PROCEEDINGS

OF THE

AMERICAN SOCIETY OF CIVIL ENGINEERS

VOL. 61 OCTOBER, 1935 No. 8, PART 1

TECHNICAL PAPERS

AND

DISCUSSIONS

Published monthly, except June and July, at 99–129 North Broadway, Albany, N. Y., by the American Society of Civil Engineers, Editorial and General Offices at 33 West Thirty-ninth Street, New York, N. Y. Reprints from this publication may be made on condition that the full title of Paper, name of Author, page reference, and date of publication by the Society, are given.

Entered as Second-Class Matter, December 28, 1931, at the Post Office at Albany, N. Y., under the Act of March 3, 1879. Acceptance for mailing at special rate of postage provided for in Section 1103, Act of October 3, 1917, authorized on July 5, 1918.

Subscription (if entered before January 1) $8.00 per annum. Price $1.00 per copy.

CURRENT PAPERS AND DISCUSSIONS

		Discussion closes
Relation Between Rainfall and Run-Off from Small Urban Areas. *W. W. Horner and F. L. Flynt*	Oct., 1934	
Discussion	May 1935	
The Silt Problem. *J. C. Stevens*	Oct., 1934	
Discussion	Feb., Mar., May, Sept., Oct., 1935	Un
Effect of Secondary Stresses Upon Ultimate Strength. *John I. Parcel and Eldred B. Murer*	Nov., 1934	
Discussion	Jan., Mar., Aug., 1935	Oct.,
Analysis of Multiple Arches. *Alexander Hrennikoff*	Dec., 1934	
Discussion	May, Sept., 1935	Oct.,
Rational Design of Steel Columns. *D. H. Young*	Dec., 1934	
Discussion	Mar., May, Aug., 1935	Oct.,
A Direct Method of Moment Distribution. *T. Y. Lin*	Dec., 1934	
Discussion	Mar., May, Aug., 1935	Oct.,
Elastic Properties of Riveted Connections. *J. Charles Rathbun*	Jan., 1935	
Discussion	Feb., May, Aug., 1935	Oct.,
Analysis of Thick Arch Dams, Including Abutment Yield. *Philip Cravitz*	Jan., 1935	
Discussion	Sept., 1935	Oct.,
Hydraulic Laboratory Results and Their Verification in Nature. *Herbert D. Vogel*	Jan., 1935	
Discussion	May, Aug., 1935	Oct.,
The Hydraulic Jump in Terms of Dynamic Similarity. *Boris A. Bakhmeteff and Arthur E. Matzke*	Feb., 1935	
Discussion	Mar., May, Aug., Sept., 1935	Oct.,
Frictional Resistance in Artificially Roughened Pipes. *Victor L. Streeter*	Feb., 1935	
Discussion	Aug., 1935	Oct.,
Stabilizing Constructed Masonry Dams by Means of Cement Injections. *D. W. Cole*	Feb., 1935	
Discussion	Aug., Sept., Oct., 1935	Unc
Weights of Metal in Steel Trusses. *J. A. L. Waddell*	Feb., 1935	
Discussion	May, Oct., 1935	Oct.,
Line Load Action on Thin Cylindrical Shells. *Herman Schorer*	Mar., 1935	
Discussion	Sept., 1935	Nov.,
Underground Corrosion. *K. H. Logan*	Mar., 1935	
Discussion	Apr., Aug., 1935	Nov.,
The Adjustment of a Level Net. *George H. Dell*	Apr., 1935	
Discussion	Aug., 1935	Nov.,
Structural Beams in Torsion. *Inge Lyse and Bruce G. Johnston*	Apr., 1935	
Discussion	Aug., Oct., 1935	Nov.,
Photo-Elastic Determination of Shrinkage Stresses. *Howard G. Smits*	May, 1935	
Discussion	Sept., Oct., 1935	Nov.,
The Shear-Area Method. *Horace B. Compton and Clayton O. Dohrenwend*	May, 1935	
Discussion	Aug., Oct., 1935	Nov.,
Flood-Stage Records of the River Nile. *C. S. Jarvis*	Aug., 1935	Nov.,
Distribution of Stresses under a Foundation. *A. E. Cummings*	Aug., 1935	
Discussion	Oct., 1935	Nov.,
Some Low-Temperature Characteristics of Bituminous Paving Compositions. *Hugh W. Skidmore*	Aug., 1935	Nov.,
Failure Theories of Materials Subjected to Combined Stresses. *Joseph Marin*	Aug., 1935	
Discussion	Oct., 1935	Nov.,
Adaptation of Venturi Flumes to Flow Measurements in Conduits. *Harold K. Palmer and Fred D. Bowlus*	Sept., 1935	Dec.,
The Stress Function and Photo-Elasticity Applied to Dams. *John H. A. Brahtz*	Sept., 1935	Dec.,
Flood and Erosion Control Problems and Their Solution. *E. Courtland Eaton*	Sept. 1935	Dec.,

NOTE.—The closing dates herein published, are final except when names of prospective discussers are registered for special extension of time.

CONTENTS FOR OCTOBER, 1935

PAPERS

DISCUSSIONS

CONTENTS FOR OCTOBER, 1935 (*Continued*)

For Index to all Papers, the discussion of which is current in* PROCEEDINGS, *see page 2

AMERICAN SOCIETY OF CIVIL ENGINEERS
Founded November 5, 1852
PAPERS

THE RELATION OF ANALYSIS TO STRUCTURAL DESIGN

By Hardy Cross[1], M. Am. Soc. C. E.

Synopsis

Confusion sometimes exists in structural design as to the use to be made of analyses. The designer soon realizes that precision is futile in some cases and important in others, and the experienced designer realizes fully that analysis of the conventional type is frequently a poor guide to proper proportions. That analysis shows a certain member to be overstressed commonly indicates that the member should be made larger; but the over-stress sometimes has little importance and may be disregarded. In some cases where the over-stress is serious, the best solution is not obvious; sometimes the structural layout should be changed entirely.

Critical study soon leads to recognition of important differences between load-carrying stresses and stresses which produce no appreciable resistance to the applied loads. The latter may be due either to external movement of abutments or to internal distortions, or they may be due to deformation induced in one part of a structure as a result of that in another part. The load-carrying stresses may also be diveded into two groups. The distinction in this case, however, is based upon response to changes in design; these sub-groups are not always clearly distinguishable, but they have characteristics so widely different in certain cases as to force their differentiation.

A classification is presented herein, with the idea of suggesting a convenient arrangement of certain familiar characteristics rather than with any wish to define the groups formally. The designations suggested, therefore, are for convenience of reference only. The non-load-carrying stresses will be distinguished as Deformation Stresses and Participation Stresses; and the load-carrying stresses as those normal in their characteristics and those which are hybrid.

Note.—Presented at the meeting of the Structural Division, New York, N. Y., on January 17, 1935. Discussion on this paper will be closed in January, 1936, *Proceedings*.

[1] Prof., Structural Eng., Univ. of Illinois, Urbana, Ill.

Deformation stresses are a consequence of strain and strain is a consequence of internal or external movements not due to stress in the structure, such as abutment movements, shrinkage, or the effects of temperature change.

Participation stresses are similar to deformation stresses, but they are due to a quite different cause. They include what are known as "secondary stresses" in bridge trusses and "participation stresses" in bracing systems as special cases. The designation is used herein for want of a better one, but the term is used in a wider sense than usual.

The primary action of most structures is such that the stress in any one part is independent, or nearly independent, of that of the other parts. This is termed normal, structural action. The group indicated includes all structures statically determined and, for good reasons, it includes also most of the forms of indeterminate structure that experience has shown to be useful.

There is a type of structure in which one member cannot be designed separately but must be designed with due consideration for its effect on other members. Such action is referred to as "hybrid," because it has some of the characteristics both of normal structural action and of participation action. The group of structures seems to be quite large and to have characteristics of great importance to designers.

Although the designations assigned herein may be new, the concepts involved are not new. What the writer wishes to do is to classify and arrange certain views of structural design which have an honored tradition in American practice. The paper is not intended to be quantitative, except in so far as quantitative statements may help in defining qualitative action. The classification proposed has some value in reconciling discordant views held by practical designers and those held by theoretical analysts, and seems, further, to have value in reconciling conflicting views held by theoretical students in the field. It is also of value in anticipating the characteristics of proposed structural types.

I.—Types of Structural Action

Deformation Stresses.—The outstanding characteristic of deformation stresses is that the strains in the structure are fixed and that the stresses are deduced from the strains. The stresses themselves are not fixed at all, but depend entirely upon the stress-strain relation of the material.

Another important characteristic is that strength has nothing, or practically nothing, to do with the problem. The strains are fixed by the overall dimensions of the structure and by the amount of deformation to be

accounted for. The designer finds it convenient to predetermine such strains, reduce them to equivalent stresses, and deduct these stresses from the working stresses available for load-carrying capacity.

Participation Stresses.—This term is used to include what are commonly known as secondary stresses in bridge trusses, participation stresses in bracing systems, participation stresses in cross-frames due to unequal deflection of trusses or girders, cross-flexure in the vertical members of trusses, secondary flexure in slender columns of bents, secondary flexure in slender spandrel columns of open spandrel arches, and secondary flexure in slender columns of buildings.

Participation stresses have many of the characteristics of deformation stresses: The strain is fixed; the stress is a consequence of the strain; and the strain, in general, can be affected in an important way only by changing over-all dimensions and not by changing the strength of the member. Thus, it is generally known that increasing the moment of inertia without changing the depth of truss members will affect the secondary stresses only as the primary stresses are affected.

Another important characteristic of these stresses is that they do not increase in proportion to the load up to rupture, but increase less rapidly after the yield point of the material has been passed. They are then clearly somewhat less dangerous than primary load-carrying stresses.

The interest of the designer in these secondary stresses is not to determine their value exactly but rather to be sure that this value is not too high. In order to find what value is too high, it is not sufficient to approach the problem from the analytical viewpoint. The values permissible in design vary with the material used, with the importance of the member involved, and with the type of failure that would result. At present, secondary stresses are accepted as a necessary evil. Try to keep them within a reasonable figure, and otherwise forget about them. Any effort to change this viewpoint represents a radical departure in thinking in the field of structural design. (In 1934, a valuable paper on the "Effect of Secondary Stresses Upon Ultimate Strength," was presented[2] by John I. Parcel, M. Am. Soc. C. E., and Eldred B. Murer, Jun. Am. Soc. C. E. Surely, the idea of discounting secondary stresses is not new in America; but accurate data as to the amount that may be discounted are much needed.)

An important difference between participation stress and deformation stress lies in their relation to the properties of the material. The two are affected in the same way by departures from Hooke's law for, in both cases, it is the strain that is fixed, the stress being a consequence of the strain. In so far as the ratio of stress to strain, however, changes with time (time flow of concrete) the effect is pronounced and direct in the case of deformation stresses, whereas time flow as distinguished from plastic flow has no effect at all in the case of participation stresses because, although the stress for a given participation strain is less as time goes on, the strain itself is in the same ratio greater because of flow under primary stress.

---

[2] *Proceedings*, Am. Soc. C. E., November, 1934, p. 1251.

If the participation strain is linear, as in the case of cross-bracing, the designer can control the stress only by changing the length of the member, which usually means that he cannot control it at all. If the strain is angular, the designer can control the maximum participation stress by changing the length of the member (which is usually impracticable), by changing the depth in the plane of flexure, and, to some extent, by changing the form or variation of section along the member.

Participation stresses are dangerous to the extent that they impair the primary load-carrying capacity of the member. Any generalization about them that does not consider the nature of failure from primary load is misleading.

Normal Structural Action.—The term is used herein to describe the action of those structures or structural parts in which it is possible to determine at the beginning the approximate magnitude of the forces in action, and in which the magnitude of these forces is affected comparatively little by the relative stress intensity in the parts of the structure.

The most obvious example is the ordinary statically determinate structure. In this type primary stress in one member is not affected at all by the stresses in any other member. All stresses are determined directly by statics, and the members are then proportioned for the forces which act upon them.

Most of the classical forms of indeterminate structures act normally, although their action is less definite than for structures statically determinate. A good example is the ordinary continuous truss, which, in practice, is often designed at once without any exact analysis being made after the design is complete. The experienced designer knows that for these structures such analyses will not indicate any important changes in his design.

Other examples are ribbed arches and spandrel-braced arches of steel, the so-called "rigid frame" bridges hinged at footings so far as the forces and moments at the knee are concerned. Most cases of continuous girders are included in this type.

In these structures it is possible to follow the procedure recommended in the textbooks. The engineer is told to guess at the sections, analyze, revise, and re-analyze. A bad first guess does not make much difference; the series of designs converges rapidly. In these cases, however, the designer can do much better than a bad first guess. Preliminary studies of pressure lines and of the properties of influence lines will enable him to make a good first guess—so good that the revision is trivial.

Hybrid Structural Action.—The term is used herein to mean structural action in which two or more parts participate in carrying loads to such an extent that if the strength of one part is changed the forces acting on other parts are largely affected. Clearly, there is some interaction in all indeterminate structures; the difference here indicated between normal and hybrid action is one of degree, and the two classes merge into each other. Participation stresses also are directly affected by changes in the primary stresses, but the relation is not reciprocal.

Hybrid structural action may be divided into two classes from the viewpoint of the designer's knowledge: Those in which the nature of the struc-

tural action can be foreseen; and those in which it cannot be foreseen. This says nothing except that the designer either does or does not know what he is doing; but the distinction needs to be made.

This type of action may be further divided into two classes, depending on whether the structure can or cannot be designed efficiently as laid out. It is very important to know this at once, but the knowledge depends on the designer's understanding of the problem.

A very simple example of what herein is called hybrid structural action occurs where two parallel beams are connected so that their center deflections must be the same under a single load at the center. If they are of the same span, depth, and material, they share the load in proportion to their strengths, and load can be assigned to one or the other at will. Even if the spans are different, this is still true if the depth-length ratio is the same for the two beams.

In this case the designer can foresee the action. He then designs as he chooses and knows that the stresses will be as assumed without further analysis; the analysis precedes any designing. Moreover, the structure can be designed efficiently since the stresses in the two beams will be the same. If the depth-length ratio is different for the two beams, however, they cannot be designed efficiently. No matter what the designer does, the relative stresses will be proportional to this ratio; but he can still foresee this fact. This case is simple; frequently the action of the structure is not easily predetermined and, in many cases, the efficiency of the design must be considered for several conditions of loading.

Near the center of long trusses having two diagonals in each panel, the designer may predetermine the stress intensities in these diagonals pretty accurately. In any panel the stress intensities in the diagonals are in inverse ratio to the squares of the lengths of these diagonals if there is no stress in the posts and if the stress intensities in the chords are equal and opposite. For dead load, these conditions in chords and posts are nearly fulfilled; for isolated loads, they are only approximately correct.

Knowing this and considering for the present only dead load, the designer can assign areas to the diagonals at will. If the chords are parallel, the diagonals can be designed efficiently; if the chords are not parallel, one diagonal must be inefficient. Influence lines may be helpful, but they fail to furnish at once a very illuminating picture of the essential structural action. For single concentrated loads the effect of the stresses in the posts and of unequal stresses in the chords may be pronounced. If single moving concentrated loads dominate the design, exact proportioning seems hopeless.

In these cases—parallel beams and double diagonals—the textbook recommendation to guess at a section, analyze, and re-design, to convergence will not work very well. If the layout is efficient, analysis will show the first guess to be right—and will show any guess to be right—but if it is inefficient, repetition of analysis and design will eliminate the inefficient member—after many repetitions—and result in a simpler structure.

Similarly, the king post truss cannot be designed for given working stresses in beam and sag rods except for a small range of the ratio of beam

depth to sag depth, which ratio can be predetermined. The chief interest in the king post truss is that, goemetrically, it is so obviously the familiar problem of a truss subjected to secondary stresses. Looking at the truss from this viewpoint, the engineer would first design it; then he would reduce the depth of the beam until the secondary stress in it was within safe limits, or he could, by adjusting the sag rods, produce initial stresses to offset the secondaries. If, however, he attempts to utilize these secondaries, to put them to work in carrying the load, an entirely different structural problem is presented, and new methods of study are required.

Hybrid structural action also occurs in the queen post truss, in systems of intersecting beams, in Vierendeel girders, probably in most slabs (at least where variation of depth is involved), in some problems of continuous beams, and in many problems of continuous frames. It is discussed subsequently, in the case of bents, of rectangular wind frames, and of arches integral with their spandrel structures.

Study of a Two-Legged Bent Illustrating the Types of Structural Action.—The distinctions herein presented are well illustrated by studies of a two-legged bent carrying vertical loads. It is assumed that the members are rectangular and homogeneous. It is proposed to study the flexural stresses in the columns. The girder section is assumed to be the same throughout the discussion but first the depth, and then the width, of the column is varied.

If the column is very narrow the girder acts practically as a beam simply supported. The rotation of the top of the column must be the same as that of the end of the girder. The angular strain in the column, therefore, is fixed, and the flexural stress varies almost directly with the depth. If the column is extremely rigid it takes nearly the full fixed-end moment in the girder and the flexural stress varies nearly inversely as the square of the column depth. Between these conditions is one in which the flexural stress in the column is nearly independent of the depth; the column is picking up moment as fast as it can take it.

If the width of the column is increased, it will be found that in the first stage (column slender) the flexural stress in the column is scarcely affected at all; in the last stage (column stiff) this stress varies inversely as the width; and in the transition stage, the increase in width reduces the flexural stress somewhat but not at all in proportion to the increase in strength.

The first stage represents a structure essentially statically determined (post and lintel or column and beam), but with participation stresses in the columns. When the column becomes very stiff the structure—so far as the columns are concerned—is normal in its action, the stresses in the columns being determined for a fairly definite moment. In the transition stage the structural action is hybrid and does not respond readily to ordinary design procedure; increase in depth may either increase or decrease the flexural stress or leave it unchanged; and increase in width (which amounts to increase in moment of inertia) produces comparatively little effect.

Deformation stresses would be produced in this structure by change of temperature. As the depth of column is increased, the deformation stresses

at the top of the column would vary at first almost directly as this depth, but later would be relieved by flexure of the girder.

Perhaps the most important fact revealed in this case is that if the flexural stresses indicated in the hybrid stage are dangerously high, there does not seem to be very much that can be done effectively, as long as the girder section is constant. This column may be thrown from the hybrid stage into the normal stage of action, however, by reducing the stiffness of the girder. In the rigid-frame bridge this is done by reducing the center depth of the girder.

II.—General Remarks on Hybrid Structural Action

It is difficult to identify hybrid action in an unfamiliar structural type, but after one has come to recognize the type he begins early to suspect its existence in certain cases. Probably the chief identifying characteristic of the type is that it responds sluggishly or erratically to traditional methods of structural design. Successive cycles of design and analysis may indicate a trend, but produce only slowly a definite and satisfactory conclusion. If there are discontinuities in this design procedure the traditional process may be quite misleading.

Traditional processes are not very helpful in this field, although they still have their place. In these cases there are usually many variables and the curves of variation present maxima and minima. It should not be necessary to point out to scientific men the extreme difficulty—the grave danger—of applying purely empirical methods to such problems. It is impossible, in such a case, to generalize or extrapolate beyond the range of data presented and it is almost impossible to classify the data for study no matter how numerous these data are, unless such arrangement is based on an adequate theory.

It makes a good deal of difference what the designer wants to do. Where the action is normal for given proportions, there is usually only one answer and that is easily approximated at once and easily determined accurately by cut and try. Where the action is hybrid there are many possible structures; the designer must make his choice. In a sense he tells the structure what he wants it to do, and the structure will try to do it. If, however, it is something that the structure cannot do at all, the designer has erred; if it is something that the structure cannot do efficiently, the design is penalized. To apply the more erudite terminology of mechanics to this conception, the fiber stresses desired may involve incompatible strains.

This type of structural action is often best approached from a direct study of the fiber stresses. H. V. Spurr, M. Am. Soc. C. E., has done this in his wind-frame studies,[8] and, without discussing herein whether his method of design is necessary, sufficient, or invariably satisfactory, the writer feels that his contribution to the direct method of attack is of great value.

Rigid-Frame Bent Subject to Vertical Loads.—Consider a bent of the so-called rigid-frame type sometimes used for building frames consisting of a roof girder, curved or polygonal, carried by two columns. The pressure

[8] "Wind Bracing", by H. V. Spurr, McGraw-Hill Book Co., 1930.

line for dead load in this structure may lie anywhere between that for a simple curved beam supported on columns and that for a three-hinged arch (hinges at the center of the girder and at the bases of the columns).

The action of the structure may be studied by either of two methods. Choose some pressure line which is expected to give a good distribution of material, determine the moments for this pressure line, and then vary the moment of inertia along the section so as to satisfy the conditions of continuity. The depths of the sections may then be varied by choice. By this method the designer tells the moments where he wants them and then decides whether he likes the result.

As an alternative procedure which has some advantage, he chooses the desired pressure line, selects working stresses along this line, and then varies the depths to provide the requisite conditions of continuity. This requires judgment, but may be done quite well by eye. The moments of inertia may then be determined for these moments, stresses, and depths. The important fact is that the design may be predetermined—and predetermined over a wide range.

If at three points of the structure the moments of inertia are intentionally reduced compared with the sections elsewhere, the structure now becomes a normal structure (a three-hinged arch) with participation stresses at the weakened sections, which now act as hinges.

Rectangular Wind Frames.—The problem of analyzing rectangular frames for horizontal forces due to wind or to earthquake accelerations continues to occupy an important place in structural literature. It seems particularly illuminating to discuss the problem from the viewpoint proposed herein. It is assumed that the columns have been designed for vertical loads and that their sections will not be changed; discussion, then, is directed entirely to the design of the girders. The effect of offsets is not considered.

It is not intended to discuss the participation stresses induced in the girders of upper floors by departures from planarity at floor levels. The writer's studies indicate that the problem is neither so important nor so difficult as some have indicated.

Assume that the girders have been designed by some of the conventional methods. An analysis is now made and it is found that some girders are overstressed and some under-stressed. Tradition indicates re-design by increasing the size of the overstressed girder and decreasing that of the girder under-stressed. However, analysis will show in many cases practically the same stresses as before; in other cases, it may show a slight improvement in the stress distribution which will be further improved by repeated re-design to a certain point; but numerous cycles of re-design may be necessary to produce much improvement.

The girders of a symmetrical rectangular frame, carrying horizontal loads, may be designed on the following assumptions: (*a*) Points of inflection are at the mid-points of all members; (*b*) column shears are proportional to moments of inertia of columns; and (*c*) design stresses in girders are proportional to depth-length ratios of girders. If so designed, it will act as

designed except near the fixed base. The analysis precedes and dictates the design; after design, no analysis is needed.

If points of inflection in the columns and distributions of column shears are assumed throughout the building, the designer can, by working from irrotational footings, determine relative stiffness, or K-values for the girders all the way up the building. Negative values for K would indicate impossible assumptions and positive values of K might be unsatisfactory because, for a given working stress, too deep a girder would be indicated or, for a given depth, too great a fiber stress would result.

The object is not to recommend this method of design, although it has value, but rather to indicate that as an alternative to the procedure, now popular, of assuming a structure and, by analysis, determining the stresses in it, presumably with a view to re-design, the designer may predetermine the function that the bracing is to perform, design directly, and then see whether the design is satisfactory as regards girder depths or working stresses. Of the two procedures, the second is often the more satisfactory. Each method is useful for certain purposes.

Note that the sensitiveness of the procedure depends upon the relative stiffness of columns and girders. If the columns are very stiff relative to the girders the moments can be applied almost anywhere without disturbing the desirable condition of inflection points very near the mid-points of the girders; the moments in the girders will be proportional to their K-values.

It seems futile to ask which of several conventional methods of analysis most nearly conforms to the results of so-called exact analysis; the answer depends on the proportions of the structure. Special attention is directed, therefore, to the dangers of induction from specific data whether obtained by computation, from models, or from tests in a laboratory, unless the range of the data covers all variables.

Arches Integral with Their Spandrel Structures.—An important example of hybrid structural action occurs in arches that are integral with their spandrel construction. It has long been recognized that there is interaction of the rib and the spandrels, but such interaction is commonly neglected in design.

In special cases applying to such structures, the engineer can see certain controlling relations. If the columns of an arch having open spandrels are quite flexible and very closely spaced, angular changes along the arch rib must be the same as those along the deck girder, since the vertical deflections of the two are every where the same. In this case, then, the entire structure could be designed at once as an arch made up of two members placed side by side as in a flitch beam. The relative flexural stresses in the rib and deck can be predicted and may be controlled by varying their relative depths.

Clearly, in this case, the designer may put all flexural resistance in the rib, or in the deck girder; or he may divide this flexural resistance between the two members at will; arches have been built of all three types—a stiff arch without stiffening girder; a flexible arch with stiffening girder; and a stiff arch reinforced with a stiffening girder. Of course, in any case, there

must be some flexural resistance in the flexible member and some flexural resistance in the columns. These, however, will have the well-defined characteristics of participation stresses.

If the columns are not closely spaced the simplicity of the picture is marred both because the flitch-beam picture is less simple and also because the deck girder now has primary stresses as a continuous beam.

As the columns become quite stiff, however, the picture becomes very complicated. Such a structure is clearly hybrid in its action and the nature of the inter-relations is not at once apparent. Methods of studying such cases have been developed by Nathan M. Newmark, Jun. Am. Soc. C. E.[4]

It is important to question whether it is good practice to change from normal structural action with participation stresses to hybrid action with obvious reduction in the factor of safety of the rib, with little promise of economy, and with much complication and uncertainty in design. There is little, if any, evidence that the participation stresses in these structures are dangerous or even objectionable. The idea of putting secondary stresses to work is not usually very promising.

III.—General Remarks on Indeterminacy

Thirty-four years ago Mr. Frank H. Cilley presented a paper under the title "The Exact Design of Statically Indeterminate Frameworks. An Exposition of Its Possibility but Futility."[5] The main thesis was that "statical indetermination in a structure is always to be regarded as self-interference with efficiency." The paper followed a previous paper by the same author,[6] and revived a discussion of long standing as to the relative advantages of determinate and indeterminate systems. Two discussions of the paper were presented by distinguished American engineers and several by foreign engineers.

There is little question that Mr. Cilley's views represented those of many, and probably of a large majority, of the leading American structural engineers of his day. To-day, on the other hand, literature contains numerous articles extolling the virtues of indeterminacy and some writers even go so far as to attribute to indeterminate structures virtues which appear to be contradictory. They are referred to as "reservoirs of resilience," their rigidity is praised, as are their economy and their strength.

Since 1900, many indeterminate steel trusses have been built in America with claims, apparently well supported, of considerable economy. More important still, a new material—concrete—which is more conveniently made continuous, has come into general use.

The rather awkward methods of analysis current at the beginning of this century undoubtedly delayed the development of continuous structural types. At that time the analysis of some of the more complicated types now proposed

[4] Some phases of Mr. Newmark's extensive studies are reported in "Interaction Between Rib and Superstructure in Concrete Arch Bridges", by Nathan M. Newmark, Jun. Am. Soc. C. E. Thesis presented to the University of Illinois in 1934, in partial fulfillment of the requirement for the degree of the Doctor of Philosophy.

[5] *Transactions*, Am. Soc. C. E., Vol. XLIII (1900), p. 353.

[6] "Some Fundamental Propositions Relating to the Design of Frameworks", by Frank H. Cilley, *Technology Quarterly*, June, 1897.

was impracticable. The profession has made progress in this field. It may be well now to divert the attention of structural designers from the endless elaboration of analytical technique to the more important matter of interpretation of analyses.

It appears that Mr. Cilley's paper was directed too much to a consideration of what is herein termed hybrid structural action. The degree of self-interference in normal structures is quite negligible. Each normal indeterminate structure usually has a determinate analogue in comparison with which it has certain virtues and which has certain virtues in comparison with it. No generalization is possible, but the indeterminate structure has won consideration and is often indicated.

Structures in which hybrid action predominates are also sometimes indicated. If their action can be clearly foreseen and if they are designed for one controlling load condition, they may be designed economically. Often they are indicated for reasons entirely apart from structural efficiency, as in the case of rectangular wind-bracing; but where their action cannot be clearly visualized, conventional procedures of analysis by computation or by model may furnish little help.

IV.—Concluding Remarks

The paper has indicated four types of structural action the characteristics of which make their separate discussion worth while. These are (*a*) the action that produces deformation stresses; (*b*) that which produces participation stresses; (*c*) normal structural action; and (*d*) hybrid structural action. Deformation stresses and participation stresses have many characteristics in common, but are essentially different in cause and sometimes in action. Hybrid structural action represents a transition stage between participation stress and normal structural action.

Deformation stresses cannot be avoided except by avoiding the deformation that produces them. They may be slightly modified so that a little more strain takes place at one point and a little less at another, but about the same total strain—angular or linear— will inevitably occur. Linear strain due to angular strain may be reduced by decreasing the depth.

The designer's interest in participation stresses is that they shall not be too high; he does not want their exact values. If they are too high, he changes either the over-all dimensions or the details of construction. What is "too high" will always remain a matter of judgment. In normal structural types only is the traditional procedure, of first computing the forces and then designing for them, applicable.

Hybrid structures may be designed in many ways. In order that analysis may guide to design, it should precede design so that the designer may see in what ways the structure can act. Then, in a quite literal sense, he tells it how to act and makes it act in that way. The difficulty is that he may blunder in trying to have it act in a way in which it cannot possibly act or that, of the many ways in which it can act, he chooses an inefficient one.

Structures characterized by hybrid action are difficult to design and are often inefficient in any case. Study of them is made difficult by the inadequacy of traditional methods; it is almost hopeless, and may be dangerous, to study them by emprical methods.

Generalizations as to relative advantages of determinate and indeterminate systems are difficult in any case. Some conflicting opinions in the literature may be reconciled by recognizing the distinction indicated.

AMERICAN SOCIETY OF CIVIL ENGINEERS

Founded November 5, 1852

PAPERS

TUNNEL AND PENSTOCK TESTS AT CHELAN STATION, WASHINGTON

By Ellery R. Fosdick, Esq.[1]

Synopsis

A thorough and detailed analysis of flow-line losses was computed from data obtained by tests on the unusually long flow line leading to the hydro-electric generating plant at Chelan, Wash. This paper contains the results of that analysis, and includes:

(1) The losses that occur in each part of the flow line;

(2) The coefficients of roughness that are applicable to the large concrete and steel lined pipes of this installation;

(3) An unusual and complete analysis of the losses that occurred in the wye-branch; and

(4) A segregation of the diversion losses (see heading, "Definitions of Symbols") in the wye-branch and lower penstock bends from the losses due to frictional resistance, as a means of checking laboratory tests and research work that was being conducted along this line.

The tests were made and a report was prepared as a means of facilitating the most economical operation of the generating station and to supply additional data in the furtherance of engineering knowledge and its application to future designs involving these features.

Introduction

In 1927, after the hydro-electric generating plant at Chelan, Wash., had been completed and put into service, it was found desirable (because of the unusually long flow line) to conduct a series of tests to determine the flow-line losses. By means of these tests it was expected to obtain more or less detailed information concerning: (1) The total flow-line loss from which it would be possible to compute, easily and accurately, the water consumption of the turbines; (2) coefficients of roughness that apply to the flow of water

Note.—Discussion on this paper will be closed January, 1936, *Proceedings*.

[1] Asst. Engr., State of Washington. Dept. of Public Service, Spokane, Wash.

in large concrete and steel pipes; (3) an analysis of the losses that occur in the wye-branch; and (4) the laws governing diversion and eddy losses in the pipe bends.

Item (1) was desired for use in operating the plant and Items (2), (3), and (4) were for the purpose of adding to the available knowledge of hydraulic losses that occur in large conduits, thereby facilitating their future design. Practically nothing of a definite nature had been done at the time these tests were made toward analyzing the losses that occur in a wye-branch and little more had been done toward an understanding of the losses in pipe bends.

Description of the Chelan Development

The Chelan hydro-electric development utilizes Chelan Lake as a storage reservoir, the potential head between this lake and the Columbia River being about 400 ft. The lake has been formed by a glacial fill across the lower end of the former Chelan Gorge. Its outlet, the Chelan River, flows through what now remains of the Chelan Gorge for a distance of about 2.5 miles to the Columbia River.

The dam that regulates the level of Chelan Lake, is built across the river about 0.5 mile from the lake. The intake of the flow line leading to the power house, situated near the junction of the Chelan and Columbia Rivers, is incorporated in the dam.

Fig. 1 is a profile drawing of the flow line and penstock from the intake to the tail-race. The intake to the flow line is of a commercial, draft distributor type from which the water enters a concrete pressure tunnel, 14.00 ft in diameter, constructed to a 0.312% grade for a distance of 10 578 ft. The concrete tunnel was cast around steel forms which produced a smooth regular finish on the interior surface. At the end of this distance the tunnel lining is changed from concrete to a double-butt, strap-riveted, steel shell and the grade is changed to 35% for a distance of 397.79 ft, at which point a 14-ft steel-lined pipe rises vertically to the surge tank. Square-edged butt-straps and button-head rivets were used to fasten adjoining sections of steel together, as may be seen in Fig. 2. The interior surface was protected only with the customary factory coat of red lead paint. Consequently, the surface was somewhat rough at the time these tests were run because the steel began rusting soon after the flow line was filled with water. Since the tests were run the interior has been cleaned and repainted with a bituminous enamel, but no observations have been made to ascertain what effect this has upon the losses. The penstock grade continues the same as before, for 604 ft more, to the wye-branch, the diameter converging in this distance from 14.00 ft to 12.50 ft, where it divides through the wye-branch into two 8.83-ft, double-butt strap-riveted, steel-lined, penstock pipes, as shown in Fig. 2. At a point 40 ft below the wye-branch the two diverging penstocks bend in opposite directions through an angle of 29° 13′ 26″, so that they are parallel to each other in a horizontal plane. The total length of each penstock branch is 138 ft, the lower end connecting to a hydraulically operated needle-valve from which the water passes through a reducing section which converges to a diameter of 6.50 ft at the point where it connects to the turbine scroll-case.

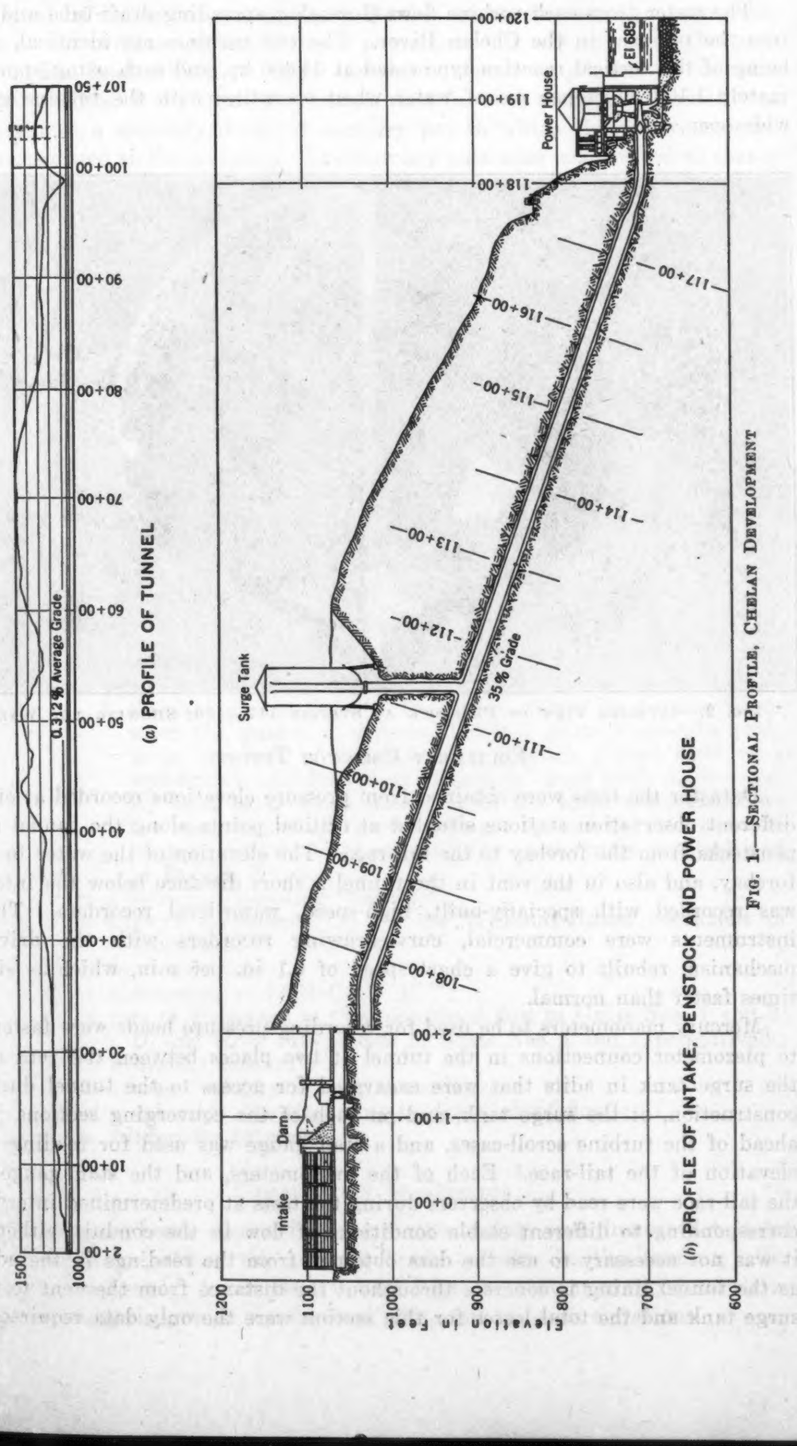

FIG. 1—SECTIONAL PROFILE, CHELAN DEVELOPMENT

The water from each turbine flows through a spreading draft-tube and out into the tail-race in the Chelan River. The two turbines are identical, each being of the vertical reaction type rated at 34 600 hp, and each using approximately 1 100 cu ft per sec of water when operating with the turbine gates wide open.

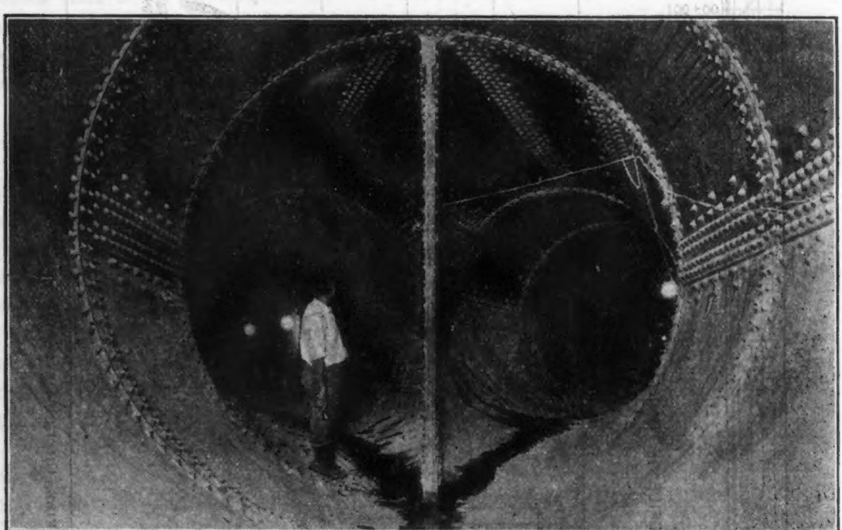

FIG. 2.—INTERIOR VIEW OF PENSTOCK AT STATION 117 + 20, SHOWING THE WYE.

EQUIPMENT USED FOR TESTS

Data for the tests were obtained from pressure elevations recorded at eight different observation stations situated at critical points along the tunnel and penstocks from the forebay to the tail-race. The elevation of the water in the forebay, and also in the vent in the tunnel a short distance below the intake, was recorded with specially-built, high-speed, water-level recorders. These instruments were commercial, curve-drawing recorders with the driving mechanism rebuilt to give a chart speed of 0.1 in. per min, which is sixty times faster than normal.

Mercury manometers to be used for recording pressure heads were fastened to piezometer connections in the tunnel at two places between the vent and the surge tank in adits that were excavated for access to the tunnel during construction, at the surge tank, and on each of the converging sections just ahead of the turbine scroll-cases, and a staff gauge was used for reading the elevation of the tail-race. Each of the manometers, and the staff gauge in the tail-race were read by observers during the tests at predetermined intervals corresponding to different stable conditions of flow in the conduit, although it was not necessary to use the data obtained from the readings in the adits as the tunnel lining is concrete throughout the distance from the vent to the surge tank and the total losses for this section were the only data required.

Instead of using the conventional U-tube manometer at the observation points on the turbine scroll-case in the power house, it was necessary (because of the high head which, in some instances, supported a mercury column approximately 28 ft high), to use a single riser for each manometer, which was connected to a specially designed mercury pot in which the water pressure was transmitted to the mercury. The mercury pots were constructed so that a relatively large surface of the mercury was exposed to the water, resulting in a relatively small change of the surface elevation of the mercury in the pot for relatively large changes in water pressure.

Test Runs

The test runs were varied so as to cover the three following conditions of load distribution between the two units: (1) One unit operating with the turbine gates wide open, the other increasing its load by steps until it was wide open; (2) two units with balanced loads decreasing the loads by steps to zero; and (3) one unit only, increasing its load by steps until wide open.

To prevent governor hunting and the attendant variation of flow, the governors were cut out, and the turbines were controlled manually throughout these tests.

Definition of Symbols

The symbols introduced in this paper are defined as follows:

e = a subscript denoting "due to eddies";

h = head loss; h_e = head loss due to eddies above the wye-branch tie-plate; h_a = loss of head that occurs in flowing water when the stream is diverted laterally from a straight path, as in the case of water flowing through a pipe bend or a wye-branch (referred to as "diversion" head loss); h_v = velocity head in Q when measured in the main penstock above the wye; h_{v1} and h_{v2} corresponding to Q_1 and Q_2; Δh_v = velocity-head difference between the flow in the main penstock and in Branch No. 2;

v = a subscript denoting "velocity";

C = Chezy's coefficient; C_w = the Williams-Hazen coefficient of roughness;

H = total head loss;

K = a constant = $1.668\ C_w^{1.852}\ R^{1.167}$;

Q = rate of discharge = total combined flow to Units Nos. 1 and 2; Q_1 and Q_2 = rate of flow to Units Nos. 1 and 2, respectively;

R = hydraulic radius;

V = average velocity at a cross-section;

a = a subscript denoting "due to diversion of flow";

Δ = "difference between".

Computation of Results

The pressure heads observed at the various points were increased to total energy heads by adding the velocity heads existing in the conduit, after which the total energy heads were converted into equivalent energy-head elevations for comparison with the forebay, vent, and tail-race elevations.

The elevation of Chelan Lake was disturbed by a seiche while these tests were being run. It was necessary, therefore, to correct slightly, all the observed elevations for this disturbance, except those in the tail-race. In addition, the manometer readings at the surge tank were corrected for an error introduced by the angularity of the riser to the penstock; and the manometer readings at the turbine scroll-cases were corrected for an error in the value of the density of the mercury. The latter errors were determined from an evident displacement of the origin on the loss curve of the wye-branch, the cause for which would not otherwise be explained.

The curves in Figs. 3, 4, 5, and 6 are plotted, therefore, from the observed losses after they have been adjusted slightly to compensate for certain inherent errors, making it possible to draw smoother and more accurate curves through the test points.

The water consumption of the turbines for different loads when operating under various heads had previously been determined by means of tests using the Gibson method.[3] These data were used in determining the flows corresponding to the loads which were carried by the units during the tunnel and penstock tests.

Entrance and Tunnel Losses

The observed losses that occur through the gathering tube and trash racks have been plotted in Fig. 3 and as may be seen are very small, reaching a

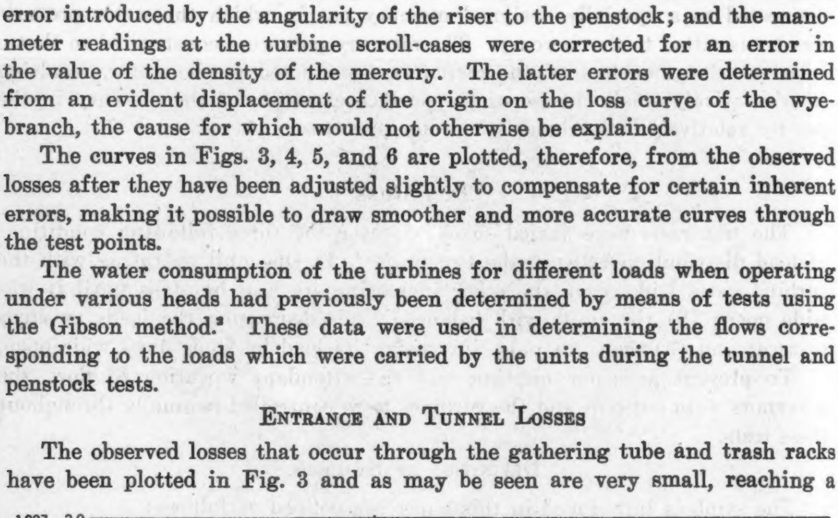

FIG. 3.—Entrance Losses Through the Gathering Tube and Trash Racks.

maximum of only 1.75 ft for the maximum flow of 2 200 cu ft per sec. The total losses in the flow line between the vent and the surge tank, a distance of 10 578 ft, are shown in Fig. 4.

[3] "Pressures in Penstocks Caused by the Gradual Closing of Turbine Gates", by Norman R. Gibson, M. Am. Soc. C. E., *Transactions*, Am. Soc. C. E., Vol. LXXXIII (1919–20), p. 707.

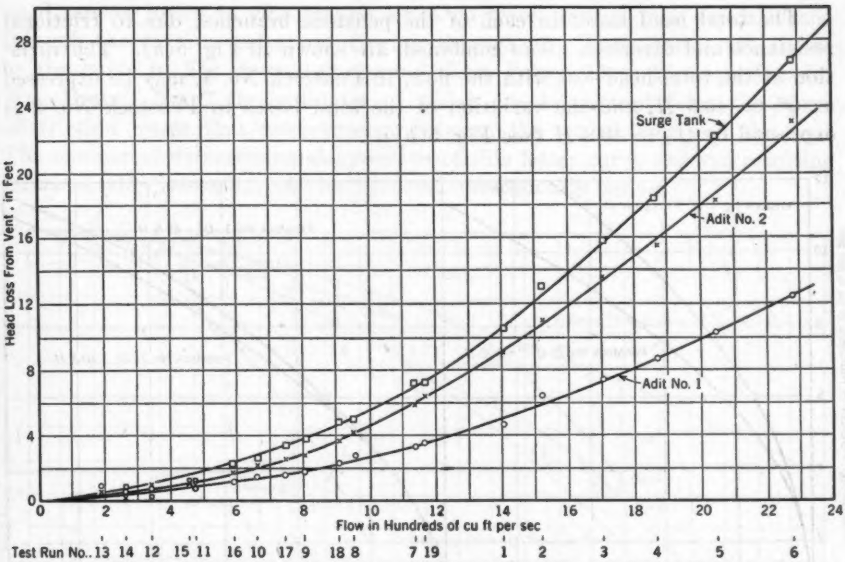

FIG. 4.—CORRECTED FLOW LINE LOSSES FROM VENT TO SURGE TANK.

BRANCH PENSTOCK LOSSES

From turbine tests which were previously conducted using the Gibson method,[3] the losses through the lower part of each penstock branch had been determined by differential pressures. In order to determine the total head loss through each penstock branch the frictional resistance component of this loss was increased proportionately to obtain the head loss due to friction for the entire length of each penstock branch. To this was added the diversion loss component which was present as a result of the bend in the lower part of each penstock branch and which obviously remained unchanged since the additional section of pipe was straight. Thus, the total loss in each penstock branch was the sum of the proportionally increased frictional resistance and the unchanged diversion losses.

Fig. 5(*a*) shows graphically the variation of the diversion losses in each of the lower penstock bends. The fact that the diversion losses through Branch No. 1 are less than in Branch No. 2 is probably due to the unsymmetrical arrangement of the spirals in the turbine scroll-case with reference to the angles through which the penstocks turn. The branches separate as they leave the wye; that is, they bend in opposite directions from the axis of the penstock above the wye whereas both the scroll-cases are spiraled in the same direction.

The equations for the curves of diversion losses in the two penstock branches are similar in character, which demonstrates that in each case the same basic laws govern these losses, although they are different in each penstock for identical flows. The equation for diversion losses in Branch No. 1 is $Q^{2.20} = 330\ H$, whereas that for diversion losses in Branch No. 2 is $Q^{2.20} = 210\ H$ (see Fig. 5(*a*)).

The total head losses in each of the penstock branches, due to frictional resistance and diversion losses combined, are shown in Fig. 5(*b*). The variation of the total head loss with the flow, in Penstock No. 1, may be expressed as $Q^2_1 = 45.5\ H$, and the variation of the total losses in Penstock No. 2 is expressed by $Q^2_2 = 40.8\ H$ (see Fig. 5(*b*)).

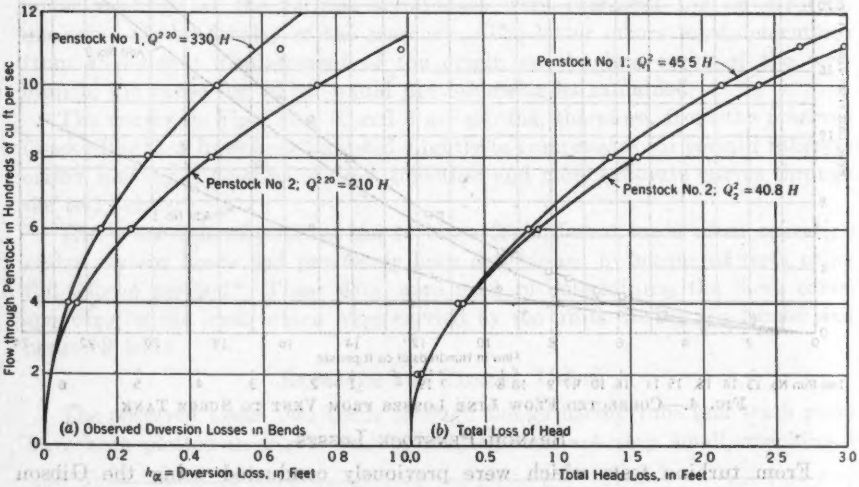

FIG. 5.—BRANCH PENSTOCK LOSSES.

The loss in head that occurred between the surge tank and points in either penstock just below the wye-branch was obtained by subtracting the head loss between the wye and either scroll-case from the corresponding total loss between the surge tank and either scroll-case.

LOSSES FROM THE SURGE TANK THROUGH THE WYE

For the purpose of studying the characteristics of the losses in the wye and penstock branches, the test loads were varied as follows:

Group (1): Unit No. 1 wide open; and Unit No. 2 increasing its load by steps until it was wide open, as shown by Test Runs 1 to 6, inclusive (see Fig. 6);

Group (2): Unit No. 1 and Unit No. 2 carrying balanced loads and decreasing loads by steps to zero as shown by Test Runs 7 to 12, inclusive; and,

Group (3): Unit No. 2 shut down and Unit No. 1 increasing its load by steps until wide open, as shown by Test Runs 13 to 19, inclusive.

To simplify the discussion that follows, these three groups of test runs will be considered in the order of Items (3), (1), and (2), instead of the order in which they actually were run.

Observed losses from the surge tank through Penstock Branch No. 2 to a point just below the wye during Group (3) of the tests, were composed of penstock friction losses from the surge tank to the wye and eddy losses that occurred above the tie-plate in the wye. It is evident that there could be

no diversion losses in this branch since no water except that which leaked through the turbine gates was flowing through it. These losses are shown by the curve in Fig. 6 passing through Test Points 13 to 19, inclusive, for Wye Branch No. 2 the ordinates of which are h_{e1} distant from the curve of friction losses that were present between the surge tank and the wye. The manner of determining the position of this latter curve and the resulting values of eddy losses, h_{e1}, will be discussed subsequently herein.

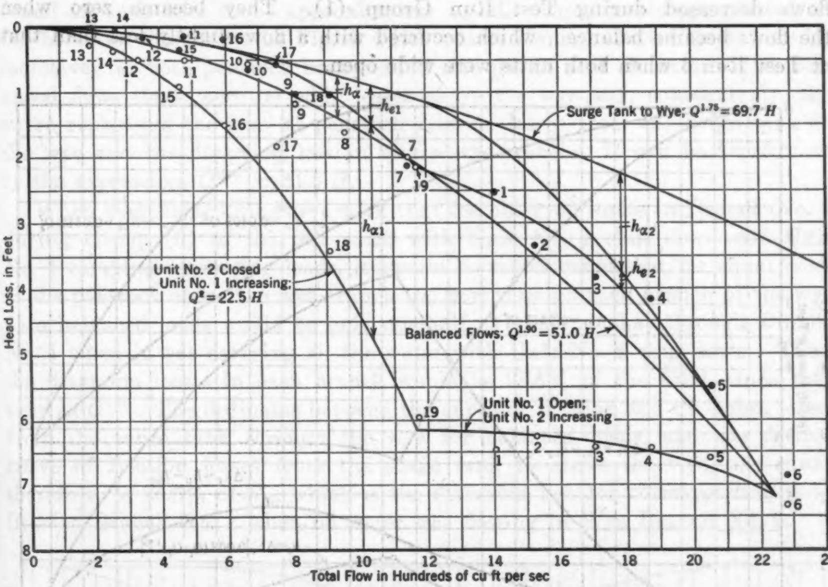

FIG. 6.—LOSSES FROM SURGE TANK THROUGH BOTH WYE BRANCHES.

During this same group of tests the observed losses through the penstock and Branch No. 1 to a point just below the wye, as in the case of losses through Branch No. 2 include (1) penstock friction losses from the surge tank to the wye; (2) eddy losses in the wye-branch above the tie-plate; and (3) the losses incurred when the water from the main penstock was diverted through an angle of 22° 30′ into Branch No. 1. The curve in Fig. 6 that passes through Test Points 13 to 19, inclusive, for Branch No. 1, with the ordinates, $h_{e1} + h_{\alpha 1}$, distant from the curve of friction losses from the surge tank to the wye, shows these losses.

It becomes evident, then, that the difference between the observed losses in Branch No. 2 and Branch No. 1 is the result of diversion losses that occur in Branch No. 1. These losses have been replotted in Fig. 7 and their relationship to the flow in Wye Branch No. 1 has been found to be $Q^{1.75} = 18.5\ h_\alpha$.

Observed losses from the surge tank through Branch No. 2 during Group (1) of the tests, with Unit No. 1 open and Unit No. 2 increasing its load, as in Group (3), consist of (1) penstock friction losses between the surge tank and the wye; (2) eddy losses above the wye; and (3) diversion losses

that occur in Branch No. 2. Diversion losses occurred during this group of tests because Unit No. 2 was running.

In Test Run Group (3) the eddy losses increased as the unbalance of flow increased between the two penstock branches, reaching a maximum at Test Run 19 when Unit No. 1 was wide open and Unit No. 2 was shut down. As the eddy losses increased when the unbalance of flows increased, during Test Run Group (3), so likewise did they decrease when the unbalance of flows decreased during Test Run Group (1). They became zero when the flows became balanced, which occurred with a flow slightly less than that at Test Run 6 when both units were wide open.

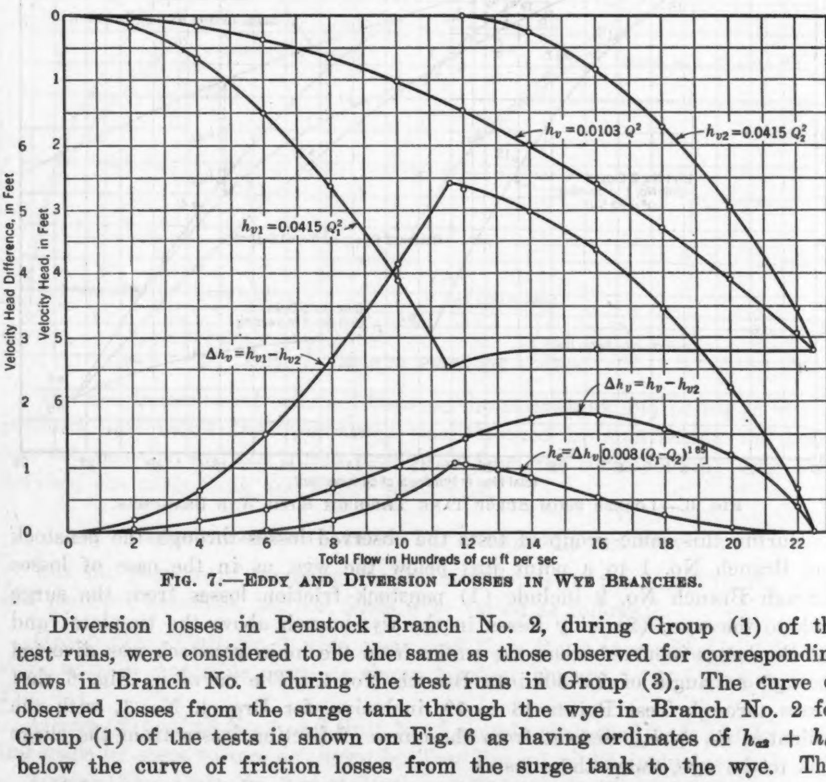

FIG. 7.—EDDY AND DIVERSION LOSSES IN WYE BRANCHES.

Diversion losses in Penstock Branch No. 2, during Group (1) of the test runs, were considered to be the same as those observed for corresponding flows in Branch No. 1 during the test runs in Group (3). The curve of observed losses from the surge tank through the wye in Branch No. 2 for Group (1) of the tests is shown on Fig. 6 as having ordinates of $h_{a2} + h_{e2}$, below the curve of friction losses from the surge tank to the wye. This curve passes through Test Points 1 to 6, inclusive, for Branch No. 2.

Observed losses from the surge tank through Wye Branch No. 1 during Group (1) of the tests are shown in Fig. 6 by the curve passing through Test Points 1 to 6, inclusive, for Branch No. 1. This curve is a continuation of the one that is distant, $h_{e1} + h_{a1}$, below the curve of friction losses from the surge tank to the wye. It slopes downward from Point 19 by an amount equal to the difference between the rate at which the friction losses between the surge tank and the wye increase with the flow of water through the penstock and the rate at which eddy losses (h_{e1}), above the wye decrease

as the flows in the two penstock branches approach a balanced condition. It is evident from the downward slope of the curve that, with the unbalance of flows that occurred during Group (1) of these tests, the friction losses from the surge tank to the wye increased more rapidly than the eddy losses above the wye decreased.

Observed losses from the surge tank through either wye-branch during the tests of Group (2) when the units were carrying equal loads, were found in each case to be approximately equal. These losses are plotted as the balanced flow curve in Fig. 6 which passes through Test Points 7 to 12, inclusive, for both penstock branches; it also passes near Point 6. With balanced flows there were no eddy losses above the wye and, consequently, the curve represents the sum of penstock friction losses from the surge tank to the wye and the diversion loss in either wye-branch. It can be reproduced by the expression, $Q^{1.90} = 51.0\, H$.

When comparing this curve with that for observed losses in Branch No. 1 during Group (3) of the test runs, with Unit No. 2 shut down and Unit No. 1 carrying increasing loads, it should be remembered that for equal flows in the penstock above the wye-branch the flow through each branch of the wye with balanced loads would be only one-half as much as that through Branch No. 1 when it was carrying all the water with Unit No. 2 shut down. Thus, the diversion losses in each branch would be 28.6% of the total, since they vary as $Q^{1.75}$. The ordinates between the curve of friction and diversion losses from the surge tank through the wye for balanced loads, and the desired curve of friction losses from the surge tank to above the wye, are equal, therefore, to 28.6% of h_{a1}, which is the diversion loss for corresponding flows in Wye Branch No. 1 when no water was flowing in Wye Branch No. 2.

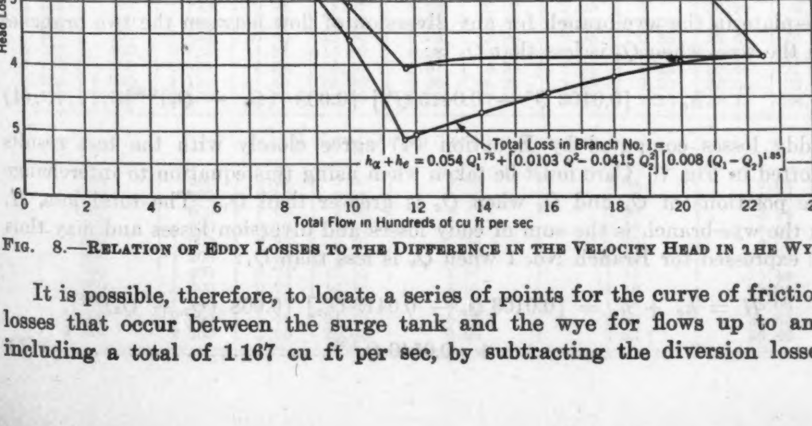

FIG. 8.—RELATION OF EDDY LOSSES TO THE DIFFERENCE IN THE VELOCITY HEAD IN THE WYE.

It is possible, therefore, to locate a series of points for the curve of friction losses that occur between the surge tank and the wye for flows up to and including a total of 1 167 cu ft per sec, by subtracting the diversion losses

from the observed losses for balanced flows. However, from this value to (but not including) a flow of 2 250 cu ft per sec, no points can be located in this manner. At 2 250 cu ft per sec the ordinate between these two curves is equal to the diversion losses that occurred when 1 125 cu ft per sec was flowing through Penstock Branch No. 1 with Unit No. 2 shut down. The curve of friction losses between the surge tank and the wye has been drawn through the points located in this manner. The equation is $Q^{1.75} = 69.7\,H$.

Eddy losses above the wye-branch tie-plate varied with, but not in proportion to, the unbalance of flows in the two branches of the wye. To study this relationship further, curves of velocity heads in each wye-branch and in the penstock above the wye, and the differences between each under the test conditions have been plotted in Fig. 8. A curve of eddy losses was likewise plotted on this sheet which shows at once, that the eddy losses are closely related to the difference between the velocity head in the penstock above the wye and in the wye-branch carrying the smaller quantity of water, which, in the case of this group of tests, was Branch No. 2. As shown in Fig. 7 the eddy losses with one unit running were found to vary as $Q^{3.85} = 12.5 \times 10^3\,h_e$.

The difference between the velocity head in the main penstock above the wye and the velocity head in Wye Branch No. 2 is:

$$\Delta h_v = h_v - h_{v2} = 0.0103\,Q^2 - 0.0415\,Q_2^2 \ldots\ldots\ldots\ldots (1)$$

Dividing h_e by Δh_v, a factor is obtained by which Δh_v may be multiplied to obtain h_e; thus:

$$\frac{\Delta h_v \left(\dfrac{Q^{3.85}}{12.5 \times 10^3}\right)}{0.0103\,Q^2 - 0.0415\,Q_2^2} = \Delta h_v \times 0.008\,Q^{1.85} \ldots\ldots\ldots\ldots (2)$$

Equation (2) equals h_e when $Q_2 = 0$. Since the eddy losses were found to vary with the unbalance of flow rather than with the total flow, Equation (2) becomes,

$$h_e = \Delta h_v\,[0.008\,(Q_1 - Q_2)^{1.85}] \ldots\ldots\ldots\ldots\ldots\ldots (3)$$

when Q_2 is less than Q_1. Expanding Equation (3) to include the expression for the difference in velocity head, the equation for eddy losses above the tie-plate in the wye-branch for any diversion of flow between the two branches in the wye, when Q_2 is less that Q_1 is:

$$h_e = [0.0103\,Q^2 - 0.0415\,Q_2^2]\,[0.008\,(Q_1 - Q_2)^{1.85}] \ldots\ldots\ldots (4)$$

Eddy losses computed by Equation (4) agree closely with the test results plotted in Fig. 7. Care must be taken when using this equation to interchange the positions of Q_1 and Q_2 when Q_2 is greater than Q_1. The total loss, H, in the wye-branch is the sum of eddy losses and diversion losses and may thus be expressed for Branch No. 1 when Q_2 is less than Q_1:

$$H = h_e + h_a = [0.0103\,Q_2 - 0.0415\,Q_2^2]\,[0.008\,(Q_1 - Q_2)^{1.85}] + 0.0540\,Q_1^{1.75} \ldots\ldots\ldots (5)$$

The expression for Branch No. 2, when Q_2 is less than Q_1, is:

$$H = [0.0103\,Q^2 - 0.0415\,Q_2^2]\,[0.008\,(Q_1 - Q_2)^{1.85}] + 0.0540\,Q_2^{1.75} \ldots (6)$$

When Q_1 is less than Q_2 the expression for Branch No. 2 is:

$$H = [0.0103\,Q^2 - 0.0415\,Q_1^2]\,[0.008\,(Q_2 - Q_1)^{1.85}] + 0.054\,Q_2^{1.75} \ldots (7)$$

Equations (5), (6), and (7), may be used to compute the total losses in Branch No. 1 and Branch No. 2 of the wye with any division of flow between the two units. The total losses that were observed in the two branches of the wye during Groups (1) and (3) of the test runs, are plotted in Fig. 7. Equations (5) and (6) apply to these curves.

Total Flow-Line Losses

With the losses in each part of the flow line and the laws governing them known, it was next desired to combine their values to determine the total flow-line losses for different divisions of flow through the two penstocks. This has been done in Table 1 for the two conditions of loading: (1) Equal flows through both turbines; and (2) unequal flows through the turbines (maximum condition of unbalance).

TABLE 1.—Total Flow-Line Losses from Forebay to Scroll-Case

Flow, in Cubic Feet per Second			Losses of Head, in Feet							
					Surge Tank Through Wye:		Penstock:		Total:	
Turbine No. 1 (1)	Turbine No. 2 (2)	Total (3)	Entrance (4)	Tunnel to surge tank (5)	No. 1 (6)	No. 2 (7)	No. 1 (8)	No. 2 (9)	No. 1 (10)	No. 2 (11)
(a) Unequal Flows Through Turbines										
200	17	217	0.02	0.50	0.21	0.05	0.08	0	0.81	0.57
400	17	417	0.05	1.40	0.75	0.17	0.38	0	2.58	1.62
600	17	617	0.10	2.40	1.66	0.37	0.86	0	5.02	2.87
800	17	817	0.18	3.90	2.90	0.76	1.48	0	8.46	4.84
1 000	17	1 017	0.32	5.50	4.13	1.44	2.30	0	12.68	7.26
1 125	17	1 142	0.46	7.00	5.88	2.02	2.95	0	16.29	9.48
1 125	200	1 325	0.66	9.40	6.23	2.45	2.95	0.08	19.24	12.59
1 125	400	1 525	0.90	12.50	6.26	2.95	2.95	0.38	22.61	16.73
1 125	600	1 725	1.21	15.90	6.38	3.73	2.95	0.86	26.44	21.70
1 125	800	1 925	1.34	19.60	6.57	4.84	2.95	1.48	30.46	27.26
1 125	1 000	2 125	1.56	23.60	6.93	6.22	2.95	2.30	35.04	33.68
1 125	1 125	2 250	1.76	26.20	7.22	7.22	2.95	2.95	38.13	38.13
(b) Equal Flows Through Turbines										
100		200	0.02	0.50	0.08		0.04		0.64	
200		400	0.05	1.40	0.30		0.08		1.83	
300		600	0.10	2.40	0.53		0.21		3.24	
400		800	0.18	3.90	1.06		0.38		5.52	
500		1 000	0.32	5.50	1.58		0.60		8.00	
600		1 200	0.53	7.70	2.20		0.86		11.29	
700		1 400	0.75	10.55	2.97		1.15		15.42	
800		1 600	0.98	13.75	3.83		1.48		20.04	
900		1 800	1.20	17.25	4.78		1.85		25.08	
1 000		2 000	1.42	21.10	5.83		2.30		30.65	
1 100		2 200	1.65	25.05	6.96		2.83		36.49	

From the data in Table 1, Fig. 9 is plotted as a working curve to be used for determining flow-line losses and net heads on the turbines. Knowing the net head it is easy to compute the turbine-water consumption. This information is much used for storage and general hydrological computations.

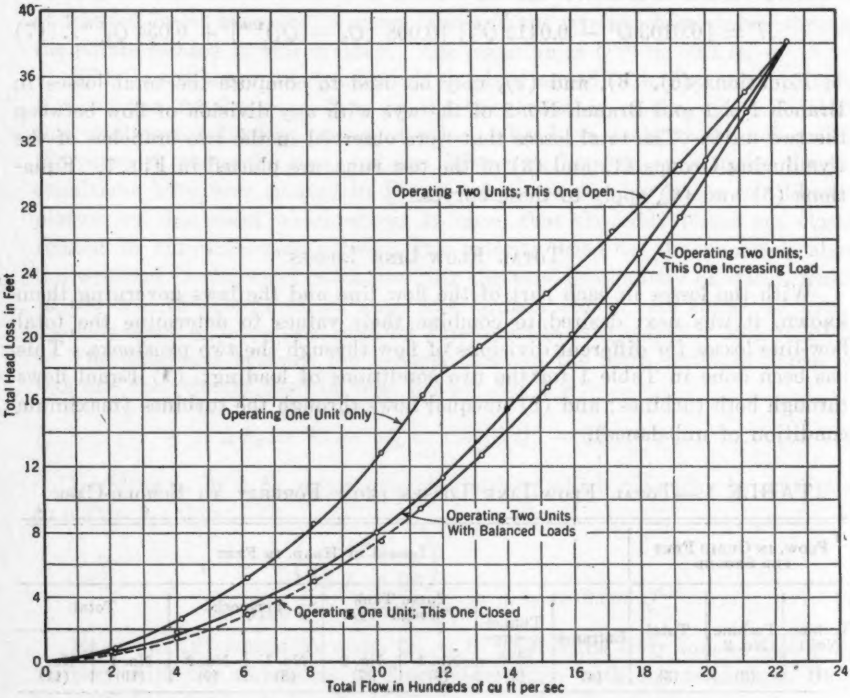

FIG. 9.—TOTAL FLOW LINE LOSS FROM FOREBAY TO SCROLL CASE.

WILLIAMS-HAZEN AND CHEZY COEFFICIENTS OF ROUGHNESS

The final step in this part of the research was first to reconcile Kutter's formula and the Williams-Hazen formula for friction losses in concrete and steel-lined tunnels to the losses actually observed in these tests, and, then, to ascertain how well the coefficients commonly recommended for use in the formula fitted this particular flow-line installation.

To do this it was first necessary to compute the coefficients of roughness which were applicable to the converging steel-lined penstock between the surge tank and the wye in which section the losses had been determined. The coefficients of roughness that were obtained in this manner were used in computing the losses which must have occurred in the steel-lined penstock from the end of the concrete-lined tunnel to the surge tank. They were also used in computing the losses in the steel-lined section of the tunnel just below the vent. The sum of these two losses was removed from the total observed losses between the vent and the surge tank, leaving those losses which occurred

in that part of the tunnel with a concrete lining. The coefficients of roughness applicable to the concrete-lined tunnel was computed from these losses by using the Williams-Hazen formula:

$$H = \frac{V^{1.852}}{1.668\, C_w^{1.852}\, R^{1.167}} \quad \ldots\ldots\ldots\ldots\ldots\ldots\ldots\ldots (8)$$

For the purpose of a comparison between the observed and the computed losses in a pipe, Equation (8) may be written

$$H = \frac{V^{1.852}}{K} \quad \ldots\ldots\ldots\ldots\ldots\ldots\ldots\ldots\ldots\ldots (9)$$

The coefficients of roughness which were obtained for the steel-lined penstock were found to vary from about 82 for very low velocities of flow to 96.5 for high velocities, as shown in Fig. 10, instead of remaining practically constant for all velocities. This variation is the result of the difference between the Williams-Hazen exponent of 1.852 which is applied to the mean velocity of flow and the exponent of 1.75 which was computed from the observed friction losses between the surge tank and the wye, the equation for these observed losses being:

$$H = \frac{V^{1.75}}{K} \quad \ldots\ldots\ldots\ldots\ldots\ldots\ldots\ldots\ldots\ldots (10)$$

The coefficients of roughness which were computed for the concrete-lined tunnel were found to remain nearly constant for all velocities, averaging

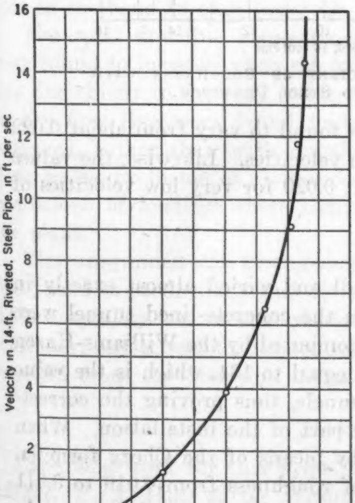

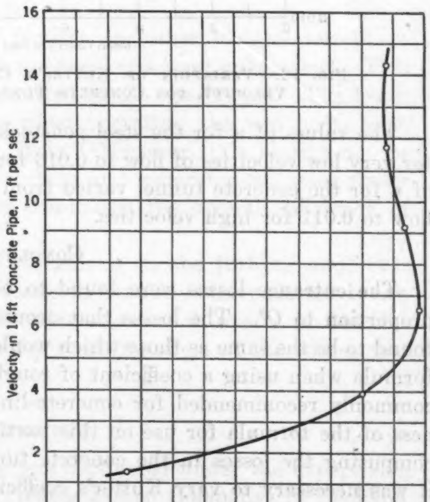

Values of C_w = Williams-Hazen Coefficient of Roughness

FIG. 10.—VARIATION IN WILLIAMS-HAZEN COEFFICIENT OF ROUGHNESS, C_w, WITH VELOCITY FOR PENSTOCK BETWEEN SURGE TANK AND WYE.

FIG. 11.—VARIATION IN THE WILLIAMS-HAZEN COEFFICIENT OF ROUGHNESS, C_w, WITH VELOCITY IN CONCRETE PRESSURE TUNNEL.

about 134, which is the value most commonly used. The computed values of these coefficients are shown in Fig. 11 where it is seen that, except for the lower velocities of flow, they varied within comparatively narrow limits.

In a similar manner the value of the Chezy coefficient, C, that was applicable to the concrete tunnel and steel penstock for different velocities of flow, was computed from the observed losses. The coefficient of roughness, n, that would be used to compute these values of C was determined from Kutter's formula. These data are plotted in Fig. 12.

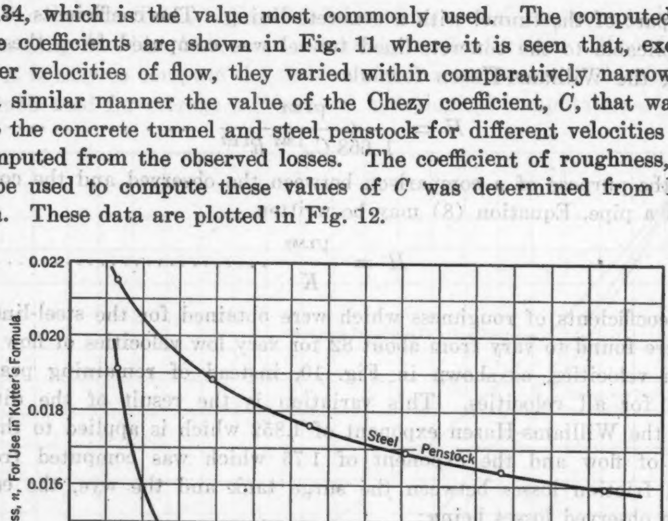

FIG. 12.—VARIATION OF KUTTER'S COEFFICIENT OF ROUGHNESS WITH VELOCITY, FOR CONCRETE TUNNEL AND STEEL PENSTOCK.

The values of n for the steel penstock were found to vary from about 0.022 for very low velocities of flow to 0.016 for high velocities. Likewise, the values of n for the concrete tunnel varied from about 0.020 for very low velocities of flow to 0.011 for high velocities.

CONCLUSIONS

The entrance losses were found to be small and varied almost exactly in proportion to Q^2. The losses that occurred in the concrete-lined tunnel were found to be the same as those which would be computed by the Williams-Hazen formula when using a coefficient of roughness equal to 134, which is the value commonly recommended for concrete-lined tunnels, thus proving the correctness of the formula for use on this particular part of the installation. When computing the losses in the concrete tunnel by means of the Chezy formula, it was necessary to vary Kutter's coefficient of roughness from 0.016 to 0.011 for different velocities, as compared to a value of 0.011 that is commonly used for designing.

The observed losses in the steel-lined penstock were found to vary with $Q^{1.76}$ instead of with $Q^{1.852}$ as would be the case when using the Williams-Hazen formula. As a consequence, in order to compute the true losses for this

particular part of the installation when using the formula, it was necessary to vary the coefficient of roughness from a value of about 82 for the lower velocities to a value of approximately 96 for the higher ones. Thus, the formula was not applicable to the steel-lined tunnel of this installation when using a constant value for the coefficient of roughness. When using the Chezy formula for computing the losses in the steel penstock, it was necessary to vary Kutter's coefficient of roughness, n, between 0.020 and 0.016 for different velocities, as compared to a value of 0.016 that is commonly used for designing.

The losses in the wye-branch, which were found to be relatively high, were composed of eddy losses occurring above the tie-plate, and diversion losses which were created as a result of the curvature in the flow line at this point. These losses varied according to definite laws which were determined as a result of these tests.

Losses in the penstock branches were found to be composed of friction losses and diversion losses in the lower penstock bends. They were of a greater magnitude than would normally be the case, due to the presence of the diversion losses.

The diversion losses in the lower penstock bends were found to vary with the 2.20 power of the flow, while those in the wye-branch were found to vary with the 1.75 power. A comparison between the diversion losses at these points is of little significance, however, because the shape of the wye-branch was determined mainly by the requirements for mechanical strength rather than by the hydraulic efficiency that could be attained. Consequently, the cross-sectional shape and curvature of each branch in the wye are not comparable to the bend in each penstock branch.

The total flow-line losses from the forebay to either turbine scroll-case were found to increase when the loads on the two units were unbalanced. This was due chiefly to the eddy losses that occurred in the wye-branch. The losses in the flow line were found to be less when operating the two units with balanced, rather than with unbalanced, flows. However, this should not be done to the exclusion of allowances for turbine and generator efficiency under conditions of loading where their effect dominated the over-all efficiency of the plant.

The unsymmetrical arrangement of the spirals in the turbine scroll-case was found to produce unequal diversion losses in the two lower penstock bends. This inequality was relatively small and unimportant with regard to flow-line efficiency, but served to demonstrate the far-reaching effect of the eddies that resulted from the diversion losses.

Acknowledgment

The field work for this investigation was conducted under the supervision of Mr. W. A. Hill, of the Washington Water Power Company, in Spokane, Wash.

particular part of the installation when using the formula, it was necessary to vary the coefficient of roughness from a value of about 82 for the lower velocities to a value of approximately 90 for the higher ones. Thus the formula was not applicable to the steel-lined tunnel of this installation when using a constant value for the coefficient of roughness. When using the Chezy formula for computing the losses in the steel penstock, it was necessary to vary Kutter's coefficient of roughness, n, between 0.020 and 0.016 for different velocities, as compared to a value of 0.0125 that is commonly used for designing.

The losses in the wye-branch, which were found to be relatively high, were composed of eddy losses occurring above the tie-plate, and diversion losses which were created as a result of the curvature in the flow line at this point. These losses varied according to definite laws which were determined as a result of these tests.

Losses in the penstock branches were found to be composed of friction losses and diversion losses in the lower penstock bends. They were of a greater magnitude than would normally be the case, due to the presence of the diversion losses.

The diversion losses in the lower penstock bends were found to vary with the 2.20 power of the flow, while those in the wye-branch were found to vary with the 1.73 power. A comparison between the diversion losses at these points is of little significance, however, because the shape of the wye-branch was determined mainly by the requirements for mechanical strength rather than by the hydraulic efficiency that could be attained. Consequently, the cross-sectional shape and curvature of each branch in the wye are not comparable to the bend in each penstock branch.

The total flow-line losses from the forebay to either turbine scroll-case were found to increase when the loads on the two units were unbalanced. This was due chiefly to the eddy losses that occurred in the wye-branch. The losses in the flow line were found to be less when operating the two units with balanced, rather than with unbalanced, flows. However, this should not be done to the exclusion of allowances for turbine and generator efficiency under conditions of loading where their effect dominated the over-all efficiency of the plant.

The unsymmetrical arrangement of the spirals in the turbine scroll-case was found to produce unequal diversion losses in the two lower penstock bends. This inequality was relatively small and unimportant with regard to flow-line efficiency, but served to demonstrate the far-reaching effect of the eddies that resulted from the diversion losses.

ACKNOWLEDGMENT

The field work for this investigation was conducted under the supervision of Mr. W. A. Hill, of the Washington Water Power Company, in Spokane, Wash.

AMERICAN SOCIETY OF CIVIL ENGINEERS

Founded November 5, 1852

PAPERS

TAPERED STRUCTURAL MEMBERS: AN ANALYTICAL TREATMENT

By Walter H. Weiskopf[1], and John W. Pickworth[1],
Assoc. Members Am. Soc. C. E.

Synopsis

The object of this paper is to present a method of analyzing structures composed of members which are not uniform in cross-section throughout their lengths. The application to some of the classical methods of analysis is indicated, and as applied to the method of moment distribution a complete development is given. Formulas for variously shaped members under various loadings are given for design use.

Introduction

The tapered member, one in which the cross-section varies from point to point along the length, is the natural and, in every respect, the correct design for a beam with restrained ends. In fact, unless the members are tapered the full advantage of continuous beams and rigidly framed structures cannot be realized. With the marked present-day trend toward the use of such structures the need increases for a satisfactory mathematical treatment of this subject.

The term, tapered member, as used herein is not confined to members in which the upper or lower edge has a curvature or haunch. Broadly stated a tapered member is one in which the moment of inertia is not constant throughout the length. In this sense a plate girder, in which the flanges are straight, but vary in area as certain parts, such as cover-plates, are added is a tapered member.

When one seeks to apply the usual theory of structures to a tapered beam difficulties appear immediately. It becomes necessary at the beginning to perform some operation, usually an integration, upon an expression of the form, $\frac{M\,dx}{E\,I}$, $\frac{M^2\,dx}{E\,I}$, or $\frac{M\,x\,dx}{E\,I}$. For a uniform member this presents no

Note.—Discussion on this paper will be closed in January, 1936, Proceedings.

[1] Cons. Engr. (Weiskopf & Pickworth), New York, N. Y.

unusual difficulties since I and E are constant. In a tapered member, however, the moment of inertia, I, is usually a complicated function of x, subject to irregularities such as occur at haunches, or involving sharp discontinuities where parts of the flange begin. Although the moment of inertia, I, may be a simple function of x, it is likely to be one which will make the integration of $\frac{M\,dx}{E\,I}$ difficult or impossible.

The method explained herein for overcoming these difficulties introduces, for the actual I of the member, a function of x, the nature of which has the properties of: (1) Closely approximating the actual I-curve; and (2) being of such a form that the expression, $\frac{M\,dx}{E\,I}$, can be integrated easily. This function,[2] which is termed the substitute I-curve, is:

$$I_x = \frac{I_0}{1 + A\left(\frac{x}{l}\right)^n} \quad \text{.........................} (1)$$

in which I_x is the moment of inertia at any point; I_0 is the moment of inertia at the end where $x = 0$; and l is the length of the member. Constants A and n are determined so as to make the substitute I-curve fit closely to the actual curve.

Fitting the I-Curve

Fig. 1 represents a member above which are plotted the actual, and a substitute, I-curve. Obviously, the substitute I-curve (Equation (1)) agrees with the actual curve where $x = 0$, both having the value, I_0, for this point. The constant A, can be determined to make the two curves coincide at the other end of the member, $x = l$. Substituting I_l for I_x, and l for x in Equation (1) and solving for A:

$$A = \frac{I_0 - I_l}{I_l} \quad \text{.........................} (2)$$

Constant A then depends solely upon the moments of inertia at the ends of the member. From Equation (2) it is evident that the greater the taper, the greater the difference between the extreme I-values, and, therefore, the greater the value of A. For this reason, A is termed the "taper modulus" of the member. For a member of uniform cross-section the taper modulus becomes zero.

Since the taper modulus, A, depends solely upon the end values of the I-curve, the constant, n, can only affect the path between these two values, or the shape of the I-curve between the ends. Therefore, n is termed the "shape exponent".

[2] Similar formulas have been suggested by George E. Large, Assoc. M. Am. Soc. C. E., and Clyde T. Morris, M. Am. Soc. C. E., *Bulletin No. 66*, Ohio State Univ., Columbus, Ohio, and by Max Ritter, *Schweitzerische Bauzeitung*, Vol. LIII, No. 18.

The effect of varying the shape exponent, n, is illustrated in Fig. 2. For the purpose of this illustration, I_o is chosen as 10, and I_l as 1. Therefore, by Equation (2) $A = 9$; and, by Equation (1):

$$I_x = \frac{10}{1 + 9\left(\frac{x}{l}\right)^n} \quad \text{.......................(3)}$$

For each value of n the substitute I-curve takes a different path between the ends of the member. As n approaches infinity, the substitute I-curve approaches that of a uniform member of moment of inertia, I_o, while as n approaches zero the curve approaches that of a uniform member, of moment of inertia, I_l. Theoretically, the shape exponent, n, can have any value between zero and plus infinity.

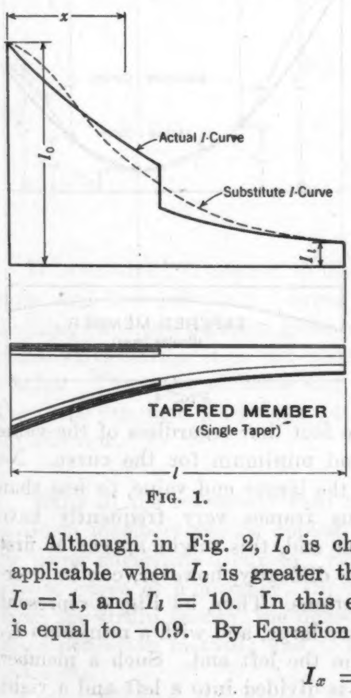

FIG. 1.

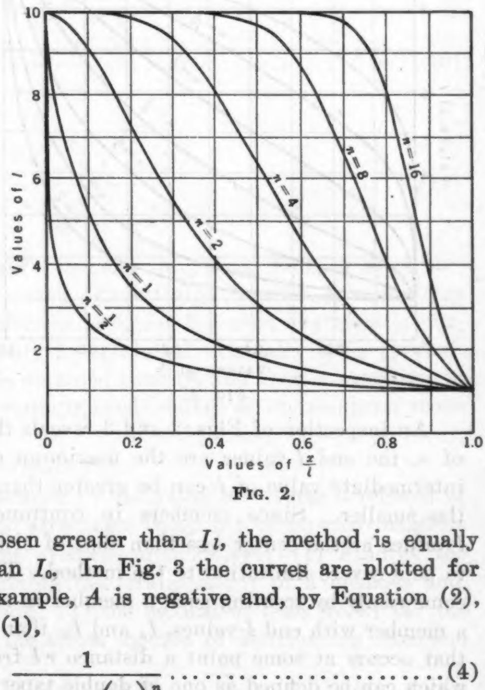

FIG. 2.

Although in Fig. 2, I_o is chosen greater than I_l, the method is equally applicable when I_l is greater than I_o. In Fig. 3 the curves are plotted for $I_o = 1$, and $I_l = 10$. In this example, A is negative and, by Equation (2), is equal to -0.9. By Equation (1),

$$I_x = \frac{1}{1 - 0.9\left(\frac{x}{l}\right)^n} \quad \text{.......................(4)}$$

As before, n can have any positive value. When it becomes infinity the curve again represents a uniform beam, of moment of inertia, I_o; and when n becomes zero the curve represents a uniform beam, of moment of inertia, I_l.

By properly choosing a value for n, the substitute I-curve can be made to approximate closely the actual I-curve. As an aid in selecting n, a value for it can be determined which will make the substitute I-curve pass through any intermediate point. Suppose it is desired that the substitute I-curve shall

have a value, I_e, where $x = x_e$. Substitute I_e for I_x, and x_e for x in Equation (1), and solve for n; then:

$$n = \frac{\log \dfrac{I_0 - I_e}{A\, I_e}}{\log \dfrac{x_e}{l}} \quad \text{.........................(5)}$$

By means of Equations (2) and (5) values of A and n can be determined, which will make the substitute I-curve coincide with the actual I-curve at the ends of the member and at one intermediate point.

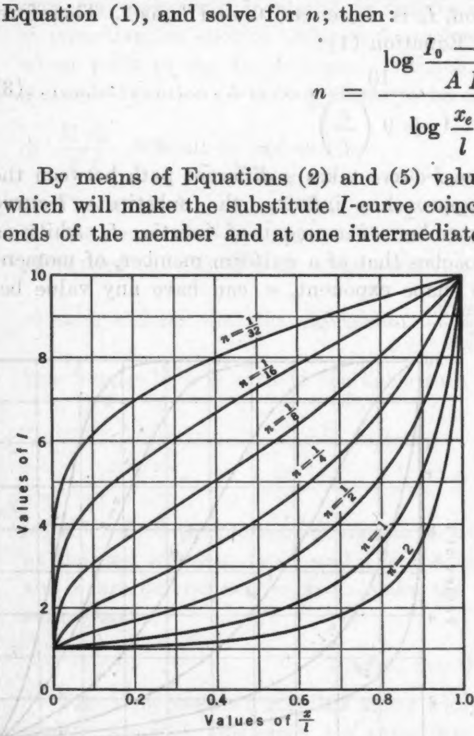

FIG. 3.

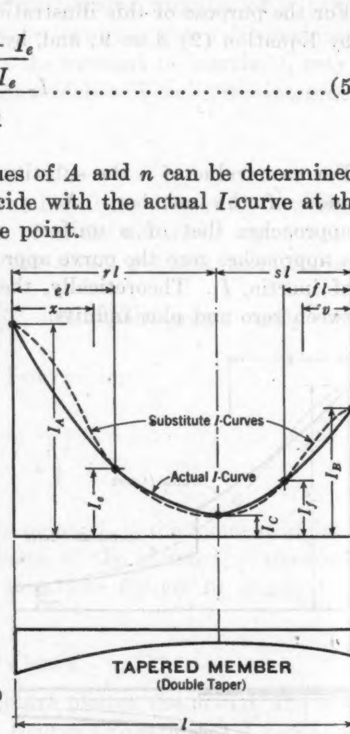

FIG. 4.

An inspection of Figs. 2 and 3 reveals the fact that regardless of the value of n, the end I-values are the maximum and minimum for the curve. No intermediate value of I can be greater than the larger end value, or less than the smaller. Since members in continuous frames very frequently have I-values at the center less than that of either end, this might appear at first to be a severe limitation to the method. The difficulty, however, can be overcome easily by treating such a member in sections. Thus, let Fig. 4 represent a member with end I-values, I_A and I_B, that are large, and with a minimum I_C, that occurs at some point a distance $r\,l$ from the left end. Such a member which can be defined as one of double taper, is divided into a left and a right section. A substitute I-curve can be fitted to the left section of the member by substituting $r\,l$ for l in Equation (1), which becomes,

$$I_x = \frac{I_A}{1 + A \dfrac{x^n}{r^n\, l^n}} \quad \text{.........................(6)}$$

For this section of the member, Equation (2) becomes,

$$A = \frac{I_A - I_C}{I_C} \quad \text{.........................(7)}$$

The substitute I-curve can also be made to pass through another point in the section of the member, (I_e), by means of Equation (5) which becomes,

$$n = \frac{\log \dfrac{I_A - I_e}{A\, I_e}}{\log \dfrac{e}{r}} \quad \text{.......................(8)}$$

For the right section of the member take the origin of co-ordinates at the other end, using v instead of x as the ordinate. If B is the taper modulus, and m, the shape exponent for this section, the equations of the substitute I-curve become,

$$I_v = \frac{I_B}{1 + B\, \dfrac{v^m}{s^m\, l^m}} \quad \text{.......................(9)}$$

and,

$$B = \frac{I_B - I_C}{I_C} \quad \text{.......................(10)}$$

and,

$$m = \frac{\log \dfrac{I_B - I_f}{B\, I_f}}{\log \dfrac{f}{s}} \quad \text{.......................(11)}$$

It is possible, of course, to divide a member into three, four, or more sections, and fit a substitute I-curve to each. Practically, however, it seems that dividing into two sections gives sufficient accuracy for most engineering purposes. Ordinarily, it is not necessary to obtain an extremely close approximation. The taper modulus can be obtained exactly, and then a variation in the shape exponent produces a surprisingly small change in the resulting stress distribution.

Applications

Many of the commonly used methods of analyzing structures composed of uniform members can be applied to structures composed of tapered members by using substitute I-curves. Some of these methods are: (1) Finding the elastic curve of a member; (2) finding the strain energy of a member and, from the strain energy, the deflection; (3) the method of least work; (4) the slope deflection method; and (5) the Cross method of distributing fixed-end moments.

(1).—Finding the Elastic Curve of a Member.—By means of a double integration of the fundamental expression, $\dfrac{d^2 y}{dx^2} = \dfrac{M}{E\, I}$, the deflection, y, is obtained as a function of x.

(2).—Finding the Strain Energy of a Member and from This Energy, the Deflection.—This problem consists of integrating between the proper limits the expression for the strain energy, W:

$$W = \int \frac{M^2\, dx}{2\, E\, I} \quad \text{.......................(12)}$$

(3).—The Method of Least Work.—To find a statically unknown force, H, this method consists in equating $\frac{dW}{dH}$ to zero and solving the resulting equation which is in the form:

$$\frac{dW}{dH} = \int \frac{M}{E\,I}\,\frac{\delta M}{\delta H}\,dx = 0 \ldots\ldots\ldots\ldots\ldots\ldots\ldots (13)$$

(4).—The Slope Deflection Method.—The fundamental equations of this method are derived by integrating the $\frac{M}{E\,I}$-diagrams; thus:

$$\theta_A - \theta_B = \int_B^A \frac{M}{E\,I}\,dx \ldots\ldots\ldots\ldots\ldots\ldots\ldots (14)$$

and,

$$y_A - \theta_A\,l = \int_B^A \frac{M\,x\,dx}{E\,I} \ldots\ldots\ldots\ldots\ldots\ldots\ldots (15)$$

in which θ_A and θ_B are the changes in slope of the points, A and B, and y_A is the deflection of one end of the member from its original position.

(5).—The Cross Method of Distributing Fixed-End Moments.—This method requires first finding the fixed-end moments, the stiffness, and the carry-over factors. By means of expressions of the form, $\int \frac{M\,x\,dx}{E\,I}$ and $\int \frac{x^2\,dx}{E\,I}$, these moments and factors can be found for tapered members. A full development of these terms is given subsequently.

INTEGRATING THE $\frac{M}{E\,I}$-CURVE

All the foregoing equations are variations and recurrences of the familiar expressions, $\int \frac{M\,dx}{E\,I}$, $\int \frac{M^2\,dx}{E\,I}$, $\int \frac{M\,x\,dx}{E\,I}$, etc. They can all be integrated according to the following general procedure.

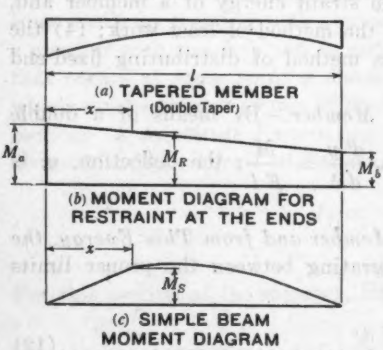

FIG. 5.

The bending moment at any point in a member can always be expressed as the algebraic sum of the moment due to restraint at the ends, and that due to the loads acting on the beam as if the ends were simply supported. These moment diagrams are shown in Fig 5. If M_R is the moment at any point due to end restraint, and M_S is the simple beam moment:

$$M = M_R + M_S \ldots\ldots\ldots (16)$$

Since the moment diagram for end restraint is a straight line,

$$M_E = M_a \frac{(l - x)}{l} + M_b \frac{x}{l} = M_a + (M_b - M_a) \frac{x}{l} \quad \ldots\ldots(17)$$

in which M_a and M_b are the end moments.

In treating the moment, M_S, the member is divided into sections between the concentrated loads. It has already been shown how the member can be divided into sections for a discontinuity in the I-curve. Each one of these can again be divided for a discontinuity in the M_S-diagram, so that sections are obtained over which both the I-curve, and the M_S-diagram are continuous functions of x. The integral of the entire member will then be the sum of the integrals of the separate sections. Subdividing the member into sections, although it increases the work, does not add to the difficulties encountered in any other respect.

For a complicated system of loading it is often easier to plot the influence line of the quantity desired for a single concentrated load at any point on the member, and then to sum up the effects of simultaneous loads. If there are no loads other than concentrations the M_S-diagram will consist of a series of straight lines, any one of which can be expressed by an equation of the form:

$$M_S = a_0 + a_1 x \quad \ldots\ldots(18)$$

If parts of the beam carry uniform loads, sections of the M_S-diagram could be expressed in the form:

$$M_S = a_0 + a_1 x + a_2 x^2 \quad \ldots\ldots(19)$$

For a uniformly varying load, there would be:

$$M_S = a_0 + a_1 x + a_2 x^2 + a_3 x^3 \quad \ldots\ldots(20)$$

When more complicated loadings occur they can be treated by the influence-line method. Therefore, it is plain that the M_S-diagram can always be divided into sections any one of which can be expressed by a formula not more complicated than Equation (20).

Furthermore, for any section of the member, from Equations (16), (17), and (20),

$$M = M_a + (M_b - M_a) \frac{x}{l} + a_0 + a_1 x + a_2 x^2 + a_3 x^3 \quad \ldots\ldots(21)$$

Using the substitute I-curve:

$$I_x = \frac{I_A}{1 + \dfrac{A\, x^n}{r^n\, l^n}} \quad \ldots\ldots(22)$$

it follows that,

$$\frac{M}{E\,I} = \frac{1}{E\,I_A} \left(1 + \frac{A\, x^n}{r^n\, l^n}\right) \left[M_a + (M_b - M_a) \frac{x}{l} + a_0 + a_1 x + a_2 x^2 + a_3 x^3\right] .(23)$$

Then,

$$\int \frac{M\,dx}{E\,I} = \int \frac{1}{E\,I_A}\left[M_a + (M_b - M_a)\,\frac{x}{l}\ + a_0 + a_1x + a_2x^2 + a_3x^3\right] dx$$

$$+ \int \frac{A}{E\,I_A\,r^n l^n}\left[M_a x^n + (M_b - M_a)\,\frac{x^{n+1}}{l} + a_0x^n + a_1x^{n+1} + a_2x^{n+2} + a_3x^{n+3}\right] dx. \quad (24)$$

In Equation (24) M_a and M_b are sometimes known (as is the case when a deflection is sought) and sometimes the unknowns which are to be found. In either case they do not vary with values of x, and are constants as far as the integration of Equation (24) is concerned. Since E, I_A, r, n, l, and the a-terms are constants, Equation (24) can be integrated term by term by the simplest processes of integral calculus.

For integrals of the form, $\int \frac{M\,x\,dx}{E\,I}$, all the terms of Equation (24) would contain values of x one power higher. For the form, $\int \frac{M^2\,dx}{E\,I}$, the terms would have still higher powers of x, but the integrations could be performed in the same general manner.

Application to the Cross Method of Distributing Fixed-End Moments

The method of moment distributions[3] introduced by Hardy Cross, M. Am. Soc. C. E., is so useful that its adaptation to tapered members will be developed in full. This will not only afford an illustration of the methods of integrating the various $\frac{M}{E\,I}$-functions, but will also furnish a set of formulas which will enable a designer to use the Cross method without integrating each time. Formulas will be derived that will give the fixed-end moments for various conditions of loading, and the stiffness and carry-over factors, for variously shaped members. Once values for these quantities have been found by means of the formulas, the designer can proceed to distribute the fixed-end moments according to the method of Professor Cross in the same manner as for uniform members.

First the expressions for beams in general will be derived. From Equations (16) and (17), a formula can be obtained for the moment at any point in a beam; thus,

$$M = M_a\,\frac{(l - x)}{l} + M_b\,\frac{x}{l} + M_s \quad (25)$$

In Equation (25), M_a and M_b are any restraining moments at the ends. The values of these moments for fixed ends are those which would make the strain energy of the member a minimum. The strain energy is:

$$W = \int_0^l \frac{M^2\,dx}{2\,E\,I_x} \quad (26)$$

[3] "Analysis of Continuous Frames by Distributing Fixed-End Moments", by Hardy Cross, *Transactions*, Am. Soc. C. E., Vol. 96 (1932), p. 1.

Then,

$$\frac{dW}{dM_A} = \int_0^l \frac{M}{E\,I_x}\,\frac{\delta M}{\delta M_A}\,dx = 0 \ldots\ldots\ldots\ldots\ldots\ldots (27)$$

with a similar equation for $\frac{dW}{dM_B}$. For fixed-end moments, Equation (25) becomes:

$$M = M_A\left(\frac{l-x}{l}\right) + M_B\,\frac{x}{l} + M_S \ldots\ldots\ldots\ldots\ldots (28)$$

Then,

$$\frac{\delta\,M}{\delta\,M_A} = \frac{l-x}{l} \ldots\ldots\ldots\ldots\ldots\ldots\ldots\ldots (29)$$

and,

$$\frac{\delta\,M}{\delta\,M_B} = \frac{x}{l} \ldots\ldots\ldots\ldots\ldots\ldots\ldots\ldots (30)$$

Substituting Equations (28) (29), and (30) in Equation (27) and its companion formula for $\frac{dW}{dM_B}$, and then simplifying and solving for M_A and M_B:

$$M_A = -\,l\,\frac{\int_0^l \frac{M_S\,(l-x)\,dx}{I_x}\int_0^l \frac{x^2\,dx}{I_x} - \int_0^l \frac{M_S\,x\,dx}{I_x}\int_0^l \frac{x\,(l-x)\,dx}{I_x}}{\int_0^l \frac{x^2\,dx}{I_x}\int_0^l \frac{(l-x)^2\,dx}{I_x} - \left[\int_0^l \frac{x\,(l-x)\,dx}{I_x}\right]^2} \ldots (31)$$

and,

$$M_B = -\,l\,\frac{\int_0^l \frac{M_S\,x\,dx}{I_x}\int_0^l \frac{(l-x)^2\,dx}{I_x} - \int_0^l \frac{M_S\,(l-x)\,dx}{I_x}\int_0^l \frac{x\,(l-x)\,dx}{I_x}}{\int_0^l \frac{x^2\,dx}{I_x}\int_0^l \frac{(l-x)^2\,dx}{I_x} - \left[\int_0^l \frac{x\,(l-x)\,dx}{I_x}\right]^2} \ldots (32)$$

Denote the integrals in Equations (31) and (32) as follows:

$$\int_0^l \frac{x\,(l-x)\,dx}{I_x} = \frac{l^3 F_1}{I_A} \ldots\ldots\ldots\ldots\ldots\ldots (33)$$

$$\int_0^l \frac{x^2\,dx}{I_x} = \frac{l^3 F_2}{I_A} \ldots\ldots\ldots\ldots\ldots\ldots (34)$$

and,

$$\int_0^l \frac{(l-x)^2\,dx}{I_x} = \frac{l^3 F_3}{I_A} \ldots\ldots\ldots\ldots\ldots\ldots (35)$$

If P is a concentrated load located at any point on the A-section of a member of double taper,

$$\int_0^l \frac{M_S\,x\,dx}{I_x} = \frac{P\,l^3 F_4}{I_A} \ldots\ldots\ldots\ldots\ldots\ldots (36)$$

and,

$$\int_0^l \frac{M_S\,(l-x)\,dx}{I_x} = \frac{P\,l^3\,F_5}{I_A} \quad \text{.................(37)}$$

Then,

$$M_A = -\,P\,l\,\frac{F_5\,F_2 - F_4\,F_1}{F_2\,F_3 - F_1^2} \quad \text{.................(38)}$$

and,

$$M_B = -\,P\,l\,\frac{F_4\,F_3 - F_5\,F_1}{F_2\,F_3 - F_1^2} \quad \text{.................(39)}$$

If the load, *P*, is on the *B*-section of a member of double taper,

$$\int_0^l \frac{M_S\,x\,dx}{I_x} = \frac{P\,l^3\,F_6}{I_A} \quad \text{.................(40)}$$

and,

$$\int_0^l \frac{M_S\,(l-x)\,dx}{I_x} = \frac{P\,l^3\,F_7}{I_A} \quad \text{.................(41)}$$

Then,

$$M_A = -\,P\,l\,\frac{F_7\,F_2 - F_6\,F_1}{F_2\,F_3 - F_1^2} \quad \text{.................(42)}$$

and,

$$M_B = -\,P\,l\,\frac{F_6\,F_3 - F_7\,F_1}{F_2\,F_3 - F_1^2} \quad \text{.................(43)}$$

If a member supports a uniformly distributed load, *w*, per unit length:

$$\int_0^l \frac{M_S\,x\,dx}{I_x} = \frac{w\,l^4\,F_8}{I_A} \quad \text{.................(44)}$$

and,

$$\int_0^l \frac{M_S\,(l-x)\,dx}{I_x} = \frac{w\,l^4\,F_9}{I_A} \quad \text{.................(45)}$$

Then,

$$M_A = -\,w\,l^2\,\frac{F_9\,F_2 - F_8\,F_1}{F_2\,F_3 - F_1^2} \quad \text{.................(46)}$$

and,

$$M_B = -\,w\,l^2\,\frac{F_8\,F_3 - F_9\,F_1}{F_2\,F_3 - F_1^2} \quad \text{.................(47)}$$

Carry-Over Factor

According to Professor Cross the carry-over factor is defined[4] as follows:

"If one end of a member which is on unyielding supports at both ends is rotated while the other end is held fixed the ratio of the moment at the fixed end to the moment producing rotation at the rotating end is herein called the 'carry-over factor'."

[4] "Analysis of Continuous Frames by Distributing Fixed-End Moments", by Hardy Cross, *Transactions*, Am. Soc. C. E., Vol. 96 (1932), p. 2.

Since there are no loads on the member except the end moments, Equation (25) becomes,

$$M = M_a \left(\frac{l - x}{l} \right) + M_b \frac{x}{l} \quad \text{(48)}$$

If End B is fixed, M_b in Equation (48) becomes M_B. If C_{AB} is the carry-over factor from End A to End B, the foregoing definition may be expressed algebraically, as follows:

$$C_{AB} = \frac{M_B}{M_a} \quad \text{(49)}$$

The strain energy for the member (see Equation (26)) is:

$$W = M_a^2 \int_0^l \frac{(l - x)^2 \, dx}{2 \, l^2 \, E I_x} + M_a M_B \int_0^l \frac{x (l - x) \, dx}{l^2 \, E I_x} + M_B^2 \int_0^l \frac{x^2 \, dx}{2 \, l^2 \, E I_x} \quad \text{(50)}$$

For fixation at End B:

$$\frac{dW}{dM_B} = M_a \int_0^l \frac{x (l - x) \, dx}{l^2 \, E I_x} + M_B \int_0^l \frac{x^2 \, dx}{l^2 \, E I_x} = 0 \quad \text{(51)}$$

Therefore,

$$C_{AB} = \frac{M_B}{M_a} = - \frac{\displaystyle\int_0^l \frac{x (l - x) \, dx}{I_x}}{\displaystyle\int_0^l \frac{x^2 \, dx}{I_x}} = - \frac{F_1}{F_2} \quad \text{(52)}$$

Similarly, for the other end,

$$C_{BA} = - \frac{F_1}{F_3} \quad \text{(53)}$$

Stiffness

Professor Cross defines[4] "stiffness" of a member as follows:

"'Stiffness', as herein used, is the moment at one end of a member (which is on unyielding supports at both ends) necessary to produce unit rotation of that end when the other end is fixed."

According to this definition the stiffness of a member would be $\frac{M_a}{\theta_A}$. For uniform members Professor Cross does not use this value, however, but uses instead $\frac{I}{l}$, which is proportional to it, the relation between the two values being,

$$\frac{I}{l} = \frac{M_a}{4 \, E \, \theta_A} \quad \text{(54)}$$

It is immaterial, of course, whether one uses $\frac{I}{l}$, or $\frac{M_a}{\theta_A} \left(\text{which is } \frac{4 \, E \, I}{l} \right)$ as long as one uses the same form for all the members of the structure. Since

for uniform members, $\frac{I}{l}$ is a most convenient form, and is in common use, and since uniform and tapered members may be combined in the same structure, the stiffness of a member as used herein is in a form that corresponds to $\frac{I}{l}$, for uniform members. Therefore, the stiffness, S_A, of End A may be expressed by the formula:

$$S_A = \frac{M_a}{4\,E\,\theta_A} \quad \text{.......................(55)}$$

The slope deflection, θ_A, can be found by equating the external to the internal work; thus:

$$\frac{M_a\,\theta_A}{2} = \int_0^l \frac{M^2\,dx}{2\,E\,I_x} = M_a^2 \int_0^l \frac{(l-x)^2\,dx}{2\,l^2\,E\,I_x}$$
$$+ M_a\,M_B \int_0^l \frac{x\,(l-x)\,dx}{l^2\,E\,I_x} + M_B^2 \int_0^l \frac{x^2\,dx}{2\,l^2\,E\,I_x} \quad \text{........(56)}$$

$$\theta_A = \frac{M_a \int_0^l \frac{(l-x)^2\,dx}{I_x} + 2\,M_B \int_0^l \frac{x\,(l-x)\,dx}{I_x} + \frac{M_B^2}{M_a} \int_0^l \frac{x^2\,dx}{I_x}}{E\,l^2} \quad \text{..(57)}$$

and,

$$\theta_A = \frac{\left(M_a\,F_3 + 2\,M_B\,F_1 + \frac{M_B^2}{M_a}\,F_2\right) l}{E\,I_A} \quad \text{...........(58)}$$

From Equation (52),

$$\frac{M_B}{M_a} = -\frac{F_1}{F_2} \quad \text{.......................(59)}$$

Then,

$$\theta_A = \frac{(M_a\,F_3 + M_B\,F_1)\,l}{E\,I_A} \quad \text{.......(60)}$$

and (see Equation (55)):

$$S_A = \frac{M_a\,I_A\,E}{4\,E\,(M_a\,F_3 + M_B\,F_1)\,l} = \frac{F_2\,I_A}{4\,(F_2\,F_3 - F_1^2)\,l} \quad \text{........(61)}$$

Similarly, for the other end,

$$S_B = \frac{F_3\,I_A}{4\,(F_2\,F_3 - F_1^2)\,l} \quad \text{.....................(62)}$$

Equations (38), (39), (42), (43), (46), (47), (52), (53), (61), and (62) are general expressions for the fixed-end moments, carry-over factors, and stiffness for members of any kind in terms of the integrals expressed by the symbols, F_1, F_2, etc. For uniform members these F-terms can be evaluated directly. For tapered members they can be found by performing the integrations indicated, using substitute I-curves.

A summary of the formulas used in this method giving values for the F-terms is given subsequently in Cases 1 to 5. In each example, the quantities, F_1, F_2, and F_3, are functions of the properties of the member and are independent of the loading. The stiffness and carry-over factors, which also depend on properties of a member only, are given in terms of F_1, F_2, and F_3. The expression, $F_2 F_3 - F_1^2$, occurs repeatedly as the denominator in formulas for stiffness and for values of the fixed-end moments. The F-terms with subscripts greater than 3 are functions of the loading as well as of the properties of the member.

Evaluation of F-Terms

Case 1.—Unsymmetrical Member of Double Taper.—This is the most general case (see Fig. 6). First, the values of A, B, n, m, C_{AB}, C_{BA}, S_A, and S_B, are determined by Equations (7), (8), (10), (11), (52), (53), (61), and (62), respectively, in which:

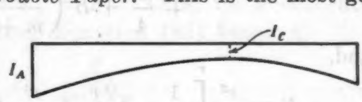

FIG. 6.—CASE 1, UNSYMMETRICAL MEMBER (DOUBLE TAPER.)

$$F_1 = r^2 \left[\frac{1}{2} - \frac{r}{3} + A \left(\frac{1}{n+2} - \frac{r}{n+3} \right) \right] + s^2 \frac{I_A}{I_B} \left[\frac{1}{2} - \frac{s}{3} + B \left(\frac{1}{m+2} - \frac{s}{m+3} \right) \right] \ldots\ldots\ldots (63)$$

$$F_2 = r^3 \left[\frac{1}{3} + \frac{A}{n+3} \right] + s \frac{I_A}{I_B} \left[1 - s + \frac{s^2}{3} + B \left(\frac{1}{m+1} - \frac{2s}{m+2} + \frac{s^2}{m+3} \right) \right] \ldots\ldots\ldots (64)$$

and,

$$F_3 = r \left[1 - r + \frac{r^2}{3} + A \left(\frac{1}{n+1} - \frac{2r}{n+2} + \frac{r^2}{n+3} \right) \right] + s^3 \frac{I_A}{I_B} \left[\frac{1}{3} + \frac{B}{m+3} \right] \ldots\ldots\ldots (65)$$

When a load, P, is placed on the left section, a distance, $k\,l$, from the origin, ($k \leqq r$), the moments are determined by Equations (38) and (39), in which:

$$F_4 = k F_1 - \frac{k^3}{6} - A \frac{k^{n+3}}{r^n (n+2)(n+3)} \ldots\ldots\ldots (66)$$

and,

$$F_5 = k F_3 - \frac{3k^2 - k^3}{6} - A \frac{k^{n+2}(n+3-kn-k)}{r^n (n+1)(n+2)(n+3)} \ldots\ldots (67)$$

When the load is on the right section, ($k \geqq r$), the moments are determined by Equations (42) and (43), in which,

$$F_6 = (1-k) F_2 - \frac{I_A (2 - 3k + k^3)}{6 I_B} - B \frac{I_A (1-k)^{m+2} (2 + km + k)}{I_B s^m (m+1)(m+2)(m+3)} \ldots (68)$$

and,

$$F_7 = (1 - k) F_1 - \frac{I_A (1 - k)^3}{6 I_B} - B \frac{I_A (1 - k)^{m+3}}{I_B s^m (m + 2)(m + 3)} \quad \text{....(69)}$$

In Equations (66) to (69) the values of F_1, F_2, *and* F_3 are those of Equations (63), (64), and (65), respectively.

The moments for a uniform load over this entire beam are determined by Equations (46) and (47), in which:

$$F_8 = \frac{r^3}{2}\left[\frac{1}{3} - \frac{r}{4} + A\left(\frac{1}{n+3} - \frac{r}{n+4}\right)\right] + \frac{s^2}{2}\frac{I_A}{I_B}\left[\frac{1}{2} - \frac{2s}{3} + \frac{s^2}{4} + B\left(\frac{1}{m+2} - \frac{2s}{m+3} + \frac{s^2}{m+4}\right)\right] \quad \text{..........(70)}$$

and,

$$F_9 = \frac{r^2}{2}\left[\frac{1}{2} - \frac{2r}{3} + \frac{r^2}{4} + A\left(\frac{1}{n+2} - \frac{2r}{n+3} + \frac{r^2}{n+4}\right)\right] + \frac{s^3 I_A}{2 I_B}\left[\frac{1}{3} - \frac{s}{4} + B\left(\frac{1}{m+3} - \frac{s}{m+4}\right)\right] \quad \text{..........(71)}$$

Case 2.—Symmetrical Member of Double Taper.—The formulas applying to the symmetrical member of double taper (see Fig. 7) are obtained by making the two ends alike in the formulas of Case 1; thus: $I_A = I_B$; $r = s = 0.5$; and $A = B$.

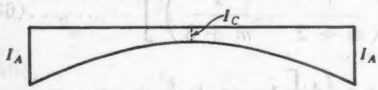

FIG. 7.—CASE 2, SYMMETRICAL MEMBER (DOUBLE TAPER.)

As before, the values of A, n, $C_{AB} = C_{BA}$, and $S_A = S_B$ are determined by Equations (7), (8), (52), and (61), respectively, in which,

$$F_1 = \frac{1}{6} + A \frac{n + 4}{4 (n + 2)(n + 3)} \quad \text{..................(72)}$$

$$F_2 = \frac{1}{3} + A \frac{(n + 1)(n + 4) + 4}{4 (n + 1)(n + 2)(n + 3)} \quad \text{...........(73)}$$

and,

$$F_3 = F_2 \quad \text{..........................(74)}$$

In applying Equation (61) to this case it is to be noted that since $F_3 = F_2$ in a symmetrical member, the denominator for the stiffness and fixed-end moments becomes $F_2^2 - F_1^2$.

When the load is on the left section, ($k \leqq \frac{1}{2}$), the moments are determined by Equations (38) and (39) in which,

$$F_4 = k F_1 - \frac{k^3}{6} - A \frac{2^n k^{n+3}}{(n + 2)(n + 3)} \quad \text{..............(75)}$$

and,

$$F_5 = k F_2 - \frac{3 k^2 - k^3}{6} - A \frac{2^n k^{n+2} (n + 3 - k n - k)}{(n + 1)(n + 2)(n + 3)} \quad \text{....(76)}$$

When the load is on the right section, ($k \geqq \frac{1}{2}$), the moments are determined by Equations (42) and (43), in which:

$$F_6 = (1 - k)\,F_2 - \frac{2 - 3\,k + k^3}{6} - A\,\frac{2^n\,(1 - k)^{n+2}\,(2 + k\,n + k)}{(n + 1)\,(n + 2)\,(n + 3)} \quad \ldots.(77)$$

and,

$$F_7 = (1 - k)\,F_1 - \frac{(1 - k)^3}{6} - A\,\frac{2^n\,(1 - k)^{n+3}}{(n + 2)\,(n + 3)} \quad \ldots\ldots\ldots(78)$$

In Equations (75) to (78) the values of F_1 and F_2 are those of Equations (72), and (73), respectively.

When the loading is symmetrical a further simplification occurs in the fixed-end moments due to the fact that $F_4 = F_5$. Thus, for a concentrated load at the center of a symmetrical beam, Equation (38) becomes,

$$M_A = M_B = -\,P\,l\,\frac{F_{10}}{F_2 + F_1} \quad \ldots\ldots\ldots\ldots\ldots(79)$$

in which,

$$F_{10} = \frac{1}{16} + \frac{A}{8\,(n + 2)} \quad \ldots\ldots\ldots\ldots\ldots(80)$$

Similarly, for a uniformly distributed load, $F_9 = F_8$, Equation (46) becomes,

$$M_A = M_B = -\,w\,l^2\,\frac{F_8}{F_2 + F_1} \quad \ldots\ldots\ldots\ldots\ldots(81)$$

in which,

$$F_8 = \frac{1}{24} + A\,\frac{n + 4}{16\,(n + 2)\,(n + 3)} \quad \ldots\ldots\ldots\ldots\ldots(82)$$

Case 3.—Unsymmetrical Member of Single Taper.—For this case (see Fig. 8), $r = 1$ and $s = 0$. Making the necessary substitutions in Equations (7), (8), (52), (53), (61), and (62), the values of A, n, C_{AB}, C_{BA}, S_A and S_B, are determined as in Case 1, with:

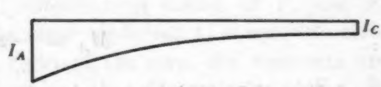

FIG. 8.—CASE 3, TAPERED MEMBER (SINGLE TAPER.)

$$F_1 = \frac{1}{6} + \frac{A}{(n + 2)\,(n + 3)} \quad \ldots\ldots\ldots\ldots\ldots(83)$$

$$F_2 = \frac{1}{3} + \frac{A}{n + 3} \quad \ldots\ldots\ldots\ldots\ldots(84)$$

and,

$$F_3 = \frac{1}{3} + \frac{2\,A}{(n + 1)\,(n + 2)\,(n + 3)} \quad \ldots\ldots\ldots\ldots\ldots(85)$$

The moments with a concentrated load at any distance, $k\,l$, from the left end are determined by Equations (38) and (39), with:

$$F_4 = k\,F_1 - \frac{k^3}{6} - A\,\frac{k^{n+3}}{(n + 2)\,(n + 3)} \quad \ldots\ldots\ldots\ldots\ldots(86)$$

and,

$$F_5 = k\,F_3 - \frac{3\,k^2 - k^3}{6} - A\,\frac{k^{n+2}\,(n + 3 - k\,n - k)}{(n + 1)\,(n + 2)\,(n + 3)} \quad\ldots\ldots(87)$$

In Equations (86) and (87) the values of F_1, F_2, and F_3 are those of Equations (83), (84), and (85), respectively.

The moments for a uniform load over the entire beam, are determined by Equations (46) and (47), in which:

$$F_8 = \frac{1}{24} + \frac{A}{2\,(n + 3)\,(n + 4)} \quad\ldots\ldots(88)$$

and,

$$F_9 = \frac{1}{24} + \frac{A}{(n + 2)\,(n + 3)\,(n + 4)} \quad\ldots\ldots(89)$$

Since members of this kind are sometimes required to withstand earth pressure, formulas are necessary for triangular loading. For example, when

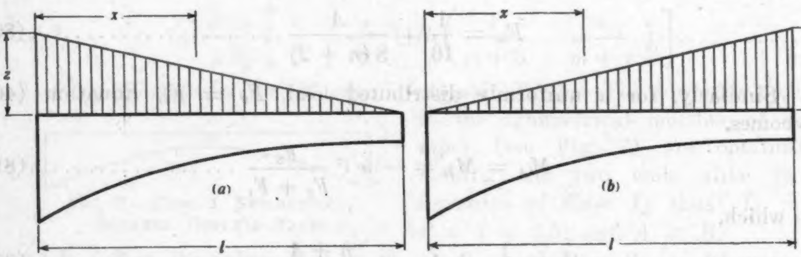

FIG. 9.—TRIANGULAR LOADINGS.

the member is loaded as shown in Fig. 9(*a*), Equation (31) becomes,

$$M_A = -\,z\,l^2\,\frac{F_{12}\,F_2 - F_{11}\,F_1}{F_2\,F_3 - F_1^2} \quad\ldots\ldots(90)$$

and Equation (32) becomes,

$$M_B = -\,z\,l^2\,\frac{F_{11}\,F_3 - F_{12}\,F_1}{F_2\,F_3 - F_1^2} \quad\ldots\ldots(91)$$

in which,

$$F_{11} = \frac{7}{360} + \frac{A\,(n + 7)}{6\,(n + 3)\,(n + 4)\,(n + 5)} \quad\ldots\ldots(92)$$

and,

$$F_{12} = \frac{1}{45} + \frac{A\,(n + 8)}{3\,(n + 2)\,(n + 3)\,(n + 4)\,(n + 5)} \quad\ldots\ldots(93)$$

When the member is loaded as shown in Fig. 9(*b*), Equations (31) and (32) become,

$$M_A = -\,z\,l^2\,\frac{F_{14}\,F_2 - F_{13}\,F_1}{F_2\,F_3 - F_1^2} \quad\ldots\ldots(94)$$

and,

$$M_B = -z\,l^2\,\frac{F_{13}\,F_3 - F_{14}\,F_1}{F_2\,F_3 - F_1^{\,2}} \quad\ldots\ldots\ldots\ldots\ldots\ldots\ldots\ldots(95)$$

in which,

$$F_{13} = \frac{1}{45} + \frac{A}{3\,(n+3)\,(n+5)} \quad\ldots\ldots\ldots\ldots\ldots\ldots\ldots\ldots(96)$$

and,

$$F_{14} = \frac{7}{360} + \frac{A\,(2\,n+7)}{3\,(n+2)\,(n+3)\,(n+4)\,(n+5)} \quad\ldots\ldots\ldots\ldots(97)$$

By adding the moments due to uniform and triangular loadings, moments for a trapezoidal loading diagram can be obtained.

Case 4.—"Stepped" Member, without Taper.—The stepped member (see Fig. 10) finds application in the columns of mill buildings, for example. In this case, A and B are equal to zero and C_{AB}, C_{BA}, S_A, and S_B are determined by Equations (52), (53), (61), and (62), in which:

FIG. 10.—CASE 4, STEPPED MEMBER.

$$F_1 = r^2\left(\frac{1}{2} - \frac{r}{3}\right) + s^2\,\frac{I_A}{I_B}\left(\frac{1}{2} - \frac{s}{3}\right) \ldots\ldots\ldots\ldots(98)$$

$$F_2 = \frac{r^3}{3} + \frac{s\,I_A}{I_B}\left(1 - s + \frac{s^2}{3}\right) \ldots\ldots\ldots\ldots\ldots\ldots(99)$$

and,

$$F_3 = r\left(1 - r + \frac{r^2}{3}\right) + \frac{s^3\,I_A}{3\,I_B} \ldots\ldots\ldots\ldots\ldots\ldots(100)$$

When the concentrated load is to the left of the step the moments are determined by Equations (38) and (39), substituting values of F_4 and F_5 from Equations (66) and (67), in which the taper modulus, A, is equal to zero.

When the concentrated load is to the right of the step, the moments are determined by Equations (42) and (43), except that the taper modulus, B, in Equations (68) and (69) is zero.

The moments for a uniform load over the entire beam are determined by Equations (46) and (47) in which:

$$F_8 = \frac{r^3}{2}\left(\frac{1}{3} - \frac{r}{4}\right) + \frac{s^2\,I_A}{2\,I_B}\left(\frac{1}{2} - \frac{2\,s}{3} + \frac{s^2}{4}\right) \ldots\ldots\ldots(101)$$

and,

$$F_9 = \frac{r^2}{2}\left(\frac{1}{2} - \frac{2r}{3} + \frac{r^2}{4}\right) + \frac{s^3\,I_A}{2\,I_B}\left(\frac{1}{3} - \frac{s}{4}\right) \ldots\ldots\ldots(102)$$

Case 5.—Member with Uniform Depth and Cross-Section.—For the simplest type of member, with a uniform depth and cross-section (see Fig. 11), in which $r = 1$ and $s = 0$, the formulas are derived directly from the equations of Case 4; that is, $F_1 = \frac{1}{6}$; $F_2 = F_3 = \frac{1}{3}$;

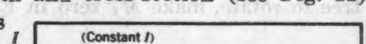

FIG. 11.—CASE 5, UNIFORM MEMBER.

$C_{AB} = C_{BA} = -\frac{1}{2}$; and $S_A = S_B = \frac{I}{l}$. With a concentrated load, the moments are determined by Equations (38) and (39), in which:

$$F_4 = \frac{k - k^3}{6} \quad \text{.......................}(103)$$

and,

$$F_5 = \frac{2k - 3k^2 + k^3}{6} \quad \text{....................}(104)$$

or simply:

$$M_A = -P\,l\,k\,(1 - k)^2 \quad \text{....................}(105)$$

and,

$$M_B = -P\,l\,k^2\,(1 - k) \quad \text{....................}(106)$$

When the concentrated load is at the center of the beam, $F_{10} = \frac{1}{16}$ and Equation (79) becomes:

$$M_A = M_B = -P\,l\,\frac{F_{10}}{F_2 + F_1} = -\frac{P\,l}{8} \quad \text{............}(107)$$

For a uniformly distributed load, $F_8 = F_9 = \frac{1}{24}$, and Equation (81) becomes:

$$M_A = M_B = -w\,l^2\,\frac{F_8}{F_2 + F_1} = -\frac{w\,l^2}{12} \quad \text{..........}(108)$$

For a triangular loading, such as that in Fig. 9(*a*), $M_A = -\frac{z\,l^2}{20}$; and $M_B = -\frac{z\,l^2}{30}$. The moments may also be determined by Equations (90) and (91), recalling that $F_2 = F_3$; $F_{11} = \frac{7}{360}$; and $F_{12} = \frac{1}{45}$. Thus, by breaking down from Case 1 to Case 5 the familiar values for uniform beams are obtained.

Variation of the Cross Method

Professor Cross gives one variation in his method well worth mention. When one end of a member is free to rotate, no moment need be carried over to it, but a modified stiffness should be used for the other end. This modified stiffness for tapered members is found as follows: Assuming End *B* as free to rotate, make M_B zero in Equation (58); thus,

$$\theta_A = \frac{M_A\,F_2\,l}{E\,I_A} \quad \text{......................}(109)$$

Then, Equation (55) becomes:

$$S'_A = \frac{M_a}{4\,E\,\theta_A} = \frac{I_A}{4\,l\,F_2} \quad \text{.......................(110)}$$

Similarly, if End A is hinged:

$$S'_B = \frac{I_A}{4\,l\,F_2} \quad \text{...........................(111)}$$

Working Lines

In applying the Cross method to framed structures composed of tapered members it is important to fix the working lines correctly. It has been found that where the curvature of a member is not too great, the working line can be taken as a straight line near the neutral axis of the minimum section. The reason for this location becomes obvious when one considers that the work terms are maximum where the moment of inertia is small, and that the working line should be located to be correct for the region contributing the greatest amount to the internal work. As an illustration Fig. 12 shows the working line for a part of a framed structure. Such lines are to be used only for the determination of the statically unknown quantities. In determining the maximum fiber stresses, the statically unknown factors having been found, the working lines, of course, should be the neutral surfaces of the members.

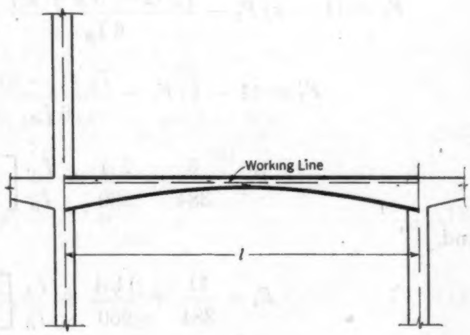

Fig. 12.

Approximate Solution

Since structures composed of tapered members are usually statically indeterminate the procedure is first to assume a trial design, analyze the stresses, modify the design, re-analyze the stresses, etc. It is very convenient in work of this nature to have an approximate solution that can be applied quickly.

Values of 2 for the shape exponent, n, have been noted frequently where the taper modulus is positive. If this value is used the work is considerably shortened, often with little sacrifice of accuracy. It has also been found in members of double taper that the I-curve is quite flat for a considerable distance near the central part of the member. There would then be small loss in accuracy by making r and s equal to one-half.

As an illustration of this procedure formulas for the F-terms of Cases 1 to 3, with the aforementioned approximations, are as follows:

In Case 1 (Equations (63) to (71)):

$$F_1 = \frac{1}{12} + \frac{3\,A}{80} + \frac{I_A}{I_B}\left[\frac{1}{12} + \frac{3\,B}{80}\right] \quad \text{.............(112)}$$

$$F_2 = \frac{1}{24} + \frac{A}{40} + \frac{I_A}{I_B}\left[\frac{7}{24} + \frac{B}{15}\right] \ldots\ldots\ldots\ldots\ldots (113)$$

$$F_3 = \frac{7}{24} + \frac{A}{15} + \frac{I_A}{I_B}\left[\frac{1}{24} + \frac{B}{40}\right] \ldots\ldots\ldots\ldots\ldots (114)$$

$$F_4 = k\,F_1 - \frac{k^3}{6} - \frac{A\,k^5}{5} \ldots\ldots\ldots\ldots\ldots\ldots\ldots (115)$$

$$F_5 = k\,F_3 - \frac{3\,k^2 - k^3}{6} - A\,\frac{k^4\,(5 - 3\,k)}{15} \ldots\ldots\ldots\ldots (116)$$

$$F_6 = (1 - k)\,F_2 - \frac{I_A\,(2 - 3\,k + k^3)}{6\,I_B} - B\,\frac{I_A\,(1 - k)^4\,(2 + 3\,k)}{15\,I_B} .(117)$$

$$F_7 = (1 - k)\,F_1 - \frac{I_A\,(1 - k)^3}{6\,I_B} - B\,\frac{I_A\,(1 - k)^5}{5\,I_B} \ldots\ldots\ldots (118)$$

$$F_8 = \frac{5}{384} + \frac{7\,A}{960} + \frac{I_A}{I_B}\left[\frac{11}{384} + \frac{11\,B}{960}\right] \ldots\ldots\ldots\ldots (119)$$

and,

$$F_9 = \frac{11}{384} + \frac{11\,A}{960} + \frac{I_A}{I_B}\left[\frac{5}{384} + \frac{7\,B}{960}\right] \ldots\ldots\ldots\ldots (120)$$

In Case 2 (Equations (72) to (82)):

$$F_1 = \frac{1}{6} + \frac{3\,A}{40} \ldots\ldots\ldots\ldots\ldots\ldots\ldots\ldots\ldots\ldots (121)$$

$$F_2 = \frac{1}{3} + \frac{11\,A}{120} = F_3 \ldots\ldots\ldots\ldots\ldots\ldots\ldots\ldots (122)$$

$$F_4 = k\,F_1 - \frac{k^3}{6} - \frac{A\,k^5}{5} \ldots\ldots\ldots\ldots\ldots\ldots\ldots (123)$$

$$F_5 = k\,F_2 - \frac{3\,k^2 - k^3}{6} - A\,\frac{k^4\,(5 - 3\,k)}{15} \ldots\ldots\ldots\ldots (124)$$

$$F_6 = (1 - k)\,F_2 - \frac{2 - 3\,k + k^3}{6} - A\,\frac{(1 - k)^4\,(2 + 3\,k)}{15} \ldots (125)$$

$$F_7 = (1 - k)\,F_1 - \frac{(1 - k)^3}{6} - A\,\frac{(1 - k)^5}{5} \ldots\ldots\ldots\ldots (126)$$

$$F_{10} = \frac{1}{16} + \frac{A}{32} \ldots\ldots\ldots\ldots\ldots\ldots\ldots\ldots\ldots\ldots (127)$$

and,

$$F_8 = \frac{1}{24} + \frac{3\,A}{160} = F_9 \qquad (128)$$

In Case 3 (Equations (83) to (97)):

$$F_1 = \frac{1}{6} + \frac{A}{20} \qquad (129)$$

$$F_2 = \frac{1}{3} + \frac{A}{5} \qquad (130)$$

$$F_3 = \frac{1}{3} + \frac{A}{30} \qquad (131)$$

$$F_4 = k\,F_1 - \frac{k^3}{6} - A\,\frac{k^5}{20} \qquad (132)$$

$$F_5 = k\,F_3 - \frac{3\,k^2 - k^3}{6} - A\,\frac{k^4\,(5 - 3\,k)}{60} \qquad (133)$$

$$F_8 = \frac{1}{24} + \frac{A}{60} \qquad (134)$$

$$F_9 = \frac{1}{24} + \frac{A}{120} \qquad (135)$$

$$F_{11} = \frac{7}{360} + \frac{A}{140} \qquad (136)$$

$$F_{12} = \frac{1}{45} + \frac{A}{252} \qquad (137)$$

$$F_{13} = \frac{1}{45} + \frac{A}{105} \qquad (138)$$

and,

$$F_{14} = \frac{7}{360} + \frac{11\,A}{2520} \qquad (139)$$

Conclusion

It is intended that this analysis be taken broadly as suggesting a general method of treating tapered members. Although the material presented gives the application to certain types of analysis and to some special kinds of members, it can be elaborated and extended to apply to many other kinds of analysis and other forms of members. It is hoped that the method of substitute *I*-curves will thus aid in the development of classes of structures which have been hampered in the past by mathematical difficulties.

$$F_2=\frac{1}{24}+\frac{A}{40}+\frac{I_A}{I_B}\left[\frac{7}{24}+\frac{B}{15}\right] \qquad (113)$$

$$F_3=\frac{7}{24}+\frac{A}{15}+\frac{I_A}{I_B}\left[\frac{1}{24}+\frac{B}{40}\right] \qquad (114)$$

$$F_4=k\,F_1-\frac{k^3}{6}-\frac{A\,k^5}{5} \qquad (115)$$

$$F_5=k\,F_2-\frac{3\,k^2-k^3}{6}-A\,\frac{k^4\,(5-3\,k)}{15} \qquad (116)$$

$$F_6=(1-k)\,F_2-\frac{I_A\,(2-3\,k+k^3)}{6\,I_B}-B\,\frac{I_A\,(1-k)^4\,(2+3\,k)}{15\,I_B} \qquad (117)$$

$$F_7=(1-k)\,F_1-\frac{I_A\,(1-k)^3}{6\,I_B}-B\,\frac{I_A\,(1-k)^5}{5\,I_B} \qquad (118)$$

$$F_8=\frac{5}{384}+\frac{7\,A}{960}+\frac{I_A}{I_B}\left[\frac{11}{384}+\frac{11\,B}{960}\right] \qquad (119)$$

and,

$$F_9=\frac{11}{384}+\frac{11\,A}{960}+\frac{I_A}{I_B}\left[\frac{5}{384}+\frac{7\,B}{960}\right] \qquad (120)$$

In Case 2 (Equations (72) to (82)):

$$F_1=\frac{1}{6}+\frac{3\,A}{40} \qquad (121)$$

$$F_2=\frac{1}{3}+\frac{11\,A}{120}=F_3 \qquad (122)$$

$$F_4=k\,F_1-\frac{k^3}{6}-\frac{A\,k^5}{5} \qquad (123)$$

$$F_5=k\,F_2-\frac{3\,k^2-k^3}{6}-A\,\frac{k^4\,(5-3\,k)}{15} \qquad (124)$$

$$F_6=(1-k)\,F_2-\frac{2-3\,k+k^3}{6}-A\,\frac{(1-k)^4\,(2+3\,k)}{15} \qquad (125)$$

$$F_7=(1-k)\,F_1-\frac{(1-k)^3}{6}-A\,\frac{(1-k)^5}{5} \qquad (126)$$

$$F_8=\frac{1}{16}+\frac{A}{32} \qquad (127)$$

and,

$$F_8 = \frac{1}{24} + \frac{3\,A}{160} = F_9 \quad \text{(128)}$$

In Case 3 (Equations (83) to (97)):

$$F_1 = \frac{1}{6} + \frac{A}{20} \quad \text{(129)}$$

$$F_2 = \frac{1}{3} + \frac{A}{5} \quad \text{(130)}$$

$$F_3 = \frac{1}{3} + \frac{A}{30} \quad \text{(131)}$$

$$F_4 = k\,F_1 - \frac{k^3}{6} - A\,\frac{k^5}{20} \quad \text{(132)}$$

$$F_5 = k\,F_3 - \frac{3\,k^2 - k^3}{6} - A\,\frac{k^4\,(5 - 3\,k)}{60} \quad \text{(133)}$$

$$F_8 = \frac{1}{24} + \frac{A}{60} \quad \text{(134)}$$

$$F_9 = \frac{1}{24} + \frac{A}{120} \quad \text{(135)}$$

$$F_{11} = \frac{7}{360} + \frac{A}{140} \quad \text{(136)}$$

$$F_{12} = \frac{1}{45} + \frac{A}{252} \quad \text{(137)}$$

$$F_{13} = \frac{1}{45} + \frac{A}{105} \quad \text{(138)}$$

and,

$$F_{14} = \frac{7}{360} + \frac{11\,A}{2520} \quad \text{(139)}$$

Conclusion

It is intended that this analysis be taken broadly as suggesting a general method of treating tapered members. Although the material presented gives the application to certain types of analysis and to some special kinds of members, it can be elaborated and extended to apply to many other kinds of analysis and other forms of members. It is hoped that the method of substitute *I*-curves will thus aid in the development of classes of structures which have been hampered in the past by mathematical difficulties.

APPENDIX

NOTATION

a_0, a_1, a_2, etc. = constants in the equation of a simple-beam moment diagram;
e = proportion of ordinate to span;
f = proportion of ordinate to span;
k = proportion of the ordinate of a concentrated load to the span;
l = length, or span, of a structural member;
m = a shape exponent;
n = a shape exponent;
r = proportion of length of section of a member to span;
s = proportion of length of section of a member to span;
v = a horizontal distance measured from the right end of a member;
w = load per unit distance;
x = horizontal distance measured from the left end of a member;
y = deflection; y_A = deflection of one end of a member from its original position;
z = maximum intensity of a uniformly varying load;
A = taper modulus;
B = taper modulus;
C_{AB} = carry-over factor from End A to End B, etc.;
E = modulus of elasticity;
F_1, F_2, F_3, etc. = constants in the Cross method of distributing fixed-end moments;
H = an unknown force in the method of least work;
I = rectangular moment of inertia; I_x = moment of inertia at any point; I_0, I_A, etc. = moment of inertia where $x = 0$, at Point A, etc.;
M = bending moment; M_R = bending moment at any point due to end restraint; M_S = moment at any point in a member, assuming the ends to be simply supported; M_a = restraining moment at End A, etc.; M_A = fixed-end moment at End A, etc.;
P = concentrated load;
S_A = stiffness of a member in the Cross method at End A, etc.;
S'_A = modified stiffness at End A of a member when End B is free to rotate, etc.;
W = work, or energy; strain energy;
θ = slope deflection; θ_A = slope deflection at Point A, etc.

AMERICAN SOCIETY OF CIVIL ENGINEERS
Founded November 5, 1852
PAPERS

PROPOSED IMPROVEMENT OF THE CAPE COD CANAL

By E. C. Harwood,[1] Esq.

Synopsis

The Cape Cod Canal has been open to navigation for twenty-one years, but could accommodate only 20% of the North Atlantic coastwise shipping in 1934 because of limited depth and width. Improvement is economically justified. For several years following the purchase of the canal by the Federal Government, plans for improvement have been under consideration. The most important question involved has been whether there should be locks, or a wider, open canal. The engineering and other difficulties involved in each case are discussed, together with the reasons for selecting the open canal. The new bridges which have been constructed are of unusual interest, one having the longest vertical lift span in the world. Construction methods include excavation by land methods as well as by dipper and by hydraulic dredging. The tide and current conditions are important because of their effect on navigation. The writer has attempted to predict the maximum current to be expected.

Introduction

The Cape Cod Canal is situated in Southeastern New England at the narrow neck where Cape Cod joins the mainland of Massachusetts. It is approximately 50 miles south of Boston and connects Cape Cod Bay on the east with Buzzards Bay on the west. The general location of the canal and the ocean routes from which the shipping through the canal is drawn, are shown in Fig. 1.

Including its approach channels in Buzzards Bay, the canal has a total length of 13 miles. Beginning at the Cape Cod end, the approximate widths at various sections of the canal (see Fig. 2) are stated in Table 1. The

Note.—Presented at the meeting of the Waterways Division, New York, N. Y., on January 16, 1935. Discussion on this paper will be closed in January, 1936, *Proceedings*.

[1] Capt., Corps of Engrs., U. S. Army, Boston, Mass.

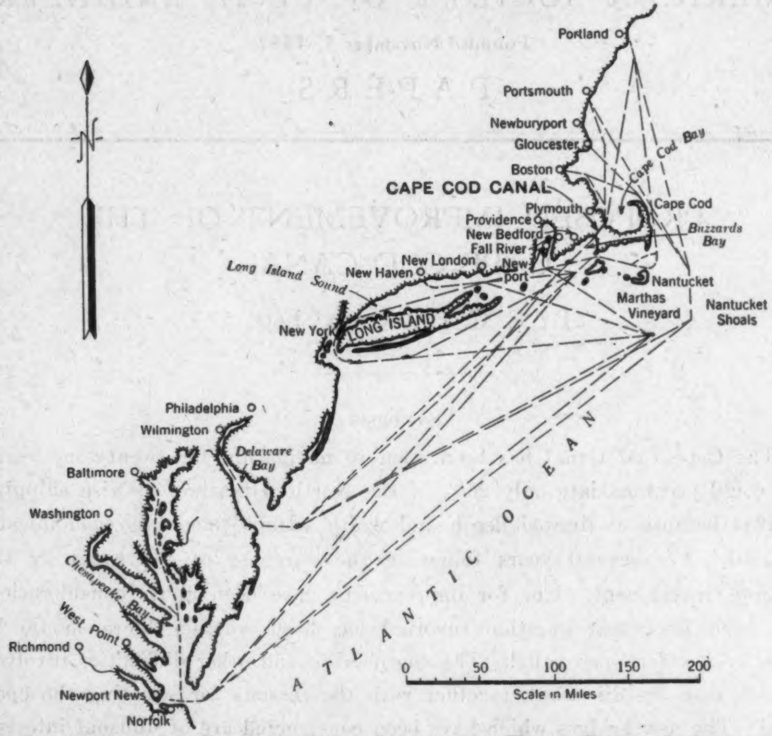

FIG. 1.—CAPE COD CANAL AND OCEAN ROUTES FROM WHICH TRAFFIC IS DRAWN.

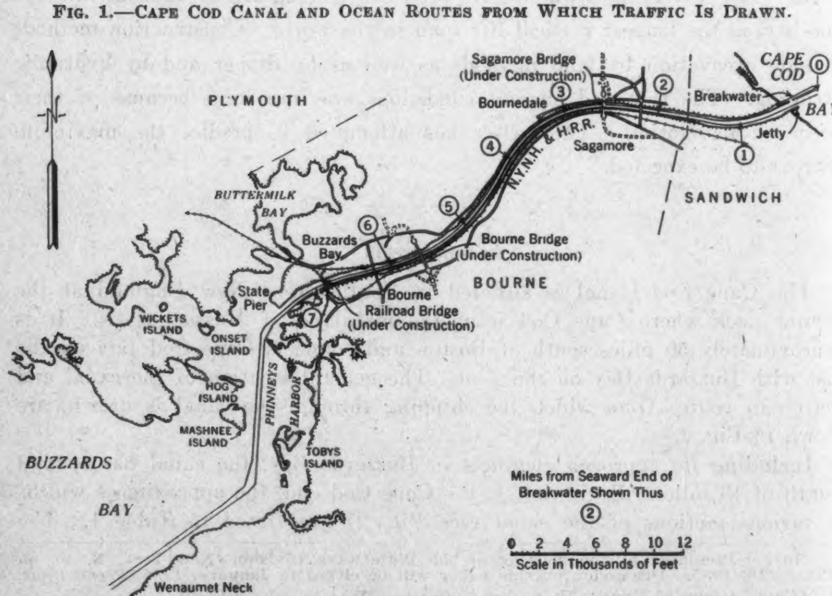

FIG. 2.—GENERAL MAP OF CAPE COD CANAL.

project depth of the canal is 25 ft but this depth has not actually been maintained for several years. At present (1935), the controlling depth is approximately 22 ft.

TABLE 1.—APPROXIMATE CHANNEL WIDTHS

Location	Bottom Width, in Feet		Length of section, in feet
	East end of section	West end of section	
Cape Cod approach	300	300	2 500
Land cut	300	300	2 000
Land cut	300	205	1 000
Land cut to a point west of railway bridge	205	205	35 800
To Buzzards Bay	205	250	200
Through Buzzards Bay	250*	250*	29 000

* At turns, the width is 450 ft.

Until June, 1935, the canal was crossed by three drawbridges, each having a horizontal clearance of 140 ft. Necessarily, these structures limited the effective width of the canal, and it was generally regarded as safe for one-way traffic only—at least as far as the larger vessels were concerned. The new bridges (which are discussed in greater detail elsewhere in this paper) have a horizontal clearance of approximately 500 ft and a vertical clearance of 135 ft.

Historical Summary

The first agitation for a canal across Cape Cod followed the establishment of the old Dutch trading post, shortly after the Pilgrims settled at Plymouth, Mass. It is reported that Miles Standish ascended the Scusset River and then crossed the intervening land to the head-waters of the Monument River, there meeting the Dutch traders from New Amsterdam. The commercial use of this narrow neck of the peninsula dates from that historic time.

As early as 1697, the General Court of Massachusetts adopted a resolution providing for a survey to determine whether or not a canal would be practicable. There is no record of the report, which undoubtedly followed, and it was nearly eighty years later that the Colony of Massachusetts again authorized a study of the problem. The Revolutionary War interfered with the completion of the survey, and, in 1791, another committee was appointed to examine and report on the project.

In 1824, Congress passed an Act directing that surveys be made and the report of Maj. P. H. Perault, U. S. Topographical Engineer, was printed in 1830, after being approved by the State of Massachusetts. The project considered at that time was for a canal having a bottom width of 36 ft and a depth of 8 ft, with locks. It is interesting to note that the general public expected the canal to be built immediately thereafter, and that it was even described abroad as one of the great public work projects about to be undertaken.

In 1860 the canal project was reviewed once more, this time by the Governor of Massachusetts. The Legislature ordered a committee of engi-

neers to report on it, and the resulting document is the first comprehensive report of the entire project.

This Committee suggested a canal with a bottom width of 120 ft and a depth of 18 ft. Although locks were contemplated, it is interesting to note that apparently the members of the Committee were among the first to realize that it might be possible to construct a canal without locks. This suggestion was stated more definitely in 1870 by Brevet Maj. Gen. J. G. Foster, of the Corps of Engineers, U. S. Army, who pointed out at that time, that in spite of the difference in head between the water levels at the two ends of the canal, the resulting currents would not be sufficiently great to require locks.

Subsequently, various charters were granted to individuals or companies that hoped to construct the long discussed canal. It was not until 1883, however, that any earth was actually excavated at the site. Mr. Frederic A. Lockwood, who was something of a mechanical genius, had invented a crude hydraulic dredge. Through his efforts, a company was formed and a channel nearly 1 mile long, 15 ft deep, and about 100 ft wide, was actually dug.

Fortunately, the land for the right of way was obtained at that time, and through the foresight of Col. Thomas L. Livermore it was held until the work was begun in earnest. Had it been permitted to revert to the original owners, there is no question but that the subsequent efforts to obtain a Cape Cod Canal would have found progress hampered by excessive costs for the land involved.

At successive intervals, the Massachusetts Legislature granted other charters to companies which proposed to build the Cape Cod Canal, but it was not until 1904 that financial interests of sufficient strength to carry the project through took an active interest in the work. At that time, Mr. DeWitt C. Flanagan presented the project to the late August Belmont, of New York, N. Y., and obtained a promise of action when the general financial outlook improved.

In 1909, Mr. Belmont decided to begin construction and a construction company was organized for that purpose. The details of the organization, the charter, and the procedure followed, have been well described by the late William Barclay Parsons, Hon. M. Am. Soc. C. E.[2]

Operation Experience

The canal was opened to traffic in 1914, at which time the depth was approximately 15 ft and the bottom width about 100 ft. Traffic never reached the anticipated tonnage, due in part to the fact that the depth was insufficient and in part to the currents existing in the canal, which made navigation hazardous in its narrow width.

During the World War, the operation of the canal was taken over by the Federal Government. Of course, traffic increased greatly during that period because of the fear of German submarines on the outer route. After the World War, the private interests that had built, and formerly operated, the canal refused to accept its return by the United States Government, and

[2] "The Cape Cod Canal", by William Barclay Parsons, M. Am. Soc. C. E., *Transactions*, Am. Soc. C. E., Vol. LXXXII (1918), p. 1.

efforts were made to persuade Congress that it should be purchased with Federal funds. After protracted negotiations and condemnation proceedings, Congress finally authorized its purchase by the United States for the sum of $11 500 000 in January, 1927.

Prior to acceptance by the United States, dredging to the full project dimensions was required so that a bottom width of 100 ft and a depth of nearly 25 ft were available throughout.

From 1928, when the Government assumed ownership, to the present time (1935) more than $1 000 000 has been spent in maintenance dredging, but the material removed is believed to have come primarily from the banks of the canal. Apparently, there has never been any tendency for sand to enter the canal at either end.

Modern Widening Operations

Since 1933, funds have been available for further widening at the bends and a 70-ft cut was completed early in December, 1934. Subsequently, two large dredges made an additional 35-ft cut into the south bank. The canal now (1935) has a bottom width of 205 ft throughout and a controlling depth of approximately 22 ft. (At the old bridge locations it has been impossible to obtain the full 205-ft bottom width for the time being. That work will be done when the old bridges have been removed.)

The canal is used by a large volume of shipping, both passenger and freight, as well as the slow-moving tows of barges. Some conception of the volume of shipping can be obtained from the record for 1934, which totaled 2 792 000 cargo tons and 11 500 vessels.

Why Improve the Canal?

There are two principal reasons for considering further improvement of the Cape Cod Canal. In the first place, the hazards of the outside route around Cape Cod are well known and by many are considered more serious than those of Cape Hatteras. These dangers may be classified under a number of different headings, as follows: Exposure, lack of refuge, shoals, zigzag courses, currents, storms, ice, and fogs.

In attempting to round Cape Cod a vessel is necessarily exposed to the elements from the time it leaves the vicinity of Martha's Vineyard to Provincetown, a distance of nearly 100 miles, and there is little or no shelter provided by the low-lying land of the Cape itself. Practically all the seriously dangerous storms in the vicinity come from either the northeast or the southwest, and the course followed is especially exposed to northeast storms. In contrast with the route through the Cape Cod Canal, which is sheltered for approximately 60% of the distance between New York and Boston, the outside route involves an equal percentage of the journey without any shelter.

There are absolutely no harbors of refuge along the outside route. Provincetown might be so regarded, but the harbor is open to the southwest storms and, therefore, is not an adequate harbor of refuge. Other minor harbors offer only 15-ft depths so that they cannot be used by the modern larger sea-going barges, motor ships, and steamers.

The shoals on the outer route have long been known to be particularly dangerous because of their shifting character and the impossibility of maintaining a straight channel through them. Although there is some shoaling in the canal itself, maintenance dredging has been sufficient to preserve a reasonable project depth, and there is every reason to believe that, when the banks have been properly riprapped, the constant shoaling that now occurs will greatly decrease.

Much has been heard of the currents in the Cape Cod Canal itself, and it is sometimes forgotten that the tidal currents over the shoals east of Cape Cod although comparatively weak, often change in direction and make the following of a given course, under some conditions, difficult indeed. At certain places on the outside route a rotary current, with a velocity of approximately 2 knots, has been observed. In the vicinity of Chatham, where it is necessary for the ships rounding the Cape to follow a zigzag course, the tidal currents are especially strong and hazardous to navigation.

In view of the foregoing difficulties, it should be obvious that fog offers a far greater hazard to vessels on the route around Cape Cod than to ships well away from land on the open sea. Furthermore, careful study extending over a long period of years has shown that the fogs on the outside route in the vicinity of the Atlantic Ocean are more frequent and of longer duration than those in the vicinity of Buzzards Bay and the Cape Cod Canal.

In navigating the shoals in Nantucket Sound it is necessary to follow a zigzag course, the angles of which at times exceed 90 degrees. During recent years a straighter channel has been dredged by the Corps of Engineers from Stonehorse Lightship northeast to the slue between Pollock Rip Shoal and Bears Shoal. Although this route is somewhat shorter and less tortuous than the outer one, it still involves several changes in direction which, in time of thick fog, means hazardous navigating.

Ice conditions are not usually such as to offer an obstacle to easy navigation, but there are occasionally very severe winters when the ice floes reach large proportions. At such times the shoal areas in the narrow channels are likely to be covered with large ice floes which introduce added hazards to the outside route. It is true that the very shallow, northern part of Buzzards Bay is even more likely to freeze, with resulting dangers to navigation. However, the proposed new straight channel will obviate much of this difficulty, and it is certain that if ice must be encountered, it is far better to grapple with it in the protected waters of Buzzards Bay than in the broader stretches of the outside route.

The outside route, furthermore, is exposed to the full fury of the northeast storms that sweep across the Northern Atlantic. These storms are widely known as among the most severe to occur on any of the oceans of the world, and the loss of property and lives that has resulted during many years past testifies to their destructive power. For example, the records of wrecks for many years past is mute evidence of the dangers of the outside route. Although the data available do not include full information as to cargo actually lost, or even as to the number of lives, the evidence is sufficiently

complete to indicate that the annual cost has been approximately $500 000, and that the number of lives lost has averaged at least 15 annually.

Commercial Reasons

In addition to the desirability of saving lives and avoiding the losses due to wrecks, there are other more definitely commercial aspects of the problem. At present (1935), the value of the shipping that passes through the canal is only a little more than one-fifth of that which might do so if ships were provided with a reasonable depth and freedom from the present hazards of canal navigation.

The traffic available, which might use the canal, can best be shown by reference to the record of coastwise cargoes entering and leaving the Port of Boston. In 1933, this amounted to 12 300 000 tons, whereas the cargo tonnage

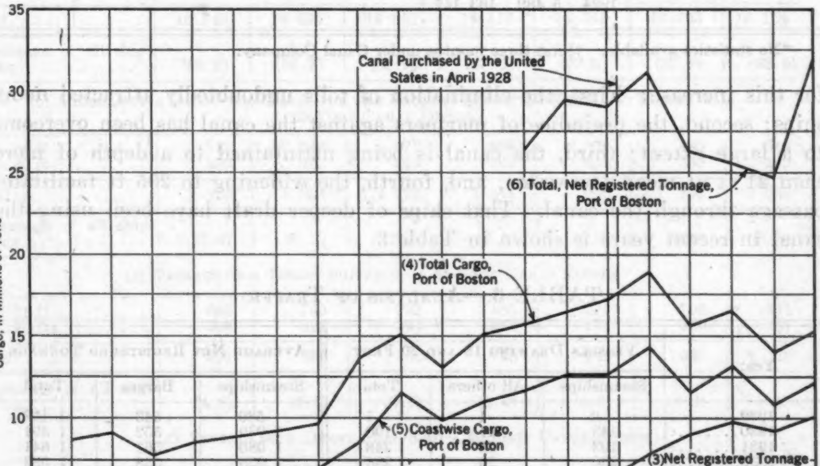

Fig. 3.—Commerce Through and Around the Cape Cod Canal.

through the canal was only 2 804 000 tons. Fig. 3, with Table 2, presents the record[3] of passages through the canal from the date of its opening to, and including 1934.

The canal was in operation only two years before the World War. When it first opened, late in 1914, it was not completed to full project dimensions and attracted only a small volume of traffic (see Curve 1, Fig. 3). During the war, many ships used the canal to avoid the submarine dangers of the outside route. The increase continued until 1920, after which traffic dropped until 1928. In April, 1928, the canal was taken over by the Federal Government.

[3] H. R. Doc. No. 795, 71st Congress, 3d Session.

The volume of traffic then rose rapidly, reaching a peak in 1930, so far as the number of ships are concerned (see Table 2). However, both gross and net registered tonnage have increased steadily in recent years, except for the one year, 1932 (see Fig. 3, Curves 2 and 3). There appear to be several reasons

TABLE 2.—TRAFFIC THROUGH THE CAPE COD CANAL

Year (1)	Number of: Vessels (2)	Number of: Passengers (3)	Year (1)	Number of: Vessels (2)	Number of: Passengers (3)	Year (1)	Number of: Vessels (2)	Number of: Passengers (3)	Year (1)	Number of: Vessels (2)	Number of: Passengers (3)
1914	582	*	1919	7 452	112 128	1925	5 010	160 184	1930	11 464	253 727
1915	2 685	*	1920	8 140	119 088	1926	5 259	166 787	1931	11 291	230 707
1916	4 635	139 917	1921	7 013	112 731	1927	5 745	202 849	1932	10 417	189 275
1917	3 330	117 109	1922	7 180	113 318	1928†	9 312	231 426	1933	11 022	178 642
1918	4 738	81 998	1923	6 771	116 309	1929	10 317	232 824	1934	11 516	201 520
			1924	5 489	133 117						

*No statistics available. †First three months under Canal Company.

for this increase: First, the elimination of tolls undoubtedly attracted many ships; second, the prejudice of mariners against the canal has been overcome to a large extent; third, the canal is being maintained to a depth of more than 21 ft at mean low water; and, fourth, the widening to 205 ft facilitates passage through the canal. That ships of deeper draft have been using the canal in recent years is shown in Table 3.

TABLE 3.—ANALYSIS OF TRAFFIC

Year	Vessels Drawing 18 and 20 Feet: Steamships	Vessels Drawing 18 and 20 Feet: All others	Vessels Drawing 18 and 20 Feet: Total	Average Net Registered Tonnage: Steamships	Average Net Registered Tonnage: Barges	Average Net Registered Tonnage: Total
1929........	0	1	1	580	543	1 123
1930........	143	47	190	1 039	552	1 591
1931........	193	55	248	1 080	561	1 641
1932........	260	26	286	1 025	558	1 583
1933........	492	21	513	1 083	550	1 633

It is evident that, to a large extent, mariners have ceased to fear the canal. Furthermore, the widening to 205 ft has attracted shipping, and it is logical to assume that any further improvement would attract still more traffic.

More than 80% of the total coastwise trade in and out of the Port of Boston passes around or through the Cape Cod Canal. Furthermore, most of the coastwise traffic passing Cape Cod is with the Port of Boston. Curves 4, 5, and 6, Fig. 3, show commerce in the Port of Boston for the years indicated.[4] The general trend during the years 1929 to 1933 is similar to that found in the case of the Cape Cod Canal.

A large volume of traffic which might use the canal still passes around Cape Cod. Some of it could use the canal at present. Other traffic is unable to use it because of its limiting depths. Table 4 shows the draft and number of trips for vessels entering and leaving Boston Harbor during the calendar

[4] H. R. Doc. No. 795, 71st Congress, 3d Session, p. 19.

years, 1927 to 1933, inclusive. Fig. 4 illustrates the relation between drafts and the capacities of vessels entering and leaving Boston Harbor in the years 1929 and 1933.

TABLE 4.—SUMMARY OF THE DRAFT AND NUMBER OF TRIPS OF VESSELS, DOMESTIC AND FOREIGN, ENTERING AND LEAVING BOSTON HARBOR DURING THE CALENDAR YEARS, 1927 TO 1933. (ARRIVAL AND DEPARTURE COUNT AS SEPARATE TRIPS.)

Draft	1927	1928	1929	1930	1931	1932	1933
(*a*) VESSELS OF A DRAFT SUITED TO THE PROJECT DEPTH (25 FEET) OF THE PRESENT CANAL							
Less than 18 ft..........	13 338	10 655	10 528	10 090	9 732	9 690	11 499
18 to 20 ft..........	2 115	2 548	2 648	2 664	2 320	2 305	2 283
20 to 22 ft..........	1 296	1 419	1 475	1 356	1 290	1 268	1 186
Total..........	16 749	14 622	14 651	14 110	13 342	13 263	16 154
Percentage of all shipping..........	(89.6)	(87.7)	(87.0)	(87.6)	(87.0)	(87.9)	(88.9)
(*b*) VESSELS OF A DRAFT TOO GREAT FOR THE PROJECT DEPTH (25 FEET) BUT SUITED TO A 30-FOOT CANAL DEPTH							
22 to 24 ft..........	512	546	677	679	522	480	610
24 to 26 ft..........	500	485	513	462	438	369	450
Total..........	1 012	1 031	1 190	1 141	960	849	1 060
Percentage of all shipping..........	(5.4)	(6.2)	(7.1)	(7.1)	(6.3)	(5.6)	(5.8)
(*c*) VESSELS OF A DRAFT SUITED TO A 35-FOOT CANAL DEPTH							
26 to 28 ft..........	685	743	727	580	671	705	863
28 to 30 ft..........	206	193	233	218	275	240	267
Total..........	891	936	960	798	946	945	1 130
Percentage of all shipping..........	(4.8)	(5.6)	(5.7)	(5.0)	(6.2)	(6.3)	(6.2)
(*d*) VESSELS OF A DRAFT SUITED TO A 40-FOOT CANAL DEPTH							
30 to 32 ft..........	15	48	28	39	74	30	8
32 to 35 ft..........	18	28	8	12	2	1	0
Total..........	33	76	36	51	76	31	8
Percentage of all shipping..........	(0.2)	(0.5)	(0.2)	(0.3)	(0.2)	....	....
(*e*) VESSELS OF A DRAFT TOO GREAT FOR SAFETY WITH A 40-FOOT DEPTH, EXCEPT WITH FAVORABLE TIDES							
More than 35 ft.......	6	2	7	4	2	1	0

The increase in canal passages for 1933 was 605 vessels (see Table 2), whereas the increase in shipping around Cape Cod during the same period was 350 vessels. Of the total increase, 955 vessels (63%) went through the canal and 37% went around Cape Cod. Reference to Table 5 will show that commerce is using larger vessels. A table for Boston Harbor similar to Table 5 gives approximately equivalent results. With the increase in size and draft of ships, a demand for an increase in the depth of the canal may be expected.

It is apparent from the foregoing that the popularity of the Cape Cod Canal is increasing rapidly and that the commerce which now uses the canal,

as well as that which may use it in the future, is growing in volume. It is unquestionably significant that in 1933 supposedly one of the worst years of the depression, net registered tonnage passing through the Cape Cod Canal

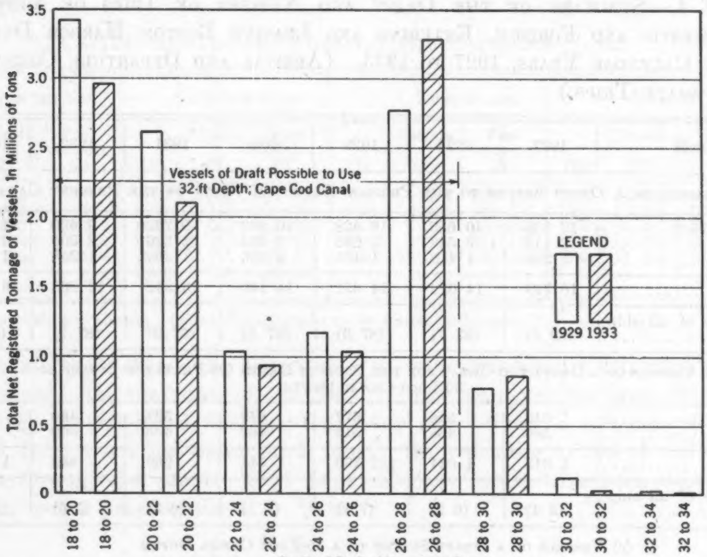

FIG. 4.—DRAFTS AND CAPACITIES OF VESSELS ENTERING AND LEAVING BOSTON HARBOR.

was the greatest in its entire history, except for a short period during the World War when the fear of submarines forced all ships that could do so to use the canal. When it is remembered that the net registered tonnage enter-

TABLE 5.—AVERAGE NET REGISTERED TONNAGE OF VESSELS PASSING THROUGH CAPE COD CANAL

Type of vessel	1929	1930	1931	1932	1933
Steamships . . .	900	1 190	1 350	1 138	1 365
Motorships . . .	90	100	121	137	148
Barges	720	770	810	790	752

ing and leaving the Port of Boston was likewise at an all-time high in 1933, and that much of this commerce will use the canal as soon as it is improved, the future usefulness of that waterway is seen to be unquestionable.

On account of the great diversity of freight and of kinds of ships involved, it would be difficult to make an accurate estimate of the savings to shippers using the canal. However, it is known that the total coastwise cargo in and out of Boston during 1933 was 12 250 000 tons. Approximately 80% of this total will probably use the canal when adequate improvements have been made.

Only 2 805 000 cargo tons were passed through the canal in 1933, leaving 6 995 000 tons which might have gone through. The total costs of all improvements contemplated, including the new bridges, is estimated at about \$31 075 000. At 3%, the annual interest charges would be \$932 000, and this is only 13 cents per cargo ton, or 0.20 cent per ton-mile, even on the basis of commerce during a depression year. (The saving in distance by using the canal is taken as 65 miles. It is true that a small portion of the coastwise tonnage in and out of Boston may never use the canal. However, any decrease in the possible economic benefits derived on that account would probably be more than counterbalanced by coastwise tonnage particularly coal and petroleum products, to ports north of Boston, and by the fact that a large proportion of the ships using the canal will save more than 65 miles in distance traveled). In recent years, the average vessel has been about 1 200 net registered tons, of which the cargo is approximately 45 per cent. This would mean an average cargo of 540 tons, and at 13 cents per ton the cost chargeable to each vessel would be about \$70 per passage. Fuel costs alone for steamers would probably be between \$50 and \$200, depending on the ship, for the additional distance involved if the canal were not used. For large tows the saving in fuel by use of the canal route would be less, but for them the safety of that route is of even greater importance.

In considering the project as a whole and not merely the justification for the proposed improvement, it would be necessary to include in the total economic benefits the annual losses by wrecks on the passage around Cape Cod. This has averaged more than \$500 000 over a period of several years.

The Problem of Improving the Canal

Hearings held in 1934 and earlier, as well as repeated contacts with masters of ships and pilots by officers and civilian employees on duty in Boston and at the canal, make it possible to state the nature of the improvement desired by interests using the canal. Briefly, it is that the channel should be deepened and widened to permit two-way traffic and that the width should be sufficient to remove the risk of being caught during a falling tide with the bow of the ship on one bank and the stern on the other; or, that the canal should be widened somewhat so as to permit two-way traffic and that locks should be installed in order to still the currents, thereby removing the risk of stranding a vessel cross-wise in the channel.

In considering this aspect of the problem, it is necessary to keep in mind the fact that there are two quite different classes of shipping which use the canal. They are the motor and steam ships on the one hand and the tows of barges on the other. In recent years, the importance of the latter has considerably diminished due to the utilization of powerful motor barges for a large part of the traffic. The shipping that operates under its own power may be further subdivided into the fast passenger-carrying vessels and the slower freight carriers, including motor barges.

The passenger carriers are naturally interested in making the passage as rapidly as possible since they operate on a schedule which gives them little

or no allowance for delays. The interests involved desire the improvement to be along the lines first mentioned (that is, without locks) in order that these ships may lose a minimum of time. The slower freight ships, including the motor barges, are not so concerned about maintaining time schedules and, therefore, would not be so strongly opposed to a lock canal, provided there was sufficient width throughout for two-way traffic. The barge proportion of the traffic, which is steadily declining in importance and now constitutes less than one-third the registered tonnage, travels at an even slower rate. It is possible that, on the average, a lock canal might somewhat reduce their time of passage. However, time is of less importance to them than to the other classes mentioned and, although the somewhat faster current in a 500-ft canal might make it necessary for tows to wait for a favoring tide, or else be taken through one barge at a time, it is certain that those tows which had the power could move on through regardless of currents. (At present (1935), even these tows must break up and go through one barge at a time because of the narrow width and the difficulty of keeping tows in line.) Furthermore, favorable currents would be encountered at least 50% of the time, and tows could proceed through without breaking up if the canal were wide enough to permit maneuvering when necessary. It has been reported that no new barges have been constructed for several years and that the trend is emphatically toward the use of motor ships. Obviously, too much consideration must not be given to a class of shipping that is becoming obsolete, which is a decreasing fraction of the whole, and which should benefit substantially under either type of improvement in any case.

The project dimensions on which the estimates are based are a depth of 32 ft and widths of 250 ft and 540 ft for the lock and open canal, respectively. This particular depth was selected because it will accommodate practically all the vessels now entering and leaving the Port of Boston which may be expected to use an improved canal. Taking into consideration the number of ships of the different drafts and their cargo capacity, it is found that this is the economic depth. That such is the case is readily seen by reference to Fig. 4, where the cargo-carrying capacity of vessels entering and leaving Boston Harbor is shown for each of several drafts. (There should be at least 4 ft of over-depth to allow for minus tides, for "squat" in a restricted channel, and for the fact that the channel bottom will not be soft material, but will be thickly strewn with boulders.) It is apparent that a depth of 30 ft would not be sufficient for the relatively large volume of cargo carried in vessels having a draft of from 26 to 28 ft, whereas 32 ft would be deep enough for these ships. The additional 2 ft of depth gives a great increase in cargo-passage capacity. On the other hand, it is equally apparent that a further increase in depth—say, to 35 ft—would result in only a small increase in cargo-passage capacity and that it would not be economically justified at this time. A width of 540 ft is considered desirable for the open canal for reasons already mentioned, and in order that the further deepening to 40 ft at some future time may be made, giving a bottom width of 500 ft, without disturbing the side slopes and bank protection.

THE LOCK *Versus* AN OPEN CANAL

Since the publication of H. R. Document No. 795, important new information has been obtained and experience has been gained which necessitates a revision of earlier ideas. New factors to be considered are: (1) Ice; (2) pile-driving; (3) excavation costs; (4) storms; (5) currents; (6) shoaling; (7) delays in passing through locks; and (8) dredging difficulties.

(1).—Ice.—The most important new development was the experience with ice conditions during the winter of 1933–34. The conditions of that period proved definitely that great difficulty would be experienced from time to time in a still-water canal. There appears to be no practicable means of avoiding ice under those conditions, and it would be most undesirable to have the canal closed for an extended period during the winter months when presumably it would be most needed because of storm hazards on the outside route.

(2).—Pile-Driving.—Another development of primary importance is the experience with the foundations for the new bridges. Great difficulty was encountered in driving the steel sheet-piling to grade because of boulders. Presumably, cut-off walls of sheet-piling would be required under the lock walls and miter-sills in order that the locks might be unwatered when necessary to make repairs. It is now believed probable that the difficulties encountered in driving such walls of sheet-piling would be extremely expensive to overcome and that the cost of locks would be increased materially for this reason.

(3).—Excavation Costs.—Apparently, the possibility of making a 500-ft canal was not previously given much consideration because of the high costs for earth removal which were formerly used as a basis for estimates. In view of the contract dredging completed in 1934, and because of the acquisition of new equipment, including very large dipper dredges (one with a capacity of 26 cu yd began working at the canal in December, 1934), it appears that costs will be lower than was considered possible a few years ago. Furthermore, there is the possibility of still further lowering excavation costs by doing a substantial portion of the work in the dry.

(4).—Storms.—Recent experience has shown conclusively that the difficulties of navigation and the hazards peculiar to the canal have been primarily due to the narrow width. Considered solely from the viewpoint of navigability, it is believed that the 500-ft open canal will be definitely superior to a 250-ft or a 300-ft lock canal. One of the hazards which will exist in either case is the fog that is frequently found in that vicinity (although not so frequently as on the route around Cape Cod). The 500-ft open canal will allow ample room for passing ships even under the worst conditions, permitting the movement of vessels. Likewise, the strong northeast gales that accompany the severe storms in this region, should be considered. In a lock canal, some difficulty would probably be experienced, especially in the case of the larger ships when loaded lightly. Because it is necessary to approach a lock very slowly, a ship would be less responsive to its rudder, and the force of the wind would be more effective. On the other hand, the most severe gales would introduce no hazard to navigation in a 500-ft open canal.

(*5*).—*Currents*.—Although it has been assumed, to be on the safe side, that currents in the 500-ft canal will be increased in accordance with accepted hydraulic formulas, the actual currents found when the improvement is made will probably be somewhat less. It appears that the volume of water passing through the 100-ft canal has somewhat affected the level of the water in Buzzards Bay, with consequent reduction of the difference between the water levels at the ends of the canal. It is only reasonable to suppose that the volume of water passing through a 500-ft canal, about five times as much, will affect the water level in Buzzards Bay to an even greater extent. The result will be to reduce the head, or the difference in level at the two ends of the canal, thereby diminishing the currents.

(*6*).—*Shoaling*.—Further study of the erosion that has occurred in the 100-ft channel, and the consequent shoaling which requires maintenance dredging, leads to the belief that most of the shoaling has been due to wave wash on the banks and the resulting caving in of large quantitites of sand. It follows that adequate bank protection in the form of rip-rap can be expected to remedy this situation. In any event, the wave wash in a 500-ft canal will be less than in the old 100-ft width. Any hazards to navigation due to shoaling and the maintenance dredging made necessary thereby will probably be of no importance in a 500-ft canal.

(*7*).—*Delays in Passing Through the Locks*.—In addition to the foregoing, there are several factors which make the lock canal less desirable. The delays incident to passage of the locks would be most objectionable to the fast passenger-carrying ships. The only shipping that would be delayed at all in the case of an open canal would be that portion of the tug-and-barges combinations, or tows, which lacked power to move against the current. However, this traffic moves slowly at best, and saves twelve or thirteen hours by using the canal. Inasmuch as the average delay involved would be less than two hours, and since the currents would expedite passages when favorable, it is clear that what the tows gained by a lock canal would be more than offset by delay to more important shipping which constitutes the largest and a growing portion of the whole. Still another consideration is that locks are vulnerable to attack in the event of war, whereas an open 500-ft canal could scarcely be blocked for any long period.

(*8*).—*Dredging Difficulties*.—A few years ago it was feared that it would be impossible to dredge in the 100-ft open canal, but this can now be forgotten, inasmuch as the canal has been widened to 170 ft throughout its length, and dredging has started on a further widening to 205 ft minimum width. Apparently, the prevention of shoaling is largely a question of proper bank protection against wave wash and that would be necessary in either type of canal.

The alternate plans of improvement which it was finally decided to consider in detail are the project recommended in H. R. Document No. 795, but with twin locks, *versus* an open canal of adequate width to eliminate the hazard of grounding across the channel during a falling tide. Estimates of cost are given in Table 6. As a result of the studies made, it is believed that

TABLE 6.—COST ESTIMATES, CAPE COD CANAL, 1934

Location (1)	Excavation, in cubic yards (2)	Flow measure (3)	Unit costs, in cents per cubic yard (4)	Total cost (5)
(a) Lock Canal, 32 by 250 Feet, Twin Locks at Station 72 (See Fig. 2)				
Prism Excavation, Including 1-Ft Over-Depth at Cape Cod Bay to Locks and 3-Ft Over-Depth from Locks to 32-Ft Contour in Buzzard's Bay:				
Cape Cod Bay to locks	3 300 000	In place	25	$825 000
Locks to Station 400 (see Fig. 2)	7 240 000	In scow	45	3 258 000
Station 400 to Wings Neck	12 438 000	In scow	45	5 597 000
Wings Neck to 32-ft contour	1 146 000	In scow	45	516 000
Sub-total	(24 124 000)	....	....	$10 196 000
Locks complete	....	....	....	11 500 000
Other Items:				
Buildings, real estate, dolphins, water supply, highway, wind break, closing dam, etc.	....	....	....	600 000
Bank protection	....	....	....	1 516 000
Lighting	....	....	....	100 000
Sub-total	....	....	....	$23 912 000
Engineering and contingencies, 15%	....	....	....	3 587 000
Total	....	....	....	$27 499 000
(b) Open Canal, 32 by 540 Feet				
Dredging, Including 1-Ft Over-Depth from Cape Cod Bay to Station 60 (see Fig. 2) and 3-Ft Over-Depth from Station 60 to 32-Ft Contour in Buzzard's Bay:				
Cape Cod Bay to Station 60 (see Fig. 2)	3 786 000	In place	25	$946 000
Station 60 to Station 400 (see Fig. 2)	17 446 000	In scow	45	7 851 000
Station 400 to Wings Neck	12 438 000	In scow	45	5 597 000
Wings Neck to 32-ft contour	1 146 000	In scow	45	516 000
Sub-total	(34 816 000	....	....	$14 910 000
Excavation in the dry, from Station 60 to Station 400	(8 785 000)	In place	25	2 196 000
Sub-total	....	....	....	$17 106 000
Other Items:				
Mooring basins and harbor of refuge	....	....	....	320 000
Bank protection	....	....	....	1 516 000
Lighting	....	....	....	100 000
Land takings, administration buildings, etc.	....	....	....	900 000
Railway and highway relocations	....	....	....	208 000
Sub-total	....	....	....	$20 150 000
Engineering and contingencies, 15%	....	....	....	3 022 000
Total	....	....	....	$23 172 000
(c) Harbor of Refuge at Buzzard's Bay				
Dredging East Mooring Basin to 32-ft depth, with a 1-ft over-depth allowance	567 000	....	25	$142 500
Dredging West Mooring Basin to 32-ft depth, with a 3-ft over-depth allowance	266 000	....	45	120 000
Dredging channel into Onset Bay to 15-ft depth, 100 ft wide, with a 1-ft over-depth allowance	78 000	....	45	35 000
Mooring dolphins, East Basin	(30 each)	....	(500)	15 000
Mooring dolphins, West Basin	(15 each)	....	$(500)	7 500
Total	....	....	....	$320 000
(d) Bank Protection				
One-man stone	175 150	....	($7)	$1 226 000
Crushed rock, or quarry spalls	58 000	....	($5)	290 000
Total	....	....	....	$1 516 000

a large part of this excavation, approximately 8 785 000 cu yd, can be done in the dry at a great saving in cost. If funds were made available only in small sums over a long period, it would probably be best to widen by dredging alone, but if the project is adopted and funds are made available so that the work can be done in the most efficient manner, a saving of approximately $2 703 000 may be expected. On this basis, the open canal would be $4 327 000 less expensive than the lock canal.

Other Features of the Improvement

In addition to the deepening and widening, other minor betterments should be provided. The additional volume of shipping anticipated will require enlargement of existing facilities and other work which is discussed briefly herein.

At times, during northerly or northeasterly gales, Cape Cod Bay becomes so rough that tows and smaller craft are unable to continue the voyage out of the canal. Therefore, it will be necessary to provide a mooring basin where vessels thus delayed may tie up until such time as they can proceed with safety. Such a mooring basin should be about 2 000 ft long and extend inshore about 300 ft from the edge of the channel (see Fig. 5). Each end of the mooring basin should be tapered so that the width required (200 ft) is reached in a distance of from 300 to 500 ft. It is planned that additional model experiments will be undertaken, and that one object of the investigation will be to ascertain what size, shape, and location of mooring basin will result in the least interference with navigation through its effects on currents and shoaling.

There are no special difficulties due to weather at the Buzzards Bay end of the canal. The waters are protected and are safe for all but the smaller craft. However, at times, it is necessary to tie up tows at that end while the tug traverses the canal with part load. A mooring basin will be needed to accommodate this traffic, and would occasionally be useful to other vessels in foggy weather. Such a basin should preferably be located northeast of Hog Island and southeast of the new straight channel. It should be about 1 000 ft long and 300 ft wide, with ends tapered. Mooring facilities should be provided.

A harbor of refuge should be provided at the Buzzards Bay end of the canal for smaller craft. For this purpose, a 15-ft channel into Onset Bay would be suitable. The estimated cost of this improvement is listed in Table 6(*c*).

Lighting.—The present lighting system in the canal consists of a series of 60 cp electric lights on piles, spaced 500 ft apart. The alignment is very poor due to erosion of the banks. This system does not meet requirements during adverse weather, because of low visibility. A system of lights should be installed which may be increased in intensity during foggy weather, or while there is vapor in the canal. The lights should be about 25 ft above the water level on poles spaced 300 ft apart. Colored lights placed at critical places in the canal may be used to indicate curves and bridges. The estimated cost of such an installation is $100 000.

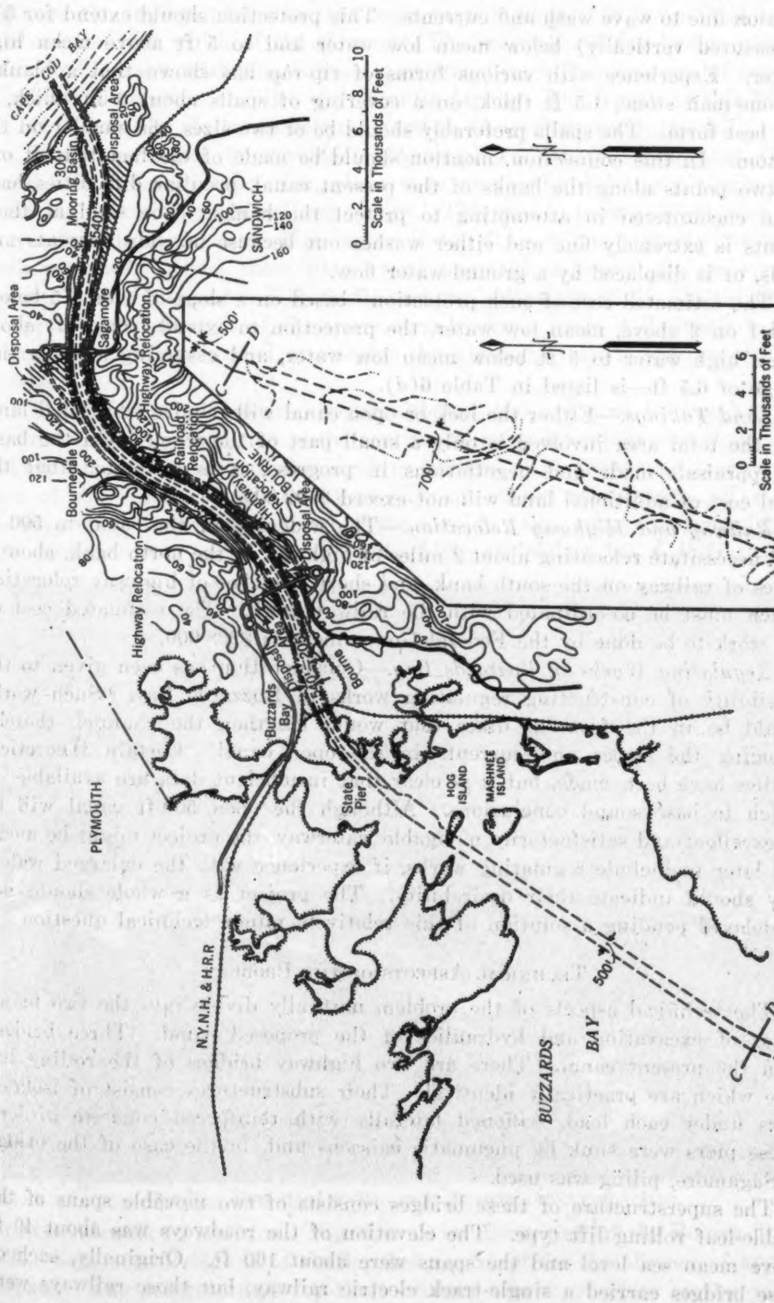

FIG 5.—PROPOSED IMPROVEMENT, CAPE COD CANAL

Bank Protection.—It will be necessary to protect the canal banks against erosion due to wave wash and currents. This protection should extend for 5 ft (measured vertically) below mean low water and to 5 ft above mean high water. Experience with various forms of rip-rap has shown that a blanket of one-man stone, 1.5 ft thick, on a covering of spalls about 6 in. thick, is the best form. The spalls preferably should be of two sizes, the smaller on the bottom. In this connection, mention should be made of the fact that at one or two points along the banks of the present canal, peculiar difficulties have been encountered in attempting to protect the banks. The sand at these points is extremely fine and either washes out because of eddy currents and boils, or is displaced by a ground-water flow.

The estimated cost of such protection—based on a slope of 1 on 2.5 below, and 1 on 2 above, mean low water, the protection to extend from 5 ft above mean high water to 5 ft below mean low water, and assuming a mean tide range of 6.5 ft—is listed in Table 6(*d*).

Land Takings.—Either the lock or open canal will require additional land, but the total area involved is only a small part of the whole. On the basis of appraisals made and negotiations in progress, it is estimated that the total cost of additional land will not exceed $592 000.

Railway and Highway Relocation.—The widening of the canal to 500 ft will necessitate relocating about 2 miles of highway on the north bank, about 3 miles of railway on the south bank, and short stretches of highway relocation which must be co-ordinated with the railway work. The estimated cost of the work to be done by the Federal Government is $208 000.

Regulating Works in Buzzards Bay.—Consideration has been given to the possibility of constructing regulating works in Buzzards Bay. Such works would be in the form of dikes that would lengthen the channel, thereby reducing the slopes and currents in the open canal. Certain theoretical studies have been made, but it is clear that insufficient data are available on which to base sound conclusions. Although the open 500-ft canal will be an excellent and satisfactorily navigable waterway, the project might be modified later to include regulating works, if experience with the enlarged waterway should indicate their desirability. The project as a whole should not be delayed pending a solution of this relatively minor technical question.

Technical Aspects of the Problem

The technical aspects of the problem naturally divide into the two major items of excavation and hydraulics of the proposed canal. Three bridges span the present canal. There are two highway bridges of the rolling lift type which are practically identical. Their substructures consist of isolated piers under each load, stiffened laterally with reinforced concrete girders. These piers were sunk by pneumatic caissons and, in the case of the bridge at Sagamore, piling was used.

The superstructure of these bridges consists of two movable spans of the double-leaf rolling lift type. The elevation of the roadways was about 40 ft above mean sea level and the spans were about 160 ft. Originally, each of these bridges carried a single-track electric railway, but those railways were

abandoned long ago and the tracks have been removed. The clearance between the fenders protecting the main piers is about 140 ft and this is the present limiting width of the channel. The existing railway bridge consists of a double-track, trunnion, bascule superstructure. The piers are of conventional solid concrete on piles with granite facing. The length of this bridge is 160 ft and the clearance between fenders is approximately 140 ft.

When the major improvements contemplated for the Cape Cod Canal were first under consideration, plans were prepared involving a single combination of highway and railway bridge. This was to have a 550-ft span and a vertical clearance above high water of 150 ft; a 6-lane highway for traffic was provided. Since those plans were prepared, however, the substantial growth in summer automobile traffic and the obligation of the United States to protect the interests of the towns near-by, have made it desirable to construct two bridges instead of one for the highways, and a separate railroad bridge.

The highway bridges are similar although the one near Bourne has four approach spans, in addition to the continuous truss extending over three spans which is found in each of the highway bridges. The three-span trusses used are of the Warren continuous type with an arched center span. The floor is supported on the upper chord of the outside spans and is suspended below the arched center spans. Each of the highway bridges has a 40-ft roadway

FIG. 6.—NEW BOURNE HIGHWAY BBIDGE AND APPROACHES.

and a sidewalk in addition. Fig. 6 is an excellent view of the Bourne Bridge. The Sagamore Bridge is of similar design, except for the absence of approach spans. The substructures for these bridges consist of piers having massive

concrete bases with two concrete shafts connected at the top by a concrete diaphragm. The concrete shafts are heavily reinforced and the end abutments are hollow reinforced concrete, with massive pylons.

In the case of the channel piers, coffer-dams were constructed, and, at first, it was expected that the piers would rest on the natural soil. However, due to the fact that there was difficulty with boulders and that it was almost impossible, therefore, to drive the steel sheet-piling as deep as originally intended, and because of the action of the saturated sand under the unequal pressures existing during construction, piles were used in the case of three of the four highway channel piers. They were driven in the wet, but even under those circumstances considerable difficulty was encountered with the blowing in of sand, because the foundation material lacks any substantial quantity of binder, such as clay.

The approaches to these highway bridges are by way of traffic circles at each end, except at the south end of the Sagamore Bridge. A special underpass has been constructed in the approach to the north end of the Bourne Bridge. The railway bridge (see Fig. 2) is the longest vertical lift bridge in the world, with a 544-ft span between end bearings. The towers are 265 ft high, and the vertical clearance of the bridge in the raised position, of course, is the same as in the case of the highway bridges, namely, 135 ft. The truss itself is of the Warren type with vertical members, the trusses being 27 ft, center to center.

This bridge is raised and lowered by four 150-hp induction motors, two of which are used to drive, and two to synchronize, the movement of the two ends of the truss. In addition, emergency motors are provided and emergency gasoline generator sets furnish energy if the commercial power facilities fail.

This structure is the first of this type in the United States to be equipped with roller bearings. Under ordinary operating conditions, it is raised or lowered through 130 ft in approximately 2 min. The bridge is normally in the raised position in contrast with the older bridge, which is normally down and has to be raised as ships approach. Parenthetically, it may be mentioned that this feature will greatly lessen the possibility of a ship striking the bridge. Ship captains will expect to find it up and when they to not find it in the raised position it is to be expected that they will take the necessary precautions to insure that the current will not sweep them into the bridge before it can be raised. Under present conditions, it is normally expected by the ship's captain that the bridge will be raised as he approaches. Consequently, when there have been difficulties with the operating mechanism, this fact has not been realized by the master of an approaching ship until too late to prevent the bridge being struck if the current made it impossible to stop within a short distance.

A few of the difficulties encountered in constructing the new bridges are of special interest. In the first place, the number of boulders which are found in the Cape Cod soil near the canal made it extremely difficult to sink the steel sheet-piling. The foundation material in some cases proved to be very loose and, although it was not compressible if held in position, it flowed

easily due to the fineness of the sand and the extremely high water content. Although piles were not contemplated originally, it was believed desirable to use them, and the coffer-dam sheeting was left in place in order to confine the sand. The wooden piles were driven under water in the case of the highway bridges, whereas the coffer-dams were unwatered before driving in the case of the railroad bridge piers. Divers cut the wooden piles used for the highway bridges, and the concrete was placed under water by bottom dump buckets. Another interesting feature of the coffer-dam work at the railroad bridge was the unwatering by the well-point method. Well-points were driven around the coffer-dam and the ground-water flow was discharged into the canal.

The north coffer-dam for the railroad bridge offered many difficulties. The material on that side of the canal seemed to be especially fluid with the result that "blow-ins" of minor proportions were frequent occurrences. Furthermore, the shifting of the earth in the immediate vicinity tended to distort the coffer-dam sheeting and place severe strains on some of the wooden brace members. At one time, it was thought that it might be necessary to place additional bracing to such an extent that driving piles in the quantity desired would have been impossible (see Fig. 7). Finally, a sufficient number

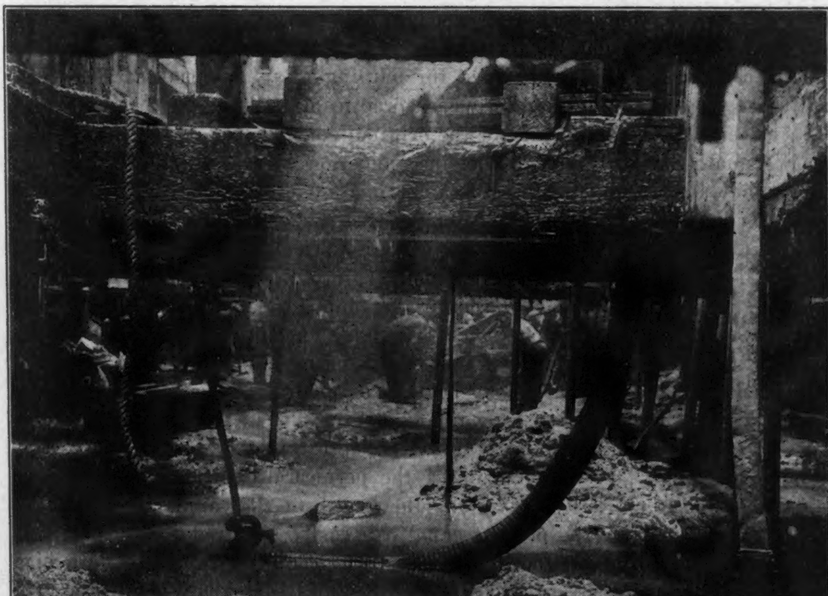

FIG. 7.—COFFER-DAM UNWATERED, NORTH MAIN PIER OF NEW RAILROAD BRIDGE.

of piles were driven so that the first few feet of concrete could be placed, and it was with a feeling of relief that the contractors, as well as the Government engineers, saw the first 3 ft of concrete sluiced into place. Of course, as soon as it had set, the danger of the complete destruction of the coffer-dam was reduced to minor proportions.

Excavation

When the canal was first constructed, it was expected that practically all the excavation could be done by hydraulic methods. Actually, however, it was found that although somewhat more than a mile of the channel from the Cape Cod end could be dredged hydraulically, the larger part of the work could not be handled by that type of equipment.

General Parsons has described[2] at great length, the attempts to operate hydraulic dredges in the land cut. When the original contractors found that they could not make further progress by hydraulic methods, they purchased second-hand dipper machines which happened to be available. Unfortunately, these machines lacked sufficient power to handle the large boulders encountered in dredging the canal channel, and, finally, it became necessary to have two 10-yd dipper dredges. The dredges were assembled at the canal and proved to be entirely satisfactory.

General Parsons had previously urged the contractors to consider the use of steam shovels and industrial railway equipment. This was done with very satisfactory results. It was found possible to excavate in the dry to a depth of 20 ft below the ground-water level. Handling the boulders with such equipment where they could easily be broken up by blasting proved to be far more practicable than the use of even the better type of dipper dredge finally obtained. Under modern conditions, with superior shovel equipment and the mobile and highly adaptable truck for hauling away material, it seems certain that excavation in the dry where practicable will be even more advantageous than it was at the time of the original construction of the canal.

Fortunately, recent contracts let in connection with the highway relocation for the new bridges make it possible to estimate closely the cost of dry excavation. Prices of 24 cents per cu yd have been obtained, even where the haul was in excess of 1 000 ft. It seems certain that on such a large volume as will be involved in the proposed widening it will pay to make use of the modern drag-line equipment, or the large steam shovels and 8 to 10-yd trucks. The material is such that no difficulty will be encountered in making roads for the truck transportation, and there are some places where heavy drag-line equipment with a sufficiently long boom can remove the dirt to be excavated in the dry without any need for haulage. With this in mind, further studies have been made in order to ascertain what depth might be reached by excavation in the dry. Tests were made of the permeability of the soil based on samples taken at various points along the length of the canal. It is believed that the seepage from the present canal can easily be cared for by pumping, even if the excavation in the dry is carried to about 18 ft below mean high water. It will be necessary to leave a substantial dam between the present canal and the new excavation, and one having a top width of 30 ft at mean high water will be used.

In addition to the advantage of handling the boulders in the dry and the fact that earth removal will be somewhat cheaper by this means, there is also a great advantage in being able to place the rip-rap in the dry. As every one who has had such experience knows, placing rip-rap under water is a

somewhat uncertain process and is likely to be wasteful of material. On the other hand, by placing the rip-rap blanket in the dry, it will be possible to have it exactly as desired with the least cost.

With a large part of the excavation in the dry, the problem of providing disposal areas is introduced. After a careful study of the territory in the immediate vicinity of the canal certain sites have been selected as indicated in Fig. 5. These sites provide more than sufficient disposal areas for the nearly 9 000 000 cu yd which can be excavated in the dry.

The excavation at the east end of the canal, with the exception of sufficient excavation in the dry for the purpose of placing the rip-rap, can be done by hydraulic methods. West of Station 70 (see Fig. 5), however, it will be necessary to make use of the most modern high-powered dipper-dredge equipment. The analysis of borings that have been taken along the site of the proposed straight channel in Buzzards Bay indicate that it may be possible to excavate a major portion of the material there by hydraulic methods.

Program of Construction

Dredging operations on the new straight channel through Hog Island can be started at the earliest practicable date. This can continue to completion without interruption if funds are provided. The approximate maximum rate at which funds can be used efficiently for this part of the work is $3 000 000 the first year, and $3 113 000 the second year. At this rate, the work would be completed in two years.

In the land cut, excavation in the dry will be the most economical. It is estimated that approximately 8 785 000 cu yd of material can be removed by means of drag-line, shovels, trucks, and other land equipment. Much of the necessary equipment would be available in this region and carrying on the work in this manner would provide jobs for the unemployed of near-by cities. The cost of such excavation will probably be little more than one-half the estimated cost of dredging through the major portion of the land cut. Furthermore, by excavating in the dry it will be possible to place the rip-rap for bank protection on dry land instead of under water. This will be more economical and in the long run will give better results. Several contracts for excavation in the dry can be projected simultaneously, and each should include placing the required rip-rap in the section excavated. Areas for the disposal of the material excavated have been selected tentatively. It is estimated that funds for this part of the work can be used efficiently at the maximum rate of $2 000 000 the first year and $1 712 000 the second. Two years will be required to complete this part of the work, including the placing of rip-rap. It is desirable that this part of the improvement be started at the earliest practicable date.

If the excavation in the dry is begun promptly, it will be possible to begin the dredging in the land cut at those sections where the excavation in the dry and the placing of rip-rap shall have been completed. Approximately 21 232 000 cu yd will have to be removed from the land cut by dredging. It is estimated that funds can be used efficiently at the rate indicated in Table 7.

TABLE 7.—MAXIMUM RATES AT WHICH FUNDS CAN BE USED

Description of work	First year	Second year	Third year	Fourth year	Fifth year
Hog Island channel...........	$3 000 000	$3 113 000	....	....	....
Land, highway, and railway, etc..	1 000 000	108 000	....	....	....
Dry excavation and rip-rap.....	2 000 000	1 712 000	....	....	....
Dredging land cut...........	....	1 000 000	$3 000 000	$3 000 000	$1 797 000
Moorings, lighting, etc...........	....	....	100 000	100 000	220 000
Totals...........	$6 000 000	$5 933 000	$3 100 000	$3 100 000	$2 017 000
Engineering and contingencies, 15%...........	900 000	890 000	465 000	465 000	302 000
Grand total...........	$6 900 000	$6 823 000	$3 565 000	$3 565 000	$2 319 000

By utilizing dry excavation as far as practicable, the foregoing program would probably effect a saving of about $2 703 000 as compared to the all-dredging method. However, if the enlargement is to be spread over a long period of years, the more costly dredging method will probably be advisable, because each expenditure would provide a more immediate benefit to navigation.

HYDRAULICS

As a very distinguished engineer has expressed it,[2] the problem presented by the flow of water in the Cape Cod Canal is "an extremely complex one in hydrodynamics, being the analysis of the motion of water in a canal of considerable magnitude connecting two seas, the tides in which differ to a great extent, both as to phase and amplitude." In comparative length and cross-section, as well as in the tidal conditions at the ends, the Cape Cod Canal differs to such an extent from the few other similar artificial waterways that methods of analysis which have been applied to some of them cannot be readily applied to it. For example, the "Reflected Wave Theory" developed by Earl I. Brown, M. Am. Soc. C. E.,[5] and applied by him to the Chesapeake and Delaware Canal is difficult to apply to the Cape Cod Canal.

Observations of tides and currents in the 100-ft canal yielded data by which the maximum velocity during a tide and the time of its occurrence could be predicted with considerable accuracy. The United States Coast and Geodetic Survey publishes tables of such values in the yearly "Current Tables." The prediction of the velocities to be anticipated in the proposed enlarged canal presents a difficult problem for which only an approximate analytical solution may be expected, since the flow in the canal is not only non-uniform (surface slope not parallel to bottom), but it is variable (continually changing with time).

The tide in Buzzards Bay (west end of the canal) precedes the tide in Cape Cod Bay (east end of the canal) by approximately 3 hr, one-half the tidal interval. The rise at the Buzzards Bay end is thus well under way while the water is still falling at the other end, and Buzzards Bay begins to fall some hours before Cape Cod Bay has reached its peak (see Fig. 8). The mean range of tide in Buzzards Bay is approximately 4 ft; in Cape Cod Bay, it is

[5] "Flow of Water in Tidal Canals", by Earl I. Brown, *Transactions*, Am. Soc. C. E., Vol. 96 (1932), p. 749.

approximately 9 ft. The phase relationship is such that the "tide head" (defined as the maximum simultaneous difference in elevation of the water surfaces occurring during any one tide at the recording gauges near the ends of the canal) occurs on the average within 1 hr after high water and within 1 hr after low water in Cape Cod Bay and averages nearly 5 ft (over-all slope, 0.000146). The greatest tide head ever recorded was 9.5 ft (over-all slope, 0.000275), but such a head is most unusual, since less than 1% of the tide heads exceed 7.5 ft.

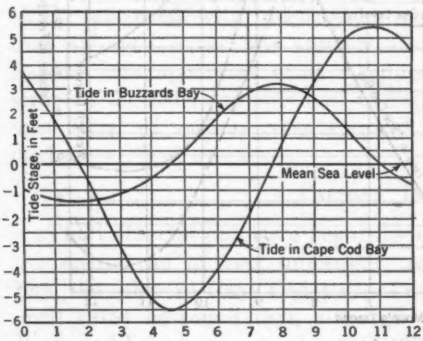

FIG. 8.—TYPICAL TIDE CURVES, FROM OBSERVATIONS, SEPTEMBER AND OCTOBER, 1932.

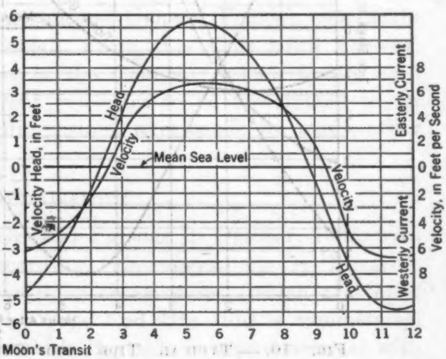

FIG. 9.—TYPICAL CURRENT CURVES, FROM OBSERVATIONS, SEPTEMBER AND OCTOBER, 1932.

Because of inertia effect, maximum velocity and maximum head during any tide do not occur simultaneously; nor do slack-water and zero head (see Fig. 9). The interval of time by which maximum velocity follows maximum head varies widely with individual tides (and is difficult to determine closely because the velocity changes are negligible for a considerable period near the time of the maximum), but it is generally less than 30 min. The interval of time by which slack-water follows zero head also varies with individual tides, and is also generally less than 30 min. For all practical purposes, slack-water may be considered to occur at virtually the same time throughout the length of the canal.

As a result of the tidal conditions at the ends, the water in the canal flows in one direction for approximately 6 hr, reverses, and flows in the opposite direction for approximately 6 hr. The current, therefore, changes direction four times a day. The maximum velocity in each direction is of approximately the same magnitude. The head between the ends of the canal and the velocity of the current in the canal are constantly changing, increasing from zero to a maximum and decreasing to zero in 6 hr. In the following comments the maximum head (tide head) and maximum velocity for any tide will be the quantities most frequently discussed. It should be understood, however, that this maximum velocity persists for a relatively short time. The general relationship between tides, head, and velocity are shown in Fig. 10.

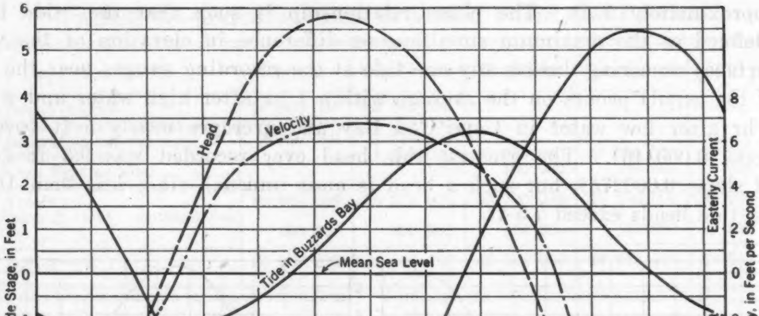

FIG. 10.—TYPICAL TIDE AND CURRENT CURVES, FROM OBSERVATIONS, SEPTEMBER AND OCTOBER, 1932.

EARLY STUDIES

Prior to the beginning of construction in 1909, a number of investigations, surveys, and reports were made. From the time Thomas Machin was commissioned, in 1776, to make surveys and plans, until 1862, all proposals for the canal involved locks. The report of the Massachusetts Joint Committee on the proposed Cape Cod Canal in 1862 contained the first recorded official discussion of the possibility of constructing a canal without locks, as has been mentioned. The Committee was advised concerning technical matters by an Advisory Council (the late Joseph G. Totten, Brigadier-General, U. S. Topographical Engineers, Hon. M. Am. Soc. C. E., the late A. D. Bache, Hon. M. Am. Soc. C. E., and Captain C. H. Davis, U. S. Navy) for which the late Henry Mitchell, M. Am. Soc. C. E., then an Assistant in the Coast and Geodetic Survey, investigated the tidal phenomena involved. The reports of the Advisory Council and of Mr. Mitchell were widely quoted in subsequent reports, and practically all investigators from that time until General Parsons began his tidal observations in 1907, based their computations and discussions of currents on Mr. Mitchell's observations of tides during one month in 1860. Unfortunately, Mr. Mitchell assumed mean tide level in Buzzards Bay to be the same as mean tide level in Cape Cod Bay, and the error was not discovered until nearly fifty years later, when it was pointed out by General Parsons. Mr. Mitchell's observations indicated that the tide head producing flow in one direction would be far from equal to that producing flow in the opposite direction, a result which would tend to make velocities computed

from his data higher, in one direction, than those computed from the correct data (a fact which may partly explain the opposition of many prominent investigators to the construction of an open canal).

Nevertheless, between the years 1870 and 1880, two eminent engineers sponsored the proposition that a canal without locks would be feasible. In his "Report on the Cape Cod Canal",[6] Gen. J. G. Foster, U. S. Army, gave results of calculations of current velocity in a proposed open canal 198 ft wide by 23 ft deep, as indicating a maximum probable velocity therein of 4 miles per hr. The late Clemens Herschel, Past-President and Hon. M. Am. Soc. C. E., supported, with independent computations, General Foster's conclusion that an open canal was entirely feasible. From this time until General Parsons was appointed Chief Engineer of the Company which finally constructed the canal, predictions of current velocities to be anticipated in an open canal of various cross-sectional dimensions were made by many other engineers.

PARSONS' INVESTIGATIONS

Tidal observations were begun by General Parsons in October, 1907, with the setting up of two, automatic, recording tide-gauges, one in Buzzards Bay, the other in Cape Cod Bay. From these observations (which continued until 1915) he found that, although the Cape Cod Bay tide is symmetrical above and below mean sea level, the Buzzards Bay tide is unsymmetrical with reference to that plane, mean high water being 2.1 ft above mean sea level, and mean low water being only 1.4 ft below it. Mean tide level, therefore, was above mean sea level and, consequently, the average values of the heads producing velocities in opposite directions do not differ appreciably, as would be the case if the Buzzards Bay mean tide level coincided with mean sea level as assumed in the 1860 tidal observations.

After the canal was completed, observation posts were selected at ten interior points in the land cut, and a series of tide and current observations were made under the direction of General Parsons[3] by observers and assistants at each post. Current velocities were measured by means of surface floats. In addition, current meter observations were made at Station 225 (nearly half way between the ends of the canal, see Fig. 2) to determine the relation between the mean velocity of the cross-section and the observed center-surface velocity. This factor was desired for the purpose of checking the results obtained from the application of various hydraulic formulas with the observed results. It was determined from these observations that: (1) The mean velocity of the entire section = 0.78 times the maximum surface velocity; (2) the maximum velocity in the section = 1.066 times the maximum surface velocity; and (3) the mean velocity of the entire section = 0.73 times the maximum velocity in the section.

Velocities computed by various methods were compared with those actually observed, and a method of solution by harmonic analysis was developed by General Parsons.[3] This method, based on the theory of tides in canals derived by Sir George Biddell Airy, as interpreted by Professor Maurice Lévy, yielded

[6] Senate Misc. Doc. No. 145, 41st Cong., 2d Session (1870).

results which checked those observed closely. The method is rather complicated, however, and this consideration, together with the fact that all analytical results must be based on important basic assumptions which may or may not be true, led General Parsons to investigate various approximate methods of solving the problem. The methods included in this study were the formulas of Bazin, Eytelwein, Ganguillet-Kutter, the French Academy of Sciences, and the method of solving the formula for permanent non-uniform flow developed by Professor Bubendey. From this investigation he concluded that the Ganguillet-Kutter formula could be used for the evaluation of velocities in the Cape Cod Canal with sufficient accuracy for all practical purposes.

Observations of Tides and Currents by the United States Corps of Engineers

Shortly after the United States purchased the canal in 1928, two automatic recording tide gauges were established in the same locations as those used from 1907 to 1915. These gauges have been maintained in continuous operation since August, 1928, for the purpose of collecting basic tidal data.

Tide and Current Observations, 1932

A comprehensive series of tide and current observations was made in 1932 when the project dimensions were 100 by 25 ft, shortly before the beginning of the dredging for widening to 170 ft. The Survey Section of the 1st New York District, Engineers, U. S. Army, supplied the equipment and technical assistance to the Boston District for this series of observations. The field work was conducted by personnel of the Boston District U. S. Army Engineers, and the records were compiled and tabulated by the 1st New York District. The purpose of the observations was to determine the laws governing the flow in the canal as well as to secure a basis for comparison with conditions after future widening.

Observation posts were selected at intervals of approximately 5 000 ft throughout the canal, the locations being made to coincide as nearly as possible with those used by General Parsons in 1915. Two parties were employed in making the velocity observations, one party remaining at the master current station, at Station 225, making continuous observations for the full period of the survey (September 28 to October 6, 1932), the other party observing at each of the other posts for a period of approximately one day. The continuous record at Station 225 served as a basis for comparisons between the shorter records at the other points. A similar arrangement for observing tides was used, three master recording gauges being maintained for the full period of the survey while the intermediate tide staffs—one at each observation post—were read by the current observer during the period his party was in position at that post.

Current observations were made from launches anchored in the center of the canal, the measurement at each observation post being confined to a single vertical located at the axis of the deep-water channel, which was also close to the point of maximum velocity. Observations were made with two cur-

rent meters simultaneously, one at three-tenths the depth, the other at seven-tenths the depth. The meters used were of the standard, large, Price type, mounted in an open rectangular iron frame. A sealed chamber of special design on the meter frame was used to protect the electrical connections against the effects of long-continued immersion in salt water. An automatic graphic recorder with pen arm was actuated by a magnet controlled by a magnetic accumulator relay connected in series with the electrical circuit of the meter. Each meter had its individual circuit with separate relay and recorder.

In order to eliminate minor fluctuations in the current velocities measured, average values over 15-min periods were taken from the records. After all these observed velocities were tabulated and platted, the observations of tides and current velocities at the subsidiary stations were reduced to mean values for the full period of the survey by reference to the master tide and current stations. For convenience, time was reduced to equivalent hours after the time of the moon's transit. From these reduced values, water-surface elevations and velocity were platted against time, as shown in Figs. 8, 9, and 10.

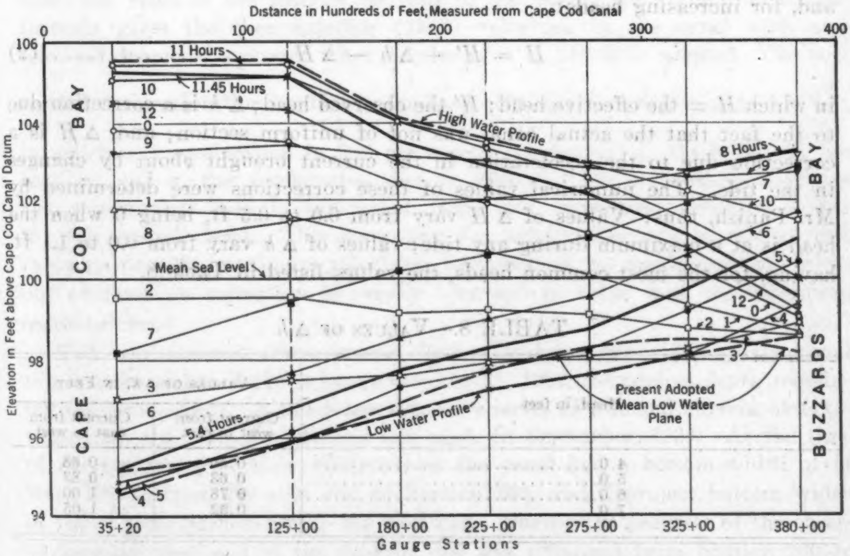

FIG. 11.—PROFILES OF WATER SURFACES: AVERAGE OF OBSERVATIONS, SEPTEMBER 28 TO OCTOBER 6, 1932.

The hourly profiles were also platted, as demonstrated by Fig. 11. The high-water and the low-water profiles were obtained by drawing lines osculatory to the hourly profiles.

As noted previously, the lag of the Cape Cod Bay tide behind the Buzzards Bay tide averages 3 hr. Therefore, high and low waters at one end of the canal occur nearly simultaneously with mean sea-level elevation at the other end. A noticeable feature, shown in Fig. 11, is the flattening of

the water surface for a distance of more than two miles from the eastern end of the canal. The profiles near the time of high water especially reflect this effect which is probably due primarily to the propagation of the Cap Cod Bay tidal wave into the canal.

Analysis of Relation Between Head and Velocity

The data obtained from the 1932 observations were used as a basis for an investigation of the relation between head and velocity by Charles K. Panish, Assistant Engineer, 1st New York District, Engineers, U. S. Army.[7] In order to establish this relationship in simple form it was found desirable to distinguish between the observed head and the ideal, or effective, head producing velocity. The effective head is defined as that existing in a canal of equivalent uniform section under conditions of steady flow, and was determined by means of the following equations:

For decreasing heads:

$$H = H' + \Delta h + \Delta H \qquad (1)$$

and, for increasing heads:

$$H = H' + \Delta h - \Delta H \qquad (2)$$

in which H = the effective head; H' the observed head; Δh is a correction due to the fact that the actual canal was not of uniform section; and, ΔH is a correction due to the acceleration in the current brought about by changes in the tide. The numerical values of these corrections were determined by Mr. Panish, thus: Values of ΔH vary from 0.0 to 0.5 ft, being 0 when the head is at a maximum during any tide; values of Δh vary from 0.0 to 1.1 ft, having, for the most common heads, the values listed in Table 8.

TABLE 8.—Values of Δh

Head, in feet	Values of Δh, in Feet	
	Current from west to east	Current from east to west
4.0	0.50	0.68
5.0	0.63	0.82
6.0	0.78	1.00
7.0	0.92	1.05

The study made by Mr. Panish of the observed velocities and the corresponding effective heads indicated that for all values of the velocity important to this paper (that is, when turbulent flow occurs), the dominating forces are hydraulic, and that the velocities in the canal as it existed at the time of the observations, could be computed approximately from:

$$V = C\sqrt{H} \qquad (3)$$

[7] "Hydraulics of the Cape Cod Canal", April 11, 1933. (Unpublished Departmental report.)

in which V is the velocity, in feet per second; H is the effective head corrected as described previously; and C has values as follows:

Definition of velocity, V	Value of C
Average over entire section	1.75
Average in the center vertical	2.24
Maximum in the section	2.40

These coefficients were determined for the canal as it was in 1932 (with project dimensions of 100 by 25 ft), and the proper values for a different cross-section can scarcely be determined analytically in advance of construction to that size of cross-section.

For predicting velocities in an enlarged canal, the method employed by Maj. Willis E. Teale, Corps of Engineers, U. S. Army, as developed from his analysis of both the Parsons' and the 1932 observations,[8] may be used. He concluded from this analysis that (with slope defined as the over-all slope determined from the head, corrected for acceleration only, between the recording gauges near the ends of the canal; and with R defined as the mean of the hydraulic radii of the interior sections of the canal) the Ganguillet-Kutter formula gives the then existing (1932) velocities in the canal with any required degree of accuracy when a value of $n = 0.0336$ is adopted. The correction for acceleration applied to the head between the recording gauges is $\frac{a\,L}{g}$, in which a is acceleration in feet per second per second; L, the length of the section; and g, the acceleration due to gravity. For increasing velocities the acceleration head is subtracted from (for decreasing velocities added to) the over-all head. This correction for acceleration can be disregarded in computing the maximum velocities, inasmuch as the maximum head without acceleration correction is usually identical in value with the maximum corrected head.

Tide and Current Observations, 1934.—Dredging for widening the canal to a bottom width of 170 ft began October 31, 1932, the project depth remaining the same—25 ft. A much less extensive series of tide and current observations than the 1932 observations was made in September, 1934. At the time of the beginning of these observations the canal had a bottom width of at least 170 ft from the east end to Station 260, and a project bottom width of 100 ft from Station 260 to the west end. During the progress of the observations the west end of the dredged cut was advanced from Station 260 to Station 282 (see Fig. 2). With the canal 170 ft wide for about 70% and 100 ft wide for the remaining 30% of its length, it was naturally anticipated that the surface slopes would be steeper, and, in consequence, the current velocities higher, in the narrow part.

The observations were made in order to: (1) Determine the maximum velocity in the, as yet, unwidened part; (2) obtain data on the distribution of velocity within the cross-section with a bottom width of 170 ft; and

[8] Cape Cod Canal—Analysis of September–October, 1932, "Velocity Observations", June 7, 1933. (Unpublished Departmental report.)

(3) determine the value of the roughness coefficient for the 170-ft section. Both the work in the field and the office computations were under the immediate direction of Donald F. Horton, Jun. Am. Soc. C. E.

The current observations were made from one launch from which were suspended two current meters of the identical type used in the 1932 observations. The Survey Section of the 1st New York District, U. S. Army Engineers, again supplied the equipment and technical assistance. Tide staffs were set up at the same locations as in 1932 and were observed as required to obtain data for the accomplishment of the specific objects outlined herein.

To determine the maximum velocity in the narrow section, observations were made at the center of the canal with one meter at three-tenths, and the other at seven-tenths, the depth. Two points had been selected as the probable locations at which the highest velocity would occur, and observations during two tides were made at each point. The highest velocities were observed at Station 346 and are as given in Table 9.

TABLE 9.—HIGHEST OBSERVED VELOCITIES AND TIDE HEADS (1934).

Direction of current	Tide head, between ends of canal, in feet	Velocity at 0.3 depth at center of canal, in feet per second
East to west	6.35	10.1
West to east	6.80	8.2

In order to eliminate minor fluctuations the velocities tabulated from the records were taken as averages over 15 min. The master current station of the 1932 observations (Station 225) was selected for the observations to obtain data on the distribution of velocity in the 170-ft cross-section. This location was chosen primarily because the canal alignment is a tangent for a considerable distance in each direction; it is also nearly mid-way between the ends of the canal. Nine measuring verticals were selected; one at the center, the others spaced 20 ft apart across the channel width. Velocity curves were observed at each of these verticals by means of the two current meters, one suspended constantly at three-tenths the depth, while, with the other meter, the velocity at each tenth the depth from surface to bottom was observed for not less than 7.5 min. The results obtained in each vertical, therefore, were a value of the velocity (average record of 7.5 min) at each tenth of the depth, and simultaneous values of the velocity at three-tenths the depth. Since the velocity is continually changing, the observed velocities at each tenth the depth were reduced to a common value of the velocity at three-tenths the depth by means of the simultaneously observed values. A vertical velocity curve was thus obtained for each of the nine verticals.

The determination of the variation in velocity across the channel was made by observations at three-tenths and seven-tenths the depth for not less than 7.5 min, successively, at each vertical. During the meter observations at each vertical the center surface velocity was determined by means of surface floats. The series of observations was made as expeditiously as pos-

sible during the period from 1 hr before, to 1 hr after, the time of maximum current, and was repeated the next day in the same manner when the water was flowing in the opposite direction. From these observations the average ratio of mean velocity of the entire cross-section to mean velocity in the center vertical was determined for four different elevations of the water surface and was found to be 0.87.

From these ratios and the relationship between the observed velocities and the mean velocity of the center vertical (which mean was determined from the vertical velocity curves observed at the center vertical), reduction factors for the convenient determination of mean velocity of the cross-section directly from the observed velocities were computed for use in:

$$V_m = F_1 V_{0.3} + F_2 V_{0.7} \dots\dots\dots\dots\dots\dots\dots (4)$$

in which V_m = the mean velocity of the cross-section; $V_{0.3}$ = the observed velocity at 0.3 depth at center; $V_{0.7}$ = observed velocity at 0.7 depth at center; and, F_1 and F_2 are reduction factors, the average values of which, as determined for four different elevations of the water surface, were found to be $F_1 = 0.51$ and $F_2 = 0.31$. The average ratio, $\frac{V_m}{V_{0.3}}$, was determined to be 0.76.

For the determination of the roughness coefficient in the 170-ft canal, the reach from Station 180 to Station 275 (Fig. 2) was selected. Tide staffs were observed at Stations 180, 225, and 275, and current meter observations were made at the center of the canal at Station 225, with one meter at three-tenths, and the other at seven-tenths, the depth. These observations were made during the period from 1.5 hr before, to 1.5 hr after, the time of maximum velocity for both directions of the current. From these observed velocities (each an average of 15-min record), by application of the reduction factors already determined, the corresponding mean velocities of the section were computed. From the tide-staff observations, the average of the hydraulic radii within the reach under consideration, and the water surface slope corresponding to each of these mean velocities were determined. (The water surface slope was determined from the carefully observed difference in elevations between Station 180 and Station 275 corrected for acceleration.) By substitution of these known values in the Ganguillet-Kutter formula, a value of n for each of the twenty mean velocities determined from the observations was computed. The average of these values of n was 0.037. The methods used in analyzing the results of these observations followed, in general, very closely those used by Major Teale in his analysis of the 1932 observations.[8]

Prediction of Velocities in an Enlarged Canal

The flow of water in the Cape Cod Canal being variable (velocity and water surface continually changing), as well as varied (non-uniform), an exact analytical determination of the velocities to be anticipated in an enlarged cross-section cannot be made by any means known to the writer. Since the maximum velocity during a given tide is of paramount practical importance,

the problem may be simplified in some respects by restricting it to the approximate determination of the maximum velocity resulting from a given tide head. Since the general equation[9] for variable-varied flow, namely,

$$S = \frac{V^2}{C^2 R} + \frac{d}{dx}\frac{(V^2)}{2g} + \frac{1}{g}\frac{\delta v}{\delta t} \quad \ldots\ldots\ldots\ldots\ldots\ldots (6)$$

differs from the general equation for varied flow only in the term, $\frac{1}{g}\frac{\delta v}{\delta t}$, which is zero at the instant of maximum velocity, the problem, as thus restricted, may be considered, for all practical purposes, one of steady varied flow in which the water surface elevations at the ends of the canal are given and the resultant discharge and velocity are desired. In Equation (6), S = slope; R = hydraulic radius; and t = time.

The ultimate size of cross-section which has been proposed is that with a bottom width of 500 ft, depth below mean low water of 40 ft (with 1 ft overdepth) and side slopes of 1 on 2.5. The maximum velocities to be anticipated at a point approximately midway between the ends of the canal (Station 225) with a cross-section of this size were computed by solution of the varied flow equation for a number of combinations of water surface elevations at the ends. The method solving the varied flow equation developed by Boris A. Bakhmeteff,[9] M. Am. Soc. C. E., was used for flow from west to east. In the other direction, flow takes place against an adverse or negative slope. In this case, the method developed by Arthur E. Matzke, Jun. Am. Soc. C. E.[10] (from equations derived by Professor Bakhmeteff), was used.

In the determination of the varied flow factors used in both these methods of solution, the Ganguillet-Kutter formula with coefficient of roughness of 0.035 was used.

The velocities first derived were obtained by dividing the computed discharge by the area of cross-section at Station 225, and, therefore, were mean velocities of the section. Mean velocity, however, is not of direct interest to navigators. The velocity at three-tenths the depth at the center—which roughly approximates in value the maximum velocity in the section—is believed (for most vessels which will use the canal) to be a better criterion of the extent to which a vessel may be affected by the current. The mean velocities first computed, therefore, were reduced to values corresponding to velocity at three-tenths the depth at the center by the application of the factor, 1.31, determined from the 1934 observations. The results are given in Table 10. These results agree closely with those obtained from the application of the method used by Major Teale previously described.[8]

Theoretically, since the surface slope is not parallel to the bottom slope, the highest velocity resulting from a given tide head would not occur at Station 225, but at one end of the canal, depending on the direction of the current. Actually, it is probable that this effect will be somewhat obscured,

[9] "Hydraulics of Open Channels", by Boris A. Bakhmeteff, M. Am. Soc. C. E., Eng. Societies Monograph, 1932.

[10] "On Varied Flow in Channels of Adverse Slope." (Unpublished paper.)

as it was observed to be in the existing canal, by unavoidable irregularities resulting from dredging operations.

Assuming the same ratio between mean velocity of the section and velocity at three-tenths the depth at the center, as determined at Station 225, these highest velocities would be as given in Table 10(*b*).

TABLE 10.—PREDICTED VELOCITIES IN THE CENTER OF THE 500 BY 40-FOOT CANAL

Tide head, in feet	Maximum Velocity at 0.3 Depth				Maximum Velocity at 0.3 Depth			
	From West to East		From East to West		From West to East		From East to West	
	In feet per second	In knots	In feet per second	In knots	In feet per second	In knots	In feet per second	In knots
	(*a*) At Station 225				(*b*) Highest Velocities at Any Section			
6.0	8.8	5.2	9.2	5.4	9.2	5.4	10.2	6.0
6.5	9.2	5.4	9.4	5.6	9.6	5.7	10.7	6.3
7.0	9.4	5.6	9.9	5.8	10.0	5.9	11.1	6.5
7.5	9.8	5.8	10.2	6.0	10.5	6.2	11.5	6.8

Since a comparable velocity of 10.1 ft per sec occurred with a tide head of 6.4 ft in the narrow section of the existing canal during the widening to 170 ft, it appears that the maximum velocities to be anticipated in a 500 by 40-ft canal will not greatly exceed those which have been actually experienced with similar tidal conditions in the short restricted 100-ft section before the completion of the 170-ft widening program. Velocities in the proposed 540 by 32-ft canal should be approximately 7% less than in the 500 by 40-ft canal.

The frequency of tide heads of the magnitudes listed in Table 10 have been approximately as follows: Higher than 6.0 ft, 15% of tides; higher than 6.5 ft, 10% of tides; higher than 7.0 ft, 5% of tides; and higher than 7.5 ft, 1% of tides. The phase relationships of the tides at the ends of the canal are such that the effect of the increased discharge through an enlarged canal will be to decrease the frequency with which heads of a given magnitude occur. It is probable, for example, that with the 500 by 40-ft canal, tide heads higher than 6.5 ft will occur during less than 10% of the tides.

The computations described herein, of velocities to be anticipated in an enlarged canal, were based on the tidal data observed with the 100 by 25-ft canal, because the changes in tidal conditions resulting from the increased discharge through an enlarged canal cannot be determined analytically with certainty. Furthermore, the exact value of the coefficient of roughness (n in the Ganguillet-Kutter formula) is not known definitely. It is thus seen that, for these reasons, if for no others, the predicted velocities can be considered approximate only and are possibly in error by as much as 10 per cent.

Model Studies

Of practical importance in the control of the dredging operations for the enlargement of the canal is the locus of the plane of mean low water which will obtain after the completion of the enlargement, since the depth is to be

determined with reference to that plane. It is anticipated that the increased discharge through an enlarged canal will change the elevation of mean low water in Buzzards Bay and in the canal proper, but no analytical method of determining this change quantitatively is known. Another problem of practical importance is the design of the proposed mooring basins, to eliminate as far as possible undesirable and dangerous eddies, which would not only menace shipping, but also would increase the difficulty and cost of maintenance. Both these problems are considered suitable for analysis by means of model studies. Therefore, it is believed desirable to undertake model studies of the enlarged canal for the purpose of studying these two problems. At the same time, determinations of velocity would be made as a check of the computed velocities, and with little additional cost, the effects of regulating works in Buzzards Bay may also be studied.

The proposed model of the enlarged canal would necessarily include enough of the upper end of Buzzards Bay to insure reaching a point at which the tide will not be affected by the increased discharge through the canal. No difficulty in this respect is anticipated for Cape Cod Bay since its characteristics are such that the increased discharge will not be large enough to affect the tide therein appreciably. Preliminary computations indicate that the area which should be reproduced will necessitate, with the scale tentatively selected, a model approximately 110 ft long.

During the investigation of a lock canal, two model studies were made. The first of these was undertaken by Thomas A. Lane, Jun. Am. Soc. C. E., and Lt. John L. Persons,[11] Corps of Engineers, U. S. Army. The purpose of the study was to determine the amount of depression below sea level of the water surface at the dock. This problem is of practical importance in the determination of the datum plane for dredging and of the design elevation of the lock sill. The study was made with a concrete model, approximately 40 ft long (scales: Horizontal, 1:1 000; vertical, 1:49). The results indicated that the depression of the water surface at the lock would be so small that for all practical purposes it could be neglected. This conclusion confirmed that reached by computations made in the office of the Boston District, U. S. Army Engineers, using the methods developed by Colonel Brown and General Parsons, to which reference has previously been made.

Model tests were also made to determine the most satisfactory design of the filling system for the lock. These tests were made by George R. Rich, M. Am. Soc. C. E.,[12] on a model to a scale of one-fortieth of a lock with a chamber 110 ft wide, 1 000 ft long, and 40 ft deep. Five different conduit designs were tested for filling time and effect on a vessel in lockage. The test ship used was a model of a standard cargo vessel, 600 ft long, with 75-ft beam, loaded to 35 000 tons displacement.

---

[11] "An Experimental Study of Tidal Action in a Lock Canal", Thesis presented to Mass. Inst. Tech., in May, 1932, in partial fulfillment of the requirements for the degree of Master of Science.

[12] "Model Tests of the Navigation Lock for the Cape Cod Canal", July 9, 1932. (Unpublished Departmental report.)

AMERICAN SOCIETY OF CIVIL ENGINEERS
Founded November 5, 1852

DISCUSSIONS

THE SILT PROBLEM

Discussion

By N. C. Grover, M. Am. Soc. C. E.

N. C. Grover,[39] M. Am. Soc. C. E. (by letter)[39a]—The silt problems of the Colorado River at the Boulder Dam are treated in this paper. Some up-to-date information has been obtained as to the effect of this dam on the silt regimen of the river, in connection with the regular activities of the U. S. Geological Survey in its program of measuring and recording the flow of surface streams. Among the 3 000 gauging stations operated, the program includes, of course, a group of stations in the Colorado River Basin. Because of the importance of silt in connection with the utility of the Colorado River, detailed silt studies were undertaken in 1925. Continuous records of the silt content of the water are kept at several of the gauging stations, including those at Grand Canyon, Willow Beach, and Topock, in Arizona.

Fig. 11(*a*) shows the quantities of silt, in millions of tons, carried by the river during each month, from January to June, 1935, at these three gauging stations. Fig. 11(*b*) shows the quantities of water, in acre-feet, carried during the same months. Grand Canyon station is situated well above the reservoir created by the Boulder Dam; Willow Beach station is 10 miles below the dam; and Topock station is about 115 miles below the dam. The Parker Dam is about 40 miles below Topock and about 155 miles below the Boulder Dam.

The construction and utilization of the Boulder Dam create a situation in the river below that dam that has great interest for engineers. The reservoir which is more than 100 miles long desilts the river so that the discharge through the dam is essentially clear water. This clear water, however, is discharged into, and flows through, a channel of silt and picks up a new load, thereby deepening the channel below the reservoir. The deposition of silt in the Boulder Reservoir and the deepening of the channel below it, of course, were anticipated. The speed with which the new load is acquired

Note.—The paper by J. C. Stevens, M. Am. Soc. C. E., was published in October, 1934, *Proceedings*. Discussion on this paper has appeared in *Proceedings* as follows: February, 1935, by Harry G. Nickle, Jun. Am. Soc. C. E.; March, 1935, by Messrs. E. W. Lane, and Frank E. Bonner; May, 1935, by Messrs. Morrough P. O'Brien, Harry F. Blaney, W. W. Waggoner, and Philip R. R. Bisschop; and September, 1935, by Herman Stabler, M. Am. Soc. C. E.

[39] Chf. Hydr. Engr., U. S. Geological Survey, Washington, D. C.

[39a] Received by the Secretary August, 26, 1935.

has general interest as has also the deposition of the new load in the reservoir formed by the Parker Dam which will rapidly lose its storage capacity. The ultimate silt content of the water as it leaves the Parker Dam will affect the problems related to the diversion into Southern California by the Metropolitan Water District of Southern California.

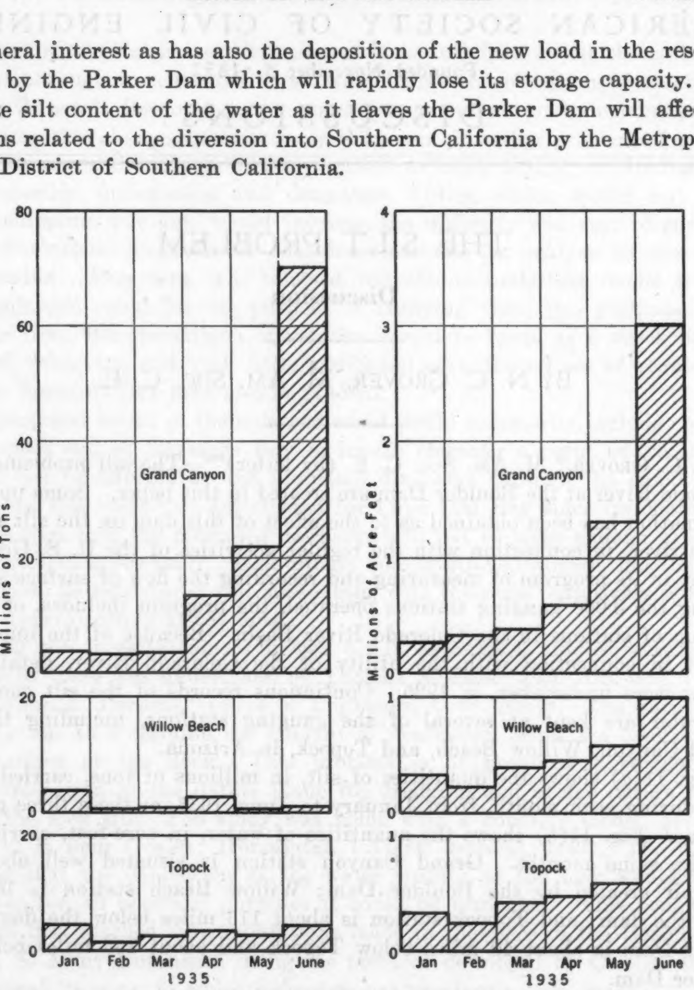

FIG. 11.—SUSPENDED MATTER, IN TONS, AND DISCHARGE, IN ACRE-FEET, AT GAUGING STATIONS ON COLORADO RIVER, IN ARIZONA.

The Colorado River above the Boulder Dam carries apparently an annual load of, say 200 000 000 to 300 000 000 tons of silt. This load, which prior to the construction of the dam was carried through to Yuma, essentially unchanged, is now deposited in the reservoir. In the five months between February 1, 1935, when storage in the reservoir began to be effective, and June 30, 1935, the load of silt that was carried past the Willow Beach gauging station amounted to about 4 000 000 tons, derived in part from operations at the dam. At the Topock gauging station the total load of sediment carried in the five months was more than 12 000 000 tons. During the same period the quantity of silt carried into the reservoir above the dam was more than 100 000 000 tons.

As a result of the pick-up of silt below the dam the channel has already been deepened. At the Willow Beach gauging station the bed was appreciably lower in September, 1935, than it was a few months previously. It is interesting to note also that the particles carried past Willow Beach and Topock are on the average much larger than the particles carried past Grand Canyon and into the reservoir.

Engineers will be interested in following the history of the new and controlled Colorado River, including not only the rates of loss of capacity of the Boulder and Parker Reservoirs, but also the rate of erosion of the river bed and banks below the Boulder Reservoir. Many years will doubtless pass before the bed, banks, and silt load are stable.

AMERICAN SOCIETY OF CIVIL ENGINEERS

Founded November 5, 1852

DISCUSSIONS

STABILIZING CONSTRUCTED MASONRY DAMS BY MEANS OF CEMENT INJECTIONS

Discussion

BY V. L. MINEAR, ASSOC. M. AM. SOC. C. E.

V. L. MINEAR,[8] Assoc. M. Am. Soc. C. E. (by letter).[8a]—A notable contribution to the knowledge of the theory and practice of cement injection is contained in this paper. It has been read and re-read by those entrusted with pressure grouting at Boulder Dam and appurtenant works. The methods developed for this great dam correspond to a remarkable degree with the methods and practices adopted in India by the author, notwithstanding the vastly different conditions under which the two jobs were carried forward.

The author placed 64 000 bbl of cement at a maximum pressure of 80 lb per sq in. in inferior masonry structures in India, using native labor. At Boulder Dam, more than 100 000 bbl of cement have been placed at maximum pressures of 1 000 lb per sq in., and with high-grade American labor. Notwithstanding the wide variation in conditions and objectives sought, it is thought that the one job affords an independent check upon the methods of injection used and the conclusions reached upon the other. Recounting all the similarities would become tiresome, but the writer wishes to re-emphasize some of Mr. Cole's more important conclusions regarding methods, that experience at Boulder Dam tends to verify:

(1) The degree of hardness and strength (of injected grout) is proportional in general to the pressure of placement with accompanying extrusion of water.

(2) For cement injection into tight ground some better efficiency is attained by the use of extra finely ground and resifted cement. Many thousands of sacks of cement, 98% of which passed the 200-mesh screen were injected at Boulder Dam, and it was definitely established that, other conditions being the same, a tight hole will admit as much as 10% more rescreened, than ordinary, cement in a given interval of time. How-

NOTE.—The paper by D. W. Cole, M. Am. Soc. C. E., was published in February, 1935, *Proceedings*. Discussion on the paper has appeared in *Proceedings*, as follows: August, 1935, by Messrs. Oren Reed, F. F. Fergusson, and Joseph Wright; and September, 1935, by Charles W. Comstock, M. Am. Soc. C. E.

[8] Care U. S. Bureau of Reclamation, Denver, Colo.

[8a] Received by the Secretary September 18, 1935.

ever, rescreening costs are relatively high, and it is thought that the apparent advantage can be more than overcome by slightly increasing the pressure applied to ordinary cement (conditions permitting).

(3) Sand is not effective for general use. It is kept in suspension within the pipe with the greatest of difficulty. It cannot be carried very far in the rock passages due to their variable cross-section and the consequent variable velocity with which the grout flows through them. In many cases sand undoubtedly clogs not only the pipe and fittings, but also the hole.

(4) Isolated grouting effects no benefits but shows a tendency to hinder the flow of grout from subsequent holes. In effect, it places obstructions in the grout passages deliberately, making it difficult or impossible to vent the air, water, and thin grout that precedes the thicker grout stream. Theory indicates, and practice seems to confirm, that a channel that has been tapped should be filled in one operation, and holes that have given a return flow should be connected in the order in which they showed grout.

(5) There is always the danger of choking the hole and sacrificing the penetration of the finer connecting passages by too much cement, too much pressure, or too much speed of delivery. The water-cement ratio, pump speed, and induced pressure must be co-ordinated in conformity with the type of grouting being done and the requirements of the individual hole. Each hole is "a law unto itself." It seems probable that more holes have been lost through inexperienced men attempting to use a thicker grout than the hole will accommodate, than from any other single cause. A sudden increase in either the speed of delivery or the pumping pressure, frequently results in the loss of a hole, especially if a water-hammer effect is present. Changes should be made gradually.

(6) Subaqueous or other inaccessible leaks can often be sealed effectively by a manipulation of the water-cement ratio and the pressure applied. The method is superior to the introduction of a sanded mixture in most cases.

(7) All joints should be left open for the free escape of water, and caulking should be resorted to only when the grout that escapes is of the same approximate density as the mixture that is being injected.

(8) The routine of grout injection developed at Boulder Dam is almost identical with that described by Mr. Cole, except for the water-cement ratio and the pressures. At Boulder Dam, the engineers strove from start to finish of a hole to maintain the maximum permissible pumping pressure, but never more than this pressure. Speed was controlled by adjustment of the mixture.

(9) There is need of a safe and reliable means of sealing the voids in otherwise completed masonry structures, in order to make them virtually impermeable by water. This is especially true of structures founded upon pervious rock. From the study of numerous cores recovered, the writer has reached the conclusion that the benefits to be derived from the injection of Portland cement grout into rock are limited to the filling of cavities and fissures within the rock, and that results are negligible so far as securing a cut-off in water-bearing rock itself is concerned.

AMERICAN SOCIETY OF CIVIL ENGINEERS
Founded November 5, 1852

DISCUSSIONS

WEIGHTS OF METAL IN STEEL TRUSSES

Discussion

BY MESSRS. H. H. ALLEN, AND JOHN VENABLE HANNA

H. H. ALLEN,[26] M. AM. SOC. C. E. (by letter).[26a]—The results of the studies and investigations reported in this paper are borne out remarkably well by the extensive office records available to the writer. He has used the nine Type *A* cantilever bridges which he (with Wilson T. Ballard, M. Am. Soc. C. E.) presented in the discussion of the author's paper entitled "Economic Proportions of Weights of Modern Highway Cantilever Bridges,"[27] as a basis for the data submitted herewith, and, in addition, one other Type *A* cantilever bridge designed and constructed by the writer's firm, namely, the cantilever bridge across the Kanawha River, at St. Albans, W. Va.

Table 3 is an arrangement of these ten Type *A* cantilever bridges in a manner similar to Table 2 of the paper. In addition, Table 3 contains similarly arranged data for the suspended spans of the Type *A* cantilevers. Data for four simple spans are also included, namely, the 156-ft simple spans that form the approaches at each end of the cantilever bridge across the Ohio River, at Ashland, Ky.; the 144-ft simple approach span to the cantilever bridge across the Ohio River, at Huntington, W. Va.; the 300-ft lift span of the James River Bridge, at Newport News, Va.; and the 208-ft approach spans of the same bridge.

All the Type *A* cantilever bridges, except the one at Ashland, Ky., were designed for the use of medium structural grade steel with a basic working stress of 18 000 lb per sq in. The Ashland Bridge was designed for the use of silicon steel and heat-treated eye-bars in the main members of the trusses, with a basic working stress of 24 000 lb per sq in.

The percentage ratios in Table 3 (Columns (10) and (11)) are based on an adjustment in the weight of the trusses, as described in the author's paper, in order properly to evaluate the truss weights on the basis of a working

NOTE.—The paper by J. A. L. Waddell, M. Am. Soc. C. E., was published in February, 1935, *Proceedings*. Discussion on this paper has appeared in *Proceedings*, as follows: May, 1935, by Messrs. Arthur M. Shaw, Joseph G. Shryock, Albert F. Reichmann, Robert W. Abbett, George C. Diehl, F. G. Jonah, Clarence B. Foight, A. H. Fuller, William E. Wilbur, W. N. Downey, J. R. Grant, Theron M. Ripley, and T. Kennard Thomson.

[26] Vice-Pres., The J. E. Greiner Co., Baltimore, Md.

[26a] Received by the Secretary September 17, 1935.

[27] *Transactions*, Am. Soc. C. E., Vol. 98 (1933), p. 931.

TABLE 3.—Weights of Metal Modern Highway Bridges

Structure	Type of span	Width of roadway, in feet	Foot-walks: No.	Foot-walks: Width, in feet	Main span, length, in feet	Total load, in pounds, per linear foot	Truss Metal: Weight, in pounds per linear foot	Truss Metal: Kind of metal	Percentage Ratios: Computed	Percentage Ratios: From the curves	Unit stress, in kips† per square inch
(1)	(2)	(3)	(4)	(5)	(6)	(7)	(8)	(9)	(10)	(11)	(12)
Huntington, W. Va. (Ohio River)	Cantilever	22	1	8	700	9 408*	3 165	Carbon	33.7	32.8	16
Bellaire, Ohio (Ohio River)	Cantilever	22	1	6	700	8 993*	3 210	Carbon	35.7	33.2	16
Pt. Pleasant, W. Va. (Kanawha River)	Cantilever	20	1	4.25	600	7 452	2 462	Carbon	33.0	30.6	16
Ashland, Ky. (Ohio River; Long A Arm)	Cantilever	22	1	5	739	7 800	2 426	Silicon	31.1	28.2	24
Portsmouth, Ohio (Ohio River)	Cantilever	22	1	6	700	7 090	2 790	Carbon	39.4	32.0	16
Cabin Creek, W. Va. (Long A Arm)	Cantilever	20	1	4	450	7 130	1 785	Carbon	25.0	26.2	16
Cabin Creek, W. Va. (Short A Arm)	Cantilever	20	1	4	450	7 295	1 860	Carbon	25.5	26.2	16
Ashland, Ky. (Ohio River; Short A Arm)	Cantilever	22	1	5	739	7 565	2 222	Silicon	29.0	28.2	24
Norfolk, Va. (Elizabeth River)	Cantilever	36	2	10	1 198.5	22 620*	9 280	Carbon	41.0	38.6	16
St. Albans, W. Va. (Kanawha River)	Cantilever	20	1	4.25	450	7 145	1 695	Carbon	23.7	26.4	16
Huntington, W. Va. (Ohio River)	Suspended	22	1	8	350	8 312*	2 290	Carbon	27.54	24.0	16
Bellaire, Ohio (Ohio River)	Suspended	22	1	6	350	7 844*	2 247	Carbon	28.70	24.1	16
Pt. Pleasant,- Henderson, W. Va.	Suspended	20	1	4.25	300	6 511	1 673	Carbon	25.7	20.6	16
Ashland, Ky. (Final) (Ohio River)	Suspended	22	1	5	350	7 119	1 774	Silicon	24.9	20.7	24
Portsmouth, Ohio (Ohio River)	Suspended	22	1	6	350	6 068	1 970	Carbon	32.4	23.7	16
Cabin Creek (Kanawha River)	Suspended	20	1	4	200	6 389	1 086	Carbon	17.0	12.9	16
Norfolk, Va.	Suspended	36	2	10	493.5	18 878*	4 780	Carbon	25.4	31.3	16
Ashland, Ky. (original design)	Suspended	22	1	5	350	6 516	1 460	Silicon	22.4	20.7	24
St. Albans, W. Va.	Suspended	20	1	4.25	200	6 443	1 100	Carbon	17.1	13.0	16
Ashland, Ky.	Simple	20	1	5	156	6 720	760	Carbon	10.3	10.5	16
Huntington, W. Va.	Simple	22	1	8	144	12 394*	1 370	Carbon	11.0	9.3	16
James River	Lift	22	..	....	300	5 998	1 260	Carbon	21.0	20.8	16
James River	Simple	22	..	....	208	6 860	940	Carbon	13.7	13.8	16
Typical spans	Simple	20	..	....	200	5 556	780	Carbon	14.3	13.5	16
Typical spans	Simple	45	..	....	200	13 048	1 645	Carbon	12.5	11.5	16
Typical spans	Simple	20	..	....	300	6 197	1 397	Carbon	22.5	21.0	16
Typical spans	Simple	45	..	....	300	14 259	2 804	Carbon	19.7	18.0	16
Typical spans	Simple	20	..	....	400	6 985	2 155	Carbon	30.8	29.0	16
Typical spans	Simple	45	..	....	400	15 783	4 287	Carbon	27.2	25.0	16

* Including electric street railway.
† 1 kip = 1 000 lb.

stress of 16 000 lb per sq in. instead of the 18 000 lb per sq in. used. The computed percentage ratios for the ten cantilever bridges agree very closely with those taken from Figs. 1, 2, 3, and 5. All these computed ratios are higher than those taken from the plotted curves, except the cantilever bridge at St. Albans, W. Va., which is 2.7% lower. This can be explained as being due to the use of rolled sections throughout the trusses for this bridge, thereby reducing the weights of details in the trusses materially.

The larger variations between the percentage ratios computed and taken from the curves of the paper for the nine suspended spans can be explained by the additional erection material included in the weights of the trusses for these spans, as compared with the weights of similar simple spans erected on falsework. The close agreement between the computed percentage ratios and those taken from Figs. 1 to 5 for the four simple spans listed, is remarkable.

It will be noted, however, that in each case the computed percentage of truss weights is slightly higher than that taken from the curves, except in the case of the 208-ft James River spans for which the computed percentage ratio is 0.1% less than the ratio taken from the curves. This truss is of the Warren type with the intermediate posts omitted, which may explain the reduction in truss weights.

The fact that the computed percentage ratios are uniformly higher than those taken from the curves led to a further investigation by the writer. Fig. 14 shows the ratio of truss weights to total weight carried for simple

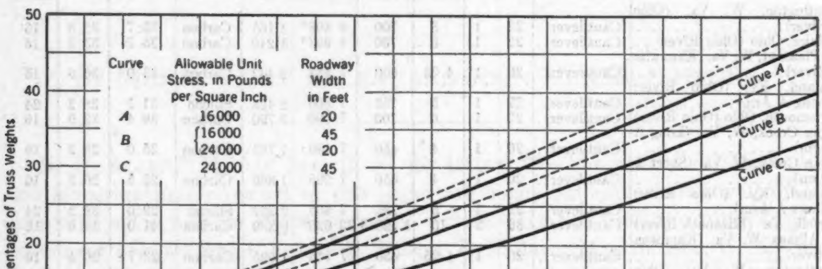

FIG. 14.—RATIO OF TRUSS WEIGHTS TO TOTAL WEIGHT CARRIED, SIMPLE HIGHWAY TRUSSES.

highway trusses on which are plotted Curves *A*, *B*, and *C*, corresponding to Curves 1, 2, and 3, Fig. 1(*b*). The curves shown in dashed lines on Fig. 14, immediately above Curves *A* and *B*, respectively, are plotted by collating office records which include the weights of steel subdivided into floor, bracing, and trusses for ideal typical simple highway spans for Class *A* loading, varying by 50 ft in length from 200 ft to 500 ft, for roadway widths varying between 16 and 36 ft by 4-ft variations, with additional weights for one or two sidewalks of 6 ft, 8 ft, or 10 ft. The curves of Fig. 14, shown in dashed lines, were obtained by using the percentage of truss weights of these typical, ideal, highway, simple, truss spans compared with the total weight of these spans, and agree more closely with the computed percentage ratios in Table 3 than those of the paper. This may be attributed to the personal equation of the designer, as expressed by the author:

"* * * each designer has personal idiosyncrasies that affect the weights of trusses he computes, and there is quite a perceptible difference in the metal weights between structures which are truly first-class in every particular and those of only mediocre excellence, or those that have been 'trimmed' to the limit."

Regardless of the relatively small differences obtained from the results of the author's investigations and the data submitted by the writer, the writer

feels that this method of approaching the problem of quickly estimating the weights of various types of trusses is an excellent one. These curves, of course, will need to be somewhat modified where the use of rolled sections reduces the weight of truss details.

JOHN VENABLE HANNA,[28] M. AM. SOC. C. E. (by letter).[28a]—In the early days of the Kansas City Terminal Railway Company's project for a new union station, and trackage in connection therewith, the writer was under the necessity of making, quickly, preliminary estimates of cost for a considerable number of structures. These structures were to carry urban highway traffic as well as railway traffic. In addition to the Union Station Building and the trackage immediately required for it, additional approach tracks were needed, which it was thought highly desirable should be entirely free from grade crossings. To estimate the cost of the structures necessary for this purpose, it was essential to determine weights of steel with a reasonable approach to the actual weights resulting from detailed designs. A method of estimating these weights, such as that set forth in the author's paper, would have been most welcome.

No doubt many engineers have been in the position of needing reliable methods of estimating weights quickly, and many will be in that position hereafter. In the light of the writer's experience, he believes that this paper will be of great value to many members of the profession.

[28] Chf. Engr., Kansas City Terminal Ry., Kansas City, Mo. Mr. Hanna died on April 30, 1935.

[28a] Received by the Secretary April 27, 1935.

AMERICAN SOCIETY OF CIVIL ENGINEERS
Founded November 5, 1852

DISCUSSIONS

STRUCTURAL BEAMS IN TORSION

Discussion

By Messrs. P. Wilhelm Werner, F. L. Ehasz, W. P. Roop and John B. Letherbury, and Alfred T. Waidelich

P. Wilhelm Werner,[19] Assoc. M. Am. Soc. C. E. (by letter).[19a]—Torsion in structural beams has been studied, theoretically and experimentally, by several investigators, the most important of whom have been cited by the authors. The names of C. Weber,[20] C. Schmieden,[21] and H. Engelmann.[22] should be added for completeness. Weber[20] has treated the double-flanged type of section in general, and obtains the H-beam and I-beam sections as a special case of the general solution. In this connection he also explains the apparent relative weakness of channels in bending when compared with beams of symmetrical cross-section with the same moment of resistance.

Perhaps the most important result of the reported investigation is the method of evaluating the torsion constant, which is defined theoretically and substantiated by the tests. In view of the extensive tests presented in the paper, it would be of interest to know whether some data are also available regarding the influence of rivet holes upon the torsional rigidity and stresses in structural beams. As far as the writer is aware, this question has hitherto been neglected entirely in problems dealing with torsion. From the hydrodynamical analogy in the torsion theory,[23] however, it is known that a small hole, or cavity, near the edge of a twisted circular shaft will cause a considerable increase of the shearing stresses around the hole. It may be expected that a similar stress concentration will occur also around rivet holes in structural beams, although the holes may not materially influence the yielding of the beam as a whole.

Note.—The paper by Inge Lyse, M. Am. Soc. C. E., and Bruce G. Johnston, Jun. Am. Soc. C. E., was published in April, 1935, *Proceedings*. Discussion on this paper has appeared in *Proceedings*, as follows: April, 1935, by Messrs. H. M. Westergaard and R. D. Mindlin, and Joseph B. Reynolds; and August, 1935, by Messrs. Harold E. Wessman, and F. B. Seely and W. J. Putnam.

[19] Civ. Engr., A. B. Vattenbyggnadsbyran, Stockholm, Sweden.

[19a] Received by the Secretary July 11, 1935.

[20] "Uebertragung des Drehmomentes in Balken mit doppelflanschigen Querschnitt," by C. Weber, *Zeitschrift für angew. Math. Mech.*, Vol. 6, 1926, p. 85.

[21] "Ueber die Torsion von Walzeisen-Profilen," by C. Schmieden, *Zeitschrift für angew. Math. Mech.*, 1930, p. 251.

[22] Experimentelle und theoretische Untersuchungen zur Drehfestigkeit der Stäbe," by H. Engelmann, *Zeitschrift für angew. Math. Mech.*, 1929, p. 386.

[23] "Theory of Elasticity," by S. Timoshenko, 1934, p. 264.

With reference to the theoretical analysis, the paper deals exclusively with the case of a beam twisted by a constant torque, T, applied at its ends. It is of interest to note, that the results thus obtained may also be derived as a special case of a more general problem—a beam twisted by a concentrated torque, T_p, applied at an arbitrary point on the span. This general case is of considerable importance for practical design purposes.

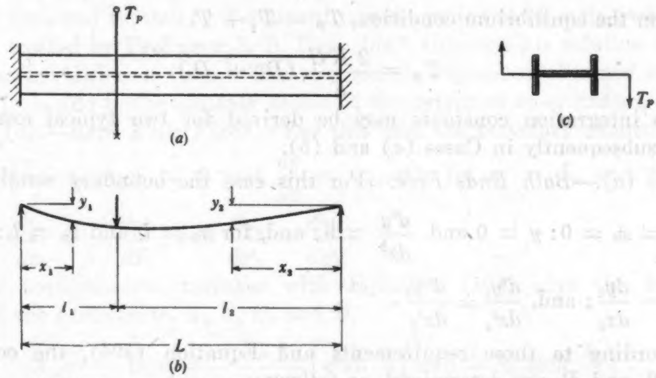

FIG. 35.—DIAGRAMMATICAL REPRESENTATION OF TWISTED I-BEAM.

Referring to Fig. 35, the general expression for the twisting moment is,

$$T_x = \frac{2\,K\,G}{h}\left(\frac{dy}{dx} - a^2\,\frac{d^3y}{dx^3}\right) \quad \text{.................(100)}$$

which is also the differential equation for the deflection of the flanges. It should be observed, however, that Equation (100), like the author's Equation (33), is strictly applicable only when the deflection is due to bending alone, which implies small ratios of $\beta = \frac{b}{L}$, or, that the flange width may be considered as small in relation to the span. From the general theory of beams in flexure it may be concluded that the ratio should be $\beta \leqq 0.25$ in order to keep the error in the calculated stresses within about 5 per cent.

If T_1 and T_2 denote the constant torque on the left and right-hand side of T_p, respectively:

$$T_1 = \frac{2\,K\,G}{h}\left(\frac{dy_1}{dx_1} - a^2\,\frac{d^3y_1}{dx^3_1}\right) \quad \text{...............(101a)}$$

and,

$$T_2 = \frac{2\,K\,G}{h}\left(\frac{dy_2}{dx_2} - a^2\,\frac{d^3y_2}{dx^3_2}\right) \quad \text{...............(101b)}$$

The solution of Equations (101) is,

$$y_1 = A_1 \sinh \frac{x_1}{a} + B_1 \cosh \frac{x_1}{a} + D_1\,x_1 + C_1 \quad \text{........(102a)}$$

and,

$$y_2 = A_2 \sinh \frac{x_2}{a} + B_2 \cosh \frac{x_2}{a} + D_2\,x_2 + C_2 \quad \text{........(102b)}$$

By differentiating Equations (102) and substituting in Equations (101):

$$T_1 = \frac{2\,K\,G}{h}\,D_1 \quad\ldots\ldots\ldots\ldots\ldots\ldots\ldots\ldots\ldots\ldots(103a)$$

and,

$$T_2 = \frac{2\,K\,G}{h}\,D_2 \quad\ldots\ldots\ldots\ldots\ldots\ldots\ldots\ldots\ldots\ldots(103b)$$

From the equilibrium condition, $T_p = T_1 + T_2$:

$$T_p = \frac{2\,K\,G}{h}\,(D_1 + D_2) \ldots\ldots\ldots\ldots\ldots\ldots\ldots\ldots(104)$$

The integration constants may be derived for two typical examples, as shown subsequently in Cases (*a*) and (*b*).

Case (*a*).—*Both Ends Free.*—For this case the boundary conditions are, for $x_1 = x_2 = 0$: $y = 0$ and $\dfrac{d^2y}{dx^2} = 0$; and, for $x_1 = l_1$ and $x_2 = l_2$: $y_1 = y_2$; $\dfrac{dy_1}{dx_1} = -\dfrac{dy_2}{dx_2}$; and, $\dfrac{d^2y_1}{dx_1^2} = \dfrac{d^2y_2}{dx_2^2}$.

According to these requirements and Equation (104), the coefficients, A, B, C, and D, are determined, as follows:

$$A_1 = -\frac{a\,h\,T_p}{2\,K\,G}\;\frac{\sinh\dfrac{l_2}{a}}{\sinh\dfrac{l_1}{a}\cosh\dfrac{l_2}{a} + \sinh\dfrac{l_2}{a}\cosh\dfrac{l_1}{a}} \ldots\ldots(105a)$$

$$A_2 = -\frac{a\,h\,T_p}{2\,K\,G}\;\frac{\sinh\dfrac{l_1}{a}}{\sinh\dfrac{l_1}{a}\cosh\dfrac{l_2}{a} + \sinh\dfrac{l_2}{a}\cosh\dfrac{l_1}{a}} \ldots\ldots(105b)$$

$$B_1 = B_2 = C_1 = C_2 = 0 \ldots\ldots\ldots\ldots\ldots\ldots\ldots\ldots\ldots\ldots(105c)$$

$$D_1 = +\frac{h\;T_p}{2\,K\,G}\,\frac{l_2}{L} \ldots\ldots\ldots\ldots\ldots\ldots\ldots\ldots\ldots\ldots(105d)$$

and,

$$D_2 = +\frac{h\;T_p}{2\,K\,G}\,\frac{l_1}{L} \ldots\ldots\ldots\ldots\ldots\ldots\ldots\ldots\ldots\ldots(105e)$$

By making $l_1 = l_2 = l = \dfrac{L}{2}$ and $T_p = 2\,T$:

$$A_1 = A_2 = -\frac{a\,h\,T}{2\,K\,G}\;\frac{l}{\cosh\dfrac{l}{a}} \ldots\ldots\ldots\ldots\ldots\ldots(106a)$$

and,

$$D_1 = D_2 = +\frac{h\,T}{2\,K\,G} \ldots\ldots\ldots\ldots\ldots\ldots\ldots\ldots\ldots\ldots(106b)$$

Then the deflection function for this case may be written,

$$y = \frac{a\,h\,T}{2\,K\,G}\left[\frac{x}{a} - \frac{\sinh\frac{x}{a}}{\cosh\frac{l}{a}}\right] \quad\ldots\ldots\ldots\ldots\ldots\ldots\ldots(107)$$

Equation (107) also represents the special case of a beam with one end fixed, the other free, and twisted by a constant torque applied at its ends—which case has been treated by Professor J. B. Reynolds,[24] although his solution is given in a somewhat different form. The very simple expression obtained in Equation, (107) is due to the suitable choice of the origin of co-ordinates.

Case (b).—Both Ends Fixed.—For this case the boundary conditions are, for $x_1 = x_2 = 0$: $y = 0$ and $\frac{dy}{dx} = 0$; and, for $x_1 = l_1$, and $x_2 + l_2$: $y_1 = y_2$; $\frac{dy_1}{dx_1} = -\frac{dy_2}{dx_2}$; and $\frac{d^2y_1}{dx^2_1} = \frac{d^2y_2}{dx^2_2}$.

These requirements, together with Equation (104) give the following values of the coefficients, A, B, C, and D,

$$\begin{aligned}A_1 = -D_1\,a = &-\frac{a\,h\,T_p}{2\,K\,G}\left[\sinh\frac{l_2}{a}\left(\sinh\frac{l_1}{a} + \sinh\frac{l_2}{a}\right)\right.\\
&+\left(\cosh\frac{l_1}{a} - \cosh\frac{l_2}{a}\right)\left(\cosh\frac{l_2}{a} - 1\right) - \frac{l_2}{a}\left.\left(\sinh\frac{l_1}{a}\cosh\frac{l_2}{a} + \sinh\frac{l_2}{a}\cosh\frac{l_1}{a}\right)\right]\\
&\div\left(\sinh\frac{l_1}{a} + \sinh\frac{l_2}{a}\right)^2 - \left(\cosh\frac{l_1}{a} - \cosh\frac{l_2}{a}\right)^2\\
&-\frac{L}{a}\left(\sinh\frac{l_1}{a}\cosh\frac{l_2}{a} + \sinh\frac{l_2}{a}\cosh\frac{l_1}{a}\right)\quad\ldots\ldots(108a)\end{aligned}$$

$$\begin{aligned}A_2 = -D_2\,a = &-\frac{a\,h\,T_p}{2\,K\,G}\left[\sinh\frac{l_1}{a}\left(\sinh\frac{l_1}{a} + \sinh\frac{l_2}{a}\right)\right.\\
&-\left(\cosh\frac{l_1}{a} - \cosh\frac{l_2}{a}\right)\left(\cosh\frac{l_1}{a} - 1\right) - \frac{l_1}{a}\left.\left(\sinh\frac{l_1}{a}\cosh\frac{l_2}{a} + \sinh\frac{l_2}{a}\cosh\frac{l_1}{a}\right)\right]\\
&\div\left(\sinh\frac{l_1}{a} + \sinh\frac{l_2}{a}\right)^2 - \left(\cosh\frac{l_1}{a} - \cosh\frac{l_2}{a}\right)^2\\
&-\frac{L}{a}\left(\sinh\frac{l_1}{a}\cosh\frac{l_2}{a} + \sinh\frac{l_2}{a}\cosh\frac{l_1}{a}\right)\quad\ldots\ldots(108b)\end{aligned}$$

$$\begin{aligned}B_1 = -C_1 = &-\frac{h\,T_p}{2\,K\,G}\left[\sinh\frac{l_2}{a}\left(l_2\sinh\frac{l_1}{a} - l_1\sinh\frac{l_2}{a}\right)\right.\\
&-\left(\cosh\frac{l_1}{a} - 1\right)\left(a\sinh\frac{l_2}{a} - l_2\cosh\frac{l_2}{a}\right)\\
&-\left(\cosh\frac{l_2}{a} - 1\right)\left.\left(a\sinh\frac{l_1}{a} - l_1\cosh\frac{l_2}{a}\right)\right]\div\left(\sinh\frac{l_1}{a} + \sinh\frac{l_2}{a}\right)^2\\
&-\left(\cosh\frac{l_1}{a} - \cosh\frac{l_2}{a}\right)^2 - \frac{L}{a}\left(\sinh\frac{l_1}{a}\cosh\frac{l_2}{a} + \sinh\frac{l_2}{a}\cosh\frac{l_1}{a}\right).(108c)\end{aligned}$$

[24] *Proceedings*, Am. Soc. C. E., April, 1935, p. 515.

and,

$$B_2 = - C_2 = - \frac{h\,T_p}{2\,K\,G} \left[\sinh \frac{l_1}{a} \left(l_1 \sinh \frac{l_2}{a} - l_2 \sinh \frac{l_1}{a} \right) \right.$$

$$- \left(\cosh \frac{l_1}{a} - 1 \right) \left(a \sinh \frac{l_2}{a} - l_2 \cosh \frac{l_1}{a} \right)$$

$$\left. - \left(\cosh \frac{l_2}{a} - 1 \right) \left(a \sinh \frac{l_1}{a} - l_1 \cosh \frac{l_2}{a} \right) \right]$$

$$\div \left(\sinh \frac{l_1}{a} + \sinh \frac{l_2}{a} \right)^2 - \left(\cosh \frac{l_1}{a} - \cosh \frac{l_2}{a} \right)^2$$

$$- \frac{L}{a} \left(\sinh \frac{l_1}{a} \cosh \frac{l_2}{a} + \sinh \frac{l_2}{a} \cosh \frac{l_1}{a} \right) \qquad \text{(108d)}$$

By making $l_1 = l_2 = l = \dfrac{L}{2}$ and $T_p = 2\,T$:

$$A_1 = A_2 = - D_1\,a = - D_2\,a = - \frac{a\,h\,T}{2\,K\,G} \qquad \text{(109a)}$$

and,

$$B_1 = B_2 = - C_1 = - C_2 = + \frac{a\,h\,T}{2\,K\,G} \tanh \frac{l}{2\,a} \qquad \text{(109b)}$$

and the deflection function for this case may be written,

$$y = \frac{a\,h\,T}{2\,K\,G} \left(- \sinh \frac{x}{a} + \tanh \frac{l}{2\,a} \cosh \frac{x}{a} + \frac{x}{a} - \tanh \frac{l}{2\,a} \right) \qquad \text{(110)}$$

Equation (110) also represents the special case treated by the authors, namely, a beam twisted by a constant torque, T, applied at its ends, with both ends restrained.

In the "General Remarks" under "Design Examples" the authors state that "the local direct stresses * * * are in the nature of secondary stresses" and suggest that "allowable fiber stresses usual in secondary stress design be applied in general to these stresses." Referring, for instance, to Loading Cases (*a*) and (*b*) in this discussion, which represent typical torsion problems in practical design, the writer would not feel inclined to accept a specification that the direct fiber stresses obtained in the flanges should generally be classed as secondary stresses. As a matter of fact, the twisting of the beam may be conceived as pure bending of the two flanges, which are supported by an elastic medium, the reacting forces of which are reflected by the torsional rigidity of the twisted elements of the beam.

Consider, now, a beam which is simply supported in both ends and subjected to a twisting moment, T_p, applied at the center. The deflection function for this case, according to Equation (107), may be written,

$$y = \frac{a\,h\,T_p}{4\,K\,G} \left(\frac{x}{a} - \frac{\sinh \dfrac{x}{a}}{\cosh \dfrac{L}{2\,a}} \right) \qquad \text{(111)}$$

The bending moment in each flange is,

$$M = -\frac{E I_y}{2} \frac{d^2 y}{dx^2} = \frac{a\, T_p}{2\, h} \frac{\sinh \frac{x}{a}}{\cosh \frac{L}{2\, a}} \quad \text{..............(112)}$$

and thus the maximum moment (at the center of the beam), is,

$$M_o = \frac{a\, T_p}{2\, h} \tanh \frac{L}{2\, a} \quad \text{....................(113)}$$

If, momentarily, the beam is assumed to have no torsional rigidity (that is, if the flanges are required to take the entire superimposed torsional load) the corresponding maximum bending moment in each flange would be,

$$M_f = \frac{T_p}{h} \frac{L}{4} \quad \text{..........................(114)}$$

The ratio between the two moments is,

$$\kappa = \frac{M_o}{M_f} = \frac{\tanh \lambda}{\lambda} \quad \text{......................(115)}$$

in which, $\lambda = \frac{L}{2\, a}$. The value of κ is given in Fig. 36 for various ratios, λ.

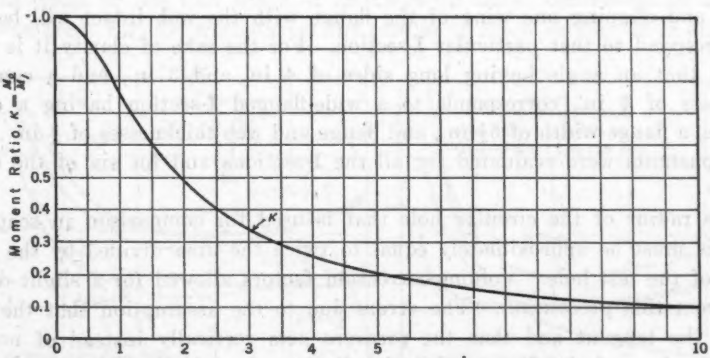

FIG. 36.—GRAPHICAL REPRESENTATION OF EQUATION (115)

As indicated, the writer's derivations are applicable only for $\beta \leq 0.25$, and the inaccuracy increases as β increases. Equation (115), however, gives a clue as to how the problem may be approached for $\beta > 0.25$. Consider, for example, a beam with the same dimensions as in the author's Design Example *B*—that is, with $b = 8.29$ in. and $2\, a = 54$ in. For $\beta = 0.25$ in this case, $L = 33.2$ in. and $\lambda = 0.615$. According to Fig. 36 this corresponds to $\kappa = 0.9$, or M_f varies as 1.11 M_o. This means that for $\beta > 0.25$ one may compute—at least for the beam under consideration—approximately (the inaccuracy is maximum 11% on the safe side) the stresses in the flanges under the assumption that each flange acts as a beam, or rather as a narrow plate, the depth

of which cannot be considered as small in relation to the span width and which is stressed by a force, $P = \frac{T_p}{h}$, in its own plane.

F. L. EHASZ,[25] JUN. AM. SOC. C. E. (by letter).[25a]—In Fig. 9 the authors demonstrate the fact that there has been considerable diversity of opinion regarding the problem of stress concentration in the fillets of twisted bars. Several analytical and experimental solutions giving widely varying results have been proffered. Consequently, the effect of size and shape of structural members on torsional behavior was investigated in an attempt to help in the final solution of this problem. More than eighty experimental solutions involving various structural shapes were found. The membrane analogy provided a fairly rapid method for determining the increase of shearing stress in fillets by means of soap films. Torsion constants were also obtained for most of the sections analyzed.

The following variables were studied: The radius of fillets, length and thickness of the components of the member, and the shape of the member, angle, or I-section. In each series, the fillet varied from about $\frac{1}{8}$ in. to $1\frac{1}{2}$ in. Eight series of angles having $\frac{1}{2}$-in. to 1-in. thicknesses and 3 to 6-in. lengths; and three series of I-beams with wide flanges, corresponding to three of the angle series, were analyzed to determine the change of the hump at the junctures. An angle formed by taking half the I-section (that is, a T-section), and clipping one wing of the flange with the web intact will be said to correspond to that particular I-section. For the sake of clarity it is mentioned that an angle having long sides of 4 in. and 3 in., and a constant thickness of $\frac{3}{4}$ in., corresponds to a wide-flanged I-section having a depth of 8 in., a flange width of $5\frac{1}{4}$ in., and flange and web thicknesses of $\frac{3}{4}$ in. Torsion constants were evaluated for all the I-sections and for six of the angle series.

The radius of the circular hole that is used for comparison in soap-film analysis must be approximately equal to twice the area divided by the perimeter of the test hole. Volume-correction factors allowed for a slight deviation from this precaution. The errors due to the assumption that the sine equals the tangent and that the pressure acts vertically instead of normal to the surface of the film are largely eliminated, and pressure correction is achieved by resorting to the volume-correction curve which was procured by testing several sections of known torsional properties against each other, two at a time. The initial height of water in the flask, an essential part of the volume-displacement apparatus, was kept, at all times, approximately equal to that prevailing in the preliminary volume-correction tests.

In contour work, the height of the circular film was checked after every five or six points to insure that conditions remained constant. Elevations were correct to within 0.001 in. It was found that a boundary angle ranging between 15° and 25° was advisable for the circular film in order to obtain a

[25] Lawrence Calvin Brink Research Fellow in Civ. Eng., Lehigh Univ., Bethlehem, Pa.

[25a] Received by the Secretary July 15, 1935.

precision of 2% in the stress concentration tests. For satisfactory volume measurements the boundary angle for the test film should not exceed 35 degrees. The minimum radius of the circular section in this investigation was ½ in., a value which, according to Taylor,[26] should be considered the minimum allowable for reliable results. In the case of a symmetrical shape, such as the I-beam, only one-half the section was studied. A vertical septum passing through the axis of symmetry provided the essential continuity. It was necessary to double the torsion constant of the reduced shape in order to obtain the desired constant.

After a few complete contour diagrams were made, it was thought best to diminish the work required for a section by adopting the so-called cross-section method wherein points spaced from 0.03 to 0.1 in. apart along a normal to the boundary were located and their elevations recorded. Especial care and smaller spacings were taken immediately near the edge, since the crux of the slope determination lies there. Tangents to enlarged drawings of the films at the boundaries gave a direct measure of the border shearing stresses. Cross-sections were taken in the case of angles at the center of the fillet and at the center of the inner straight portion of the flanges. For I-sections additional slope data were recorded for the web. The shearing stress in the fillet could thus be compared with that in the arms of angles and with the shear in the flange and web of I-sections.

The effect of size and shape of members on stress concentration may be observed from Fig. 37, which gives the results of a few series. It is apparent

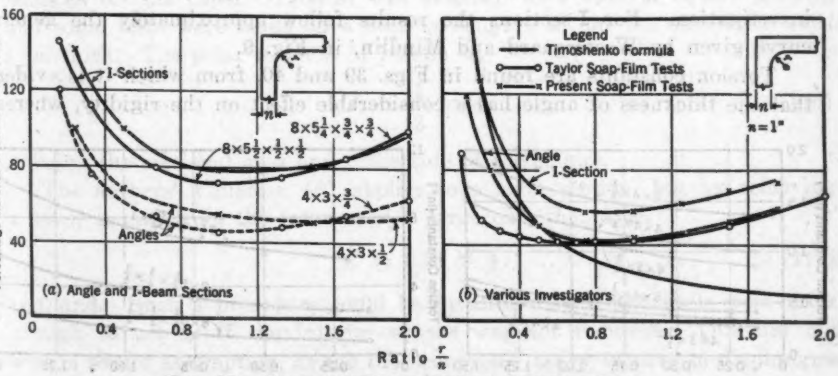

FIG. 37.—COMPARISONS OF STRESS CONCENTRATION.

from Fig. 37(*a*) that the stress concentrations of I-sections are considerably greater than for their corresponding angles. An angle, 4 by 3 in. by ½ in., is one having long sides, 4 in. and 3 in., with the thickness of both legs ½ in. An I-section, 8 by 5¼ in. by ¾ by ¾ in., has a depth of 8 in., a flange width of 5¼ in., with web and flange thicknesses of ¾ in. That the stress varies directly with the thickness may be concluded from the fact that

[26] "The Mechanical Properties of Fluids: A Collective Work," 1924, p. 236.

the fillet-stress concentration factors are inversely related to the thickness. The lowest points on the curves are peculiar in two respects. As the thickness of the straight part increases, the ratio of fillet to thickness for the minimum concentration decreases linearly according to Fig. 38, which also shows a fairly straight-line variation of the magnitude of the minimum concentration factor. This was obtained by taking averages of all the angle series.

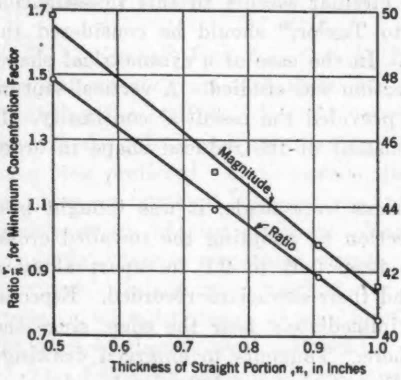

FIG. 38.

A comparison of the results of this investigation with those of Timoshenko's analytical solution and Taylor's soap-film tests is found in Fig. 37(*b*). For small fillets, including the usual radii, Timoshenko's formula proved to be superior to all others for angles. Timoshenko obtained his approximate theoretical solution[27] from the membrane analogy by assuming that the shearing stress in the fillet becomes zero at a point, $\frac{n}{2}$, from the boundary, in which n is the thickness of flange. Soap-film tests showed that this assumption is true for small radii of the fillet, r. For larger fillet sizes there is fair agreement between the tests of Taylor and those of the present investigation. For I-sections the results follow approximately the general curve given by Westergaard and Mindlin, in Fig. 9.

Torsion constants are found in Figs. 39 and 40, from which it is evident that the thickness of angle has a considerable effect on the rigidity, whereas

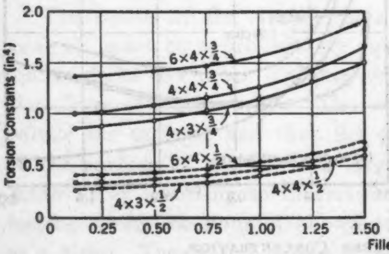

FIG. 39.—TORSION CONSTANTS FOR ANGLES

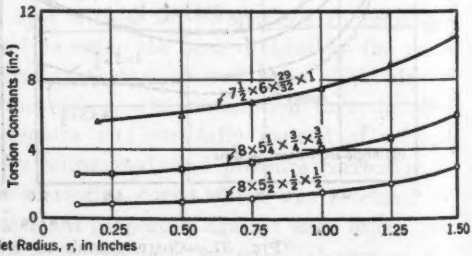

FIG. 40.—TORSION CONSTANTS FOR I-SECTIONS.

the effect of length of arm is comparatively small. Experimental results were checked analytically and a fair precision was noted.

The following are the principal deductions drawn from these tests: (1) The inherent relations of the membrane analogy have proved especially useful in determining the stress concentration factors at the fillets of a

[27] "Theory of Elasticity," by S. Timoshenko, First Edition, 1934, p. 258.

twisted rod; (2) Timoshenko's formula for stress concentration proved suitable for the usual fillet radii in the case of angles, whereas that proposed by Westergaard and Mindlin (see Fig. 9) gave results having similar tendencies manifested in the present tests on I-sections; (3) observations of the soap films in the case of I-sections confirmed the fact mentioned by the authors that the critical shearing stresses prevail at the fillets and at the center of the outer side of the flange; (4) there is a linear relation between the minimum percentage increase of stress in the fillets of angles and the thickness of the straight portion (the ratio of fillet size to flange thickness, $\frac{r}{n}$, for minimum concentration factor also shifts linearly with variation in thickness); (5) the shearing stress, in general, increases linearly with the thickness (in I-sections, however, the stress in the web is slightly greater than in the flange for the same web and flange thickness. The stress falls off rapidly at the fillet, the rate being greater for small radii); and, (6) for ductile materials not subjected to alternating stress, the use of small fillets does not involve danger because of the redistribution of stress that follows local yielding. In the case of brittle materials, however, the weakening effect of the stress concentration should be mitigated by the use of greater fillet radii.

W. P. ROOP,[28] M. AM. SOC. C. E., and JOHN B. LETHERBURY,[29] JUN. AM. SOC. C. E. (by letter).[29a]—Although in this paper no procedure is outlined for estimating torsional rigidity of tubular sections, when the writers recently had occasion to deal with such a section, an effort was made to apply the methods of this paper. Interest was attached to a tube of square section, and some tests were made on a section about 1 in. on the side with walls $\frac{1}{8}$ in. thick. The polar moment of inertia is,

$$J = \frac{1}{3}\, b^2 A \ldots\ldots\ldots\ldots\ldots\ldots\ldots\ldots (116)$$

A being the sectional area and b the side of the square.

The authors' Equation (6) applies to a solid section, but by removing a small square from the interior of a large one, the value,

$$K = 0.28\, b^2 A \ldots\ldots\ldots\ldots\ldots\ldots\ldots\ldots (117)$$

is found. Such a procedure could be justified only if the walls were thick enough to act as if the interior square was not removed. This did not seem a severe assumption, as the tube contained heavy transverse diaphragms spaced about $\frac{3}{2}\, b$. Nevertheless, when such a tube was made and an experimental value of K was found by measuring torsional deflection under known load, it proved to be only about one-fourth the value calculated by Equations (116) and (117).

[28] Lt. Comdr. (C.C.), U. S. Navy; Office of Superintending Constructor, New York Shipbuilding Co., Camden, N. J.

[29] Hull Draftsman, New York Shipbuilding Co., Camden, N. J.

[29a] Received by the Secretary July 19, 1935.

The next step was to make up another tube using more care. Both tubes were welded up, but in the second case the welding was continuous and more uniform. However, when allowance was made in the calculations for the area of the weld fillets, the result was almost the same as at first, that the effective value of K was only about one-third to one-fourth the calculated value.

One objective in this work was to obtain verification of a formula for torsion of a tube of toroidal form. When the toroid was constrained to lie in a plane, the angular deflection was found by calculation to be,

$$\theta = \frac{\pi}{8} \times \frac{M R}{K G} \qquad (118)$$

in which θ is the angle of rotation, in radians, caused by a couple, M, applied in a radial plane, R being the ring radius and G the shearing modulus.

Equation (118) was rather closely verified by test, provided the experimental value of K from the straight tube was used. This afforded some additional evidence for the correctness of the value of K, being about one-fourth the calculated value.

It is noted that a square tube is shown in Fig. 8(f), but it is not clear how the data given can be applied to the writers' problem, as it appears that tubes of equal sectional area would differ in torsional rigidity according to the wall thickness and the corresponding size of the square chosen. Comparison between cases, Fig. 8(f) and Fig. 8(h), suggests that the closed section has much greater rigidity, but in this case also the basis of the comparison is uncertain.

Application of the methods described under "Torsion Constant for H-beams and I-beams," to the closed section very naturally leads to a value that is too low by a margin greater than that by which Equation (6) is too high. It is evident that the square tubular section has a rigidity intermediate between the values as calculated by these two quite different procedures.

As compared with the open section, two powerful influences work to give the tube increased rigidity. The first is that of closing the section, as shown in comparing Cases (b) and (c), Fig. 8. The benefit obtained by the short longitudinal plates at the ends, as in Fig. 15, may be only partly in the improved end constraint; part of the benefit may consist in the partial closure of the section. The question arises whether additional benefit might not be easily obtainable by introducing additional shear connections between toes of flanges at sections other than the ends.

The other influence is that of the diaphragms. Their function is like that of the fillets, but they are naturally much more effective than fillets. This suggests that the tripping brackets now commonly fitted in certain I-sections may be of considerable benefit for torsional rigidity.

For specific comparisons, the numerical data, referring to the sections tested, are given in Table 6.

In general agreement with the developments in this paper, under the heading "Fixed-Ended Torsion," the writers have had some success in devising a

set of artificial assumptions that will give a value of K for a tubular section in fair agreement with observations. This is only hindsight, however, and the writers feel rather certain that such precarious assumptions as those which have thus been found to work (that is, flat sides are beams which remain flat under load) would not be very highly regarded if the effective

TABLE 6.—NUMERICAL DATA.

Description	First bar	Second bar	Ring
Sectional area, A, in inches ²	0.58	0.61	0.703
Equivalent side of Square b, in inches	1.06	1.08	1.06+
Polar moment of inertia, J, in inches ⁴	0.218	0.237	0.307
K by Equation (6), in inches ⁴	0.184	0.199	0.30 (?)
K by Equation (16), in inches ⁴ *	0.009	0.015	0.015—
Observed K, in inches ⁴	0.053	0.080	0.128

* Ignoring webs.

value of K were not known from test data. Possibly, a solution of some merit might be found in this way, but it would require further verification by test and, therefore, would become no rational solution, but only a somewhat rational expression of empirical data.

In the light of these considerations the decision was made to use Equation (6) and calculate K for a tubular section by subtracting the value for the inner profile from that for the outer profile; but to apply a factor of from 2 to 3 to account for the deficiency of the effective value as compared with the value thus calculated.

The models referred to were made by the New York Shipbuilding Corporation and tested in its laboratory.

ALFRED T. WAIDELICH,[30] JUN. AM. SOC. C. E. (by letter).[30a]—An important research, for which there was a very real need, is described in this paper. An obvious application is in the design of spandrel beams and other beams with eccentric loading. Not only has this research indicated the method of analysis in such a case, but already it has made available for the designer one practical set of formulas and tables[31] for the two most common cases: A beam with a full uniform load applied with constant eccentricity; and a beam with a single eccentric concentrated load at the center of the span. It should be only a short time until the standard textbooks and handbooks will treat adequately the subject of torsional loads.

The dual practical problem of designing apparatus capable of twisting the larger steel sections and, at the same time, preserving a free end connection has been given a simple solution. This problem has prevented previous investigators from testing any but the smaller and lighter sections, with the result that the tests were inconclusive.

Definitely, the authors have settled the problem of determining the torsion constant for structural I-beams and H-beams. This constant is far more

[30] Asst. Prof. in Civ. Eng., Robert Coll., Galata, Istanbul, Turkey.

[30a] Received by the Secretary August 1, 1935.

[31] Bethlehem Manual of Steel Construction, 1934, pp. 279–289.

useful than the scant attention it has received would indicate. An early structural use of it was contained in a small book on the bow girder[32] which describes some torsion tests on small English joist beams. About the same time the constant appeared in aircraft design and in the study of the elastic stability of structures.

The principles of elastic stability are of increasing importance as the use of high-strength alloy steels increases, and as structural layouts become simpler. Thus, the modern catenary-supporting bent for railway electrification is a simple H-frame, consisting of three rolled shapes lying in one plane. Designers of such structures have been handicapped by the uncertainty of the value of the torsion constant. As a result, the few available tentative tabulations of the torsion constant[33] were considerably in error on the safe side, so that the full economy of this method of analysis could not be realized.

The measurement of fiber stresses in the beams under torsion furnishes a much needed check on the theoretical stresses. It is interesting that for the shear stress in the web, Equation (26) gives values that are definitely lower than those measured. The statement by the authors that Equation (26) is in accord with torsional theory is probably based on the assumption that the web acts as a part of an infinitely long rectangle undergoing the same degree of twisting as the flanges. Apparently, the proportions of the wide-flanged shapes (a relatively thin web tying together heavy flanges) prevents the web from playing such a simple rôle. It is unfortunate that the web stresses were not measured in the tests of the beams with web and flanges of nearly the same thickness. Since the governing shear stress will rarely occur in the web, Equation (27) is acceptable, although the introduction of the radius of the fillet does not seem logical—especially since this stress occurs at the center of the side of the web. Fig. 21 is interesting in that it shows an increase in the web shear stress as the fillet is approached (but before there is any increase in the web thickness). This is confirmed by the slope of the soap film, which increases on approaching the fillet because of the steep slope at the fillet and the "hump" at the junction of the web and the flanges.

[32] "The Circular Arc Bow Girder," by Gibson and Ritchie, 1914.

[33] For example, "Elastic Equilibrium in the Theory of Structures," by H. S. Richmond, *Transactions*, Am. Soc. C. E., Vol. 94 (1930), Table 1, p. 860.

AMERICAN SOCIETY OF CIVIL ENGINEERS
Founded November 5, 1852
DISCUSSIONS

PHOTO-ELASTIC DETERMINATION OF SHRINKAGE STRESSES

Discussion

BY J. H. A. BRAHTZ, ESQ.

J. H. A. BRAHTZ,[10] Esq. (by letter).[10a]—The sections of the paper entitled "Method of Solution" and "Theory of New Method" are valuable contributions to the theory of photo-elasticity in that they demonstrate how to evaluate the stresses within the boundaries of a stressed body.[11] The membrane method described by the author has been successful in the photo-elastic laboratory of the U. S. Bureau of Reclamation. The over-all error in the experiments on heavy monolithic structures is estimated to be from 5 to 10%, depending on the type of structure and loading.

The section of the paper entitled "Application of New Method," gives numerical values of the shrinkage stresses in a gravity dam far smaller than those obtained by the writer based on theoretical considerations and photo-elastic experimentation. For example, for the horizontal stresses along the bisector of the top angle of a 45° triangular dam, set on a rigid foundation, the writer finds the following approximate solution (taking the two first terms of an infinite series):

$$\sigma = \left\{ \left(\frac{r}{h}\right)^{4.39} \left[1.82 \cos\left(2.7 \log \frac{r}{h}\right) - 0.62 \sin\left(2.7 \log \frac{r}{h}\right)\right] - \left(\frac{r}{h}\right)^{12.66} \left[0.78 \cos\left(3.8 \log \frac{r}{h}\right) + 0.15 \sin\left(3.8 \log \frac{r}{h}\right)\right]\right\} K E \quad \ldots (9)$$

in which r = the distance from the vertex; h = the height of vertex above the foundation (measured along the bisector); E = the elastic modulus of elasticity; and, K = the shrinkage per unit length. If $r = h$, the horizontal stress at the foundation becomes:

$$\sigma_1 = 1.04\, K\, E \ldots\ldots\ldots\ldots\ldots\ldots\ldots\ldots (10)$$

NOTE.—The paper by Howard G. Smits, Esq., was published in May, 1935, *Proceedings*. Discusion on this paper has appeared in *Proceedings* as follows: September, 1935 by Messrs. Thomas H. Evans, and I. K. Silverman.

[10] Engr., U. S. Bureau of Reclamation, Denver, Colo.

[10a] Received by the Secretary August 9, 1935.

[11] See, also, *Zeitschrift angew. Math.*, Vol. II, 1931, p. 156.

which value is estimated to be 10% too high due to the omission of the higher order terms in Equation (9). Using the value of K in Fig. 10, that is, $K = 0.0016$, the stress becomes $\sigma_1 = 0.001664\ E$.

The author does not give the value of E in concrete used in the calibration of the test. However, assuming E to be 2 000 000 lb per sq in., the stress would be, $\sigma_1 = 3\,328$ lb per sq in.; and, with $E = 3\,000\,000$ lb per sq in., the stress would be, $\sigma_1 = 4\,992$ lb per sq in.

These quantities are not directly comparable with the author's stresses in Figs. 10 and 11, because he assumes an elastic foundation of the same modulus as the dam. Consequently, when the dam shrinks, there will be a compromise between the foundation and the dam, the former going into compression in the region directly below the dam and the latter into tension. It will not be an even division, however, because the foundation does not deform quite as readily as the dam with its much smaller mass; and, therefore, it imposes the greater part of the shrinkage as an elongation of the elements of the dam adjacent to the foundation.

Using the stresses given in Fig. 11 at the foundation (630 in the dam and 460 in the foundation) as a basis of the compromise, the computed stress in the dam would be, $\frac{630}{630 + 460}\ \sigma_1$, or 1 920 and 2 886, respectively, depending on the value of E introduced in Equation (10). These stresses are from three to five times the value (630) given in Fig. 11, depending on the value of E that the author adopted for his calibration.

Based on the writer's theory and experiments, he concludes that the average horizontal tensile stress along the base of a dam on an elastic foundation varies from 5 to 15 lb per sq in. per degree Fahrenheit of decrease in temperature, depending on the ratio of the elastic moduli in the dam and the foundation. This range of stress shows the dire necessity of providing against shrinkage effects during construction by cooling and pressure grouting.

AMERICAN SOCIETY OF CIVIL ENGINEERS
Founded November 5, 1852

DISCUSSIONS

THE SHEAR-AREA METHOD

Discussion

BY MESSRS. ALBIN H. BEYER, JOHN M. BEATTY, R. B. PECK, RALPH W. STEWART, C. W. JOHNSON AND H. W. BIRKELAND, GARRETT B. DRUMMOND, AND HAROLD E. WESSMAN

ALBIN H. BEYER,[14] M. AM. SOC. C. E. (by letter).[14a]—The claim is advanced by the authors that the shear-area method as described in their paper has the advantage over the standard-moment area method, in that it provides a simpler figure to work with, and that its use simplifies the solution for slope and deflection. This claim would be true if the authors had not introduced the computations of moments and shears in their so-called mathematical beam, loaded by the shear-area loading and supported in a hypothetical manner. The shear-area method of computation can be applied readily to any beam and loading without introducing the hypothetical beam and loading, which complicates rather than simplifies the solution.

To use any fundamental formula intelligently, the engineer must be familiar with its derivation and the meaning and sign of every symbol used. Therefore, the writer presents briefly, first the derivation of the fundamental formulas involved and, second, their application to two comparatively simple problems.

Derivation of Fundamental Formula for the General Case of a Loaded Beam.—Fig. 36(*a*) shows the beam and loading; the end restraining moments, M_A and M_B, are indicated as negative.

Fig. 36(*b*) shows the straight beam, $B\,O\,A$, deflected under the loads to the position, $B\,O'A$, where $O\,O' = y_o$, is the desired deflection of the beam at any point, O, distant x_A from A; θ_o is the slope of the beam at this point; and θ_A and θ_B are the slopes of the beam at A and B, respectively.

Select a Cartesian system of co-ordinates with the origin at O, where the deflection and slope are desired, distant x_A, a variable, from A; x is measured positive to the right of O, and y is measured positive upward. With this system of co-ordinates, the signs which apply are indicated in Fig. 37.

NOTE.—The paper by Horace B. Compton, Assoc. M. Am. Soc. C. E., and Clayton O. Dohrenwend, Jun. Am. Soc. C. E., was published in May, 1935, *Proceedings*. Discussion on the paper has appeared in *Proceedings*, as follows: August, 1935, by Messrs. George S. Large, Samuel T. Carpenter, Roland H. Trathen, A. W. Fischer, J. Charles Rathbun, Harold R. Kapner, and Fred L. Plummer.

[14] Prof. of Civ Eng., Columbia Univ., New York, N. Y.

[14a] Received by the Secretary July 18, 1935.

The differential equation of the deflected beam is given by the classifical formula,

$$\frac{d^2y}{dx^2} = \frac{d}{dx}\left(\frac{dy}{dx}\right) = \frac{M}{E\,I} \quad \text{.....................(150)}$$

Multiplying the last two terms by $x\,dx$ gives,

$$x\,d\left(\frac{dy}{dx}\right) = \frac{M\,x\,dx}{E\,I} \quad \text{.....................(151)}$$

Integrating both sides between the limits, O and A, using the method of parts for the first term:

$$\left[x\frac{dy}{dx} - y\right]_0^{x_A} = \int_0^{x_A} \frac{M\,x\,dx}{E\,I} \quad \text{................(152)}$$

or,

$$y_o = y_A - x_A\,\theta_A + \int_0^{x_A} \frac{M\,x\,dx}{E\,I} \quad \text{................(153)}$$

Equation (153) is the fundamental general formula of the moment-area method.

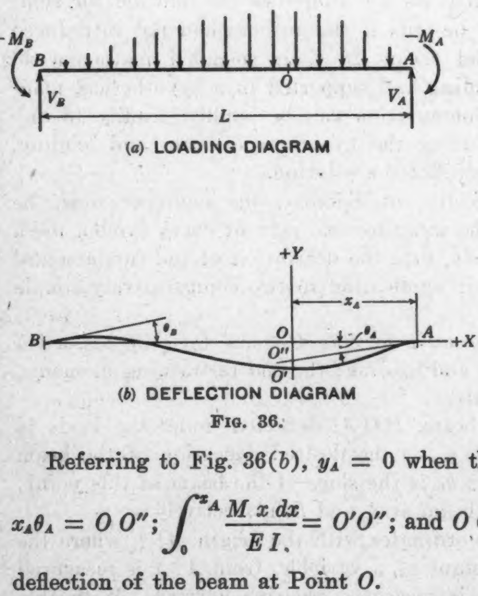

FIG. 36.

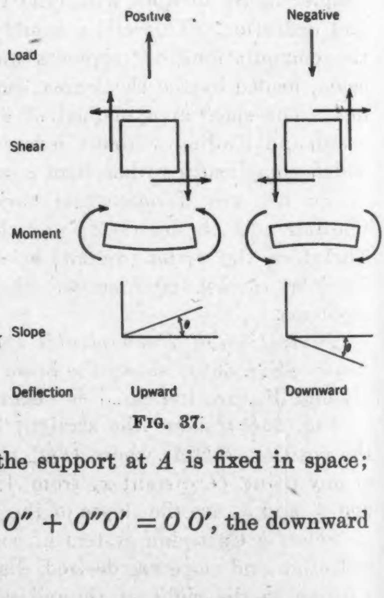

FIG. 37.

Referring to Fig. 36(b), $y_A = 0$ when the support at A is fixed in space; $x_A\theta_A = O\,O''$; $\int_0^{x_A} \frac{M\,x\,dx}{E\,I} = O'O''$; and $O\,O'' + O''O' = O\,O'$, the downward deflection of the beam at Point O.

The authors' contribution to this well-known theory consists in expressing M, the bending moment at any point, in terms of the shear area. In general, $M = M_A - \int_x^{x_A} V\,dx$, in which the last term is the shear area from x to x_A.

The equation for y_O expressed in terms of the shear area, O to A, then becomes,

$$y_o = y_A - x_A\theta_A + M_A \int_0^{x_A} \frac{x\,dx}{EI} - \int_0^{x} \left(\int_x^{x_A} \frac{V\,dx}{EI} \right) x\,dx \ldots (154)$$

a very much more complicated expression than Equation (153). Only when E and I are constant can Equation (154) be simplified to,

$$y_o = y_A - x_A\theta_A + \frac{M_A\,x^2_A}{2\,EI} - \frac{I_x}{2\,EI} \ldots\ldots\ldots\ldots\ldots (155)$$

in which I_x is the moment of inertia of the shear area (sign to be determined in accordance with Fig. 37) to the right of the origin of co-ordinates taken about the Y-axis through the origin. Taking the first derivative of y_o with respect to x_A (noting that $\frac{dy_o}{dx_A}$ is negative):

$$\theta_o = +\,\theta_A - \frac{M_A\,x_A}{EI} + \frac{A\bar{x}}{EI} \ldots\ldots\ldots\ldots\ldots\ldots (156)$$

In Equation (156) $A\bar{x}$ is the static moment of the shear area between O and A about the Y-axis through O, using the signs for the shear area as determined by Fig. 37.

Application of Formula to Beams with Constant Moment of Inertia.—The general equations to be used are,

$$y_o = y_A - x_A\theta_A + \frac{M_A\,x^2_A}{2\,EI} - \frac{I_x}{2\,EI} \ldots\ldots\ldots\ldots\ldots (157)$$

and,

$$\theta_o = +\,\theta_A - \frac{M_A\,x_A}{EI} + \frac{A\bar{x}}{EI} \ldots\ldots\ldots\ldots\ldots\ldots (158)$$

The general formulas, Equations (157) and (158), give the deflection, y_o, and the slope, θ_o at any point, O, distant x_A from A, in terms of the shear area. They can be applied directly to any beam or loading when the end shears and moments have been computed. For statically indeterminate beams, they can also be used for determining the end moments and shears. In solving these equations, the analogy of a hypothetical beam and loading is not necessary and is not recommended by the writer as the analogy does not contribute to the directness or simplicity of the solution, as can be seen from the following typical examples.

Analysis of Statically Determinate Beams (Authors' Case I).—The general formulas required are:

$$y_o = y_A - x_A\theta_A + \frac{M_A\,x^2_A}{2\,EI} - \frac{I_x}{2\,EI} \ldots\ldots\ldots\ldots\ldots (159)$$

and,

$$\theta_o = \theta_A - \frac{M_A\,x_A}{EI} + \frac{A\bar{x}}{EI} \ldots\ldots\ldots\ldots\ldots\ldots (160)$$

In this case, y_A and M_A are each equal to zero. The value of θ_A can be computed by means of Equation (159) or Equation (160). Equation (160) is used because of its simple form; also, from symmetry, $\theta_B = -\theta_A$.

Using Equation (160) (making $x_A = L$ (see Fig. 38)):

$$-\theta_A = \frac{A\bar{x}}{2EI} \qquad \text{......................(161)}$$

In Equation (161), $A\bar{x}$ is the static moment of the shaded shear area about a vertical axis through B and is equal to $-\frac{WL^3}{12}$; therefore, $\theta_A = \frac{WL^3}{24EI}$.

From Equation (159), therefore, the elastic curve is expressed by:

$$y_o = -x_A\theta_A - \frac{I_x}{2EI} \qquad \text{....................(162)}$$

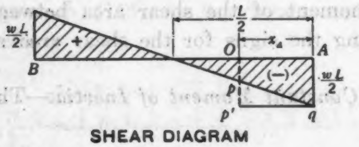

FIG. 38.

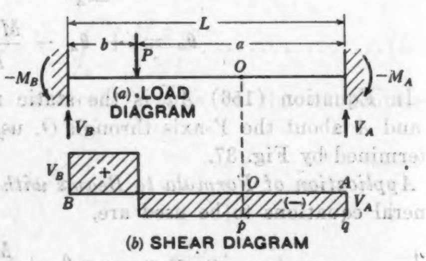

FIG. 39.

in which, I_x is the moment of inertia of the trapezodial shear area, $O\,p\,q\,A$ (Fig. 38) about $O\,p$, and is equal to the static moment of the rectangle, $O\,p'\,q\,A$, minus that of the triangle, $p\,p'\,q$, all of which is equal to $-\frac{1}{6}\,w\,L x^3_A + \frac{w x^4_A}{12}$.

The equation of the elastic curve then becomes,

$$y_o = -\frac{w L^3 x_A}{24\,EI} + \frac{w\,L\,x^3_A}{12\,EI} - \frac{w x^4_A}{24\,EI} \qquad \text{..........(163)}$$

which, for $x_A = \frac{L}{2}$, gives:

$$y_o = -\frac{5}{384}\,\frac{w L^4}{EI} \qquad \text{....................(164)}$$

The slope at O can be found by differentiating y_o with respect of x_A, keeping in mind that the origin is shifted as x_A changes, which makes $\frac{dy_o}{dx_A}$ minus; thus:

$$\theta_o = +\frac{w\,L^3}{24\,EI} - \frac{w\,L\,x^2_A}{4\,EI} + \frac{w\,x^3_A}{6\,EI} \qquad \text{..............(165)}$$

The same result for θ_o can be obtained directly from Equation (160), in which $A\bar{x}$ is now the static moment of the shear area, $O\ p\ q\ A$, about $O\ p$, and is equal to $-\frac{w\,L\,x^2_A}{4} + \frac{w\,x^3_A}{6}$, which gives,

$$\theta_o = \frac{w\,L^3}{24\,E\,I} - \frac{w\,L\,x^2_A}{4\,E\,I} + \frac{w\,x^3_A}{6\,E\,I} \quad \text{.............(166)}$$

Analysis of Statically Indeterminate Beams (Authors' Case II).—The end reactions, M_A, M_B, V_A, and V_B (Fig. 39), can be computed in the usual manner. They can also be found readily by means of Equation (159) and Equation (160), and are as follows: $M_A = -\frac{P\,a\,b^2}{L^2}$; $M_B = -\frac{P\,a^2\,b}{L^2}$; and, $V_A = -\frac{P\,b^2}{L^3}(3a + b)$. Note that θ_A, θ_B, and y_A are each equal to zero. Then,

$$y_o = +\frac{M_A\,x^2_A}{2\,E\,I} - \frac{I_x}{2\,E\,I} \quad \text{...................(167)}$$

in which, I_x is the moment of inertia (see Fig. 39), of the rectangle, $O\ p\ q\ A$, about $O\ p$, and is equal to $\frac{V_A\,x^3_A}{3}$.

Expressing M_A and V_A in terms of the load, P, and a and b, the equation of the elastic curve is:

$$y_o = -\frac{P\,a\,b^2\,x^2_A}{2\,E\,I\,L^2} + \frac{P\,b^2}{6\,E\,I\,L^3}(3\,a + b)\,x^3_A \quad \text{..........(168)}$$

in which y_o is a maximum when $\frac{dy_o}{dx_A} = 0$, provided a is $\gtreqless \frac{L}{2}$. This gives $x_A = \frac{2\,a\,L}{2\,a + L}$. The solution becomes simpler when numerical values can be substituted for M_A, V_A, I_x, and $A\bar{x}$ in Equations (159) and (160).

JOHN M. BEATTY,[15] JUN. AM. SOC. C. E. (by letter).[15a]—The "shear-area method" for the solution of the elastic functions of loaded beams as presented in this paper outlines another interesting and valuable method of analysis for both statically determinate and statically indeterminate beams. As the authors have stated it is not "the shortest method for solving slopes and deflections for all problems," but its advantages in those cases involving uniformly distributed loads become quite apparent when the method is put to the test.

The parabolic moment-curve areas involved in the solutions by the moment-area methods are always disagreeable and sometimes difficult to handle. On the other hand, the shear-curve areas for the same loadings are usually simply a combination of triangles, rectangles, and trapezoids, the properties of which are well known to every engineer and designer.

[15] Instr., Dept. of Civ. Eng., Rensselaer Polytechnic Inst., Troy, N. Y.

[15a] Received by the Secretary July 31, 1931.

There are many cases, also, in which the shear-area method may be used to advantage in combination with some other method, such as the conjugate beam method. In the case of simply supported beams, for instance, the end slopes many times may be found much more readily by the shear-area method and then these slopes may be applied as end reactions for the "conjugate beam." The problem may then be continued to completion by the latter method if an inspection seems to indicate an easier solution by that method.

For example, consider the following simple beam loaded with two patches of uniform load symmetrically placed with respect to the center of the beam (see Fig. 40(*a*)). An inspection of the shear and moment diagrams immediately suggests an easier and quicker solution of the end slopes by the shear-area method. The end slopes, which are numerically equal to each other are also equal to one-half the moment of the couple produced by the shear-area loadings. The value of the shear-area couple is equal to the value of the shear area above or below the base line, multiplied by the distance between their centers of gravity. The value of one-half this shear area couple may then be found immediately taking moments about the center line of the mathematical beam of the shear area to one side of the section. This principle may be used for all simple beams with loadings that are symmetrical with respect to the center line, providing, of course, that the beam itself is also symmetrical about the center line; thus (see Fig. 40(*b*)):

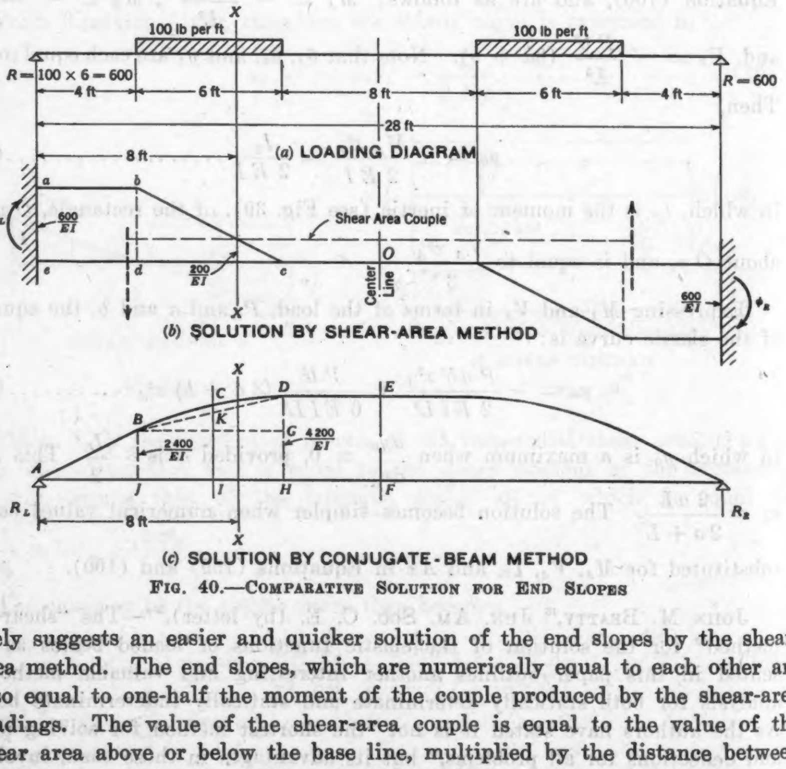

FIG. 40.—COMPARATIVE SOLUTION FOR END SLOPES

$$\phi_L = \frac{\text{Moment of Shear Area, } a\,b\,c\,d\,e, \text{ About Point } O}{E\,I} \times 144$$

or,

$$\phi_L = \frac{600 \times 4 \times 12 + 0.5 \times 600 \times 2 \times 8}{E\,I} \times 144 = \frac{6\,220\,800}{E\,I}$$

To find the same end slope by the conjugate beam method involves the solution for the end reaction, R_L, of the conjugate beam. As the moment diagram is symmetrical with respect to the center line, this reaction, R_L, must equal one-half the total moment-area loading. Of this total area, $A\,C\,E\,F\,A$, that under the curved portion (that is, Area $J\;B\;C\;D\;H$; Fig. 40(*c*)), presents the greatest difficulty. This area, of course, may be found by means of the calculus by integrating the general expression for the moment area between the limits of J and H, but this introduction of the calculus is troublesome to many and is often avoided wherever possible. Another method of finding the value of Area $J\,B\,C\,D\,H$ is to divide it into the two areas, $J\,B\,D\,H\,J$ and $B\,C\,D\,B$, and then to find each area separately. The area of the trapezoid, $J\,B\,D\,H\,J$, is readily found. The area under the curve, $B\,C\,D\,B$, may be determined by finding the value of the ordinate, $C\,K$, at the mid-point between B and D and, considering this as the mid-ordinate of a parabolic curve spanning the horizontal distance, $B\,G$, the area will then be equal to two-thirds the product of $C\,K$ times $B\,G$ (see Fig. 40(*c*)). Referring to Fig. 40(*c*): $C\,K = C\,I - K\,I = 3\,750 - 3\,300 = 450$; $M_{BJ} = 600 \times 4 = 2\,400$; $M_{CI} + 600 \times 7 - 300 \times 1.5 = 3\,750$; $M_{BF} = 600 \times 14 - 600 \times 7 = 4\,200$;

$$\text{and } R_L = \text{Areas } \frac{A\,B\,J + B\,D\,H\,J + B\,C\,D\,B + D\,E\,F\,H}{E\,I} \times 144$$

$$= \frac{1}{E\,I}\left[\frac{2\,400 \times 4}{2} + \left(\frac{2\,480 \times 4\,200}{2}\right) 6 + \frac{2}{3}\,(450 \times 6) + 4\,200 \times 4\right] \times 144$$

$$= \frac{6\,220\,800}{E\,I}.$$

Regardless of which method is used to find the total area, $A\,C\,E\,F\,A$, it is apparent that the work involved is considerably more than that incurred in the solution of ϕ_L by the shear-area method. As the values of ϕ_L and R_L are certain to be identical, both representing the end slope of the same simple beam, the shear-area method is obviously much the easier and quicker method and, at the same time, because of its simplicity, much less liable to error than the solution by the conjugate beam method.

If the values of the moment areas are known (as they now are in this problem) there is very little to choose from between the two methods in so far as the determination of the maximum deflection at the center of the beam is concerned. Each method involves about an equal amount of numerical work, although the determination of the static moments of the moment areas in the case of the conjugate beam may be preferred by some to the solution for the moments of inertia of the shear areas in the case of the shear-area

method. For example, by the shear-area method:

$$y_{\max.} = \phi_L \times x - \frac{I_x}{2} = \frac{1}{E\,I}\Bigg\{6\,220\,800 \times 14 \times 12$$

$$\left[\frac{\dfrac{600 \times 4^3}{12} + 600 \times 4 \times 12^2 + \dfrac{600 \times 6^3}{36} + \dfrac{600 \times 6}{2} \times 8^2}{2}\right] 1\,728\Bigg\}$$

$$= \frac{641\,088\,000}{E\,I}$$

and, by the conjugate beam method:

$$y_{\max.} = \frac{1}{E\,I}\Bigg\{6\,220\,800 \times 14 \times 12 - \Bigg[\frac{2\,400 \times 4}{2} \times \frac{34}{3} + 2\,400 \times 6 \times 7$$

$$+ \frac{1\,800 \times 6}{2} \times 6 + \frac{2}{3}(450 \times 6) \times 7 + 4\,200 \times 4 \times 2\Bigg] 1\,728\Bigg\}$$

$$= \frac{641\,088\,000}{E\,I}.$$

It is in the determination of the deflection at any intermediate point, such as Point X, Fig. 41, that the advantage of the shear-area principle becomes apparent.

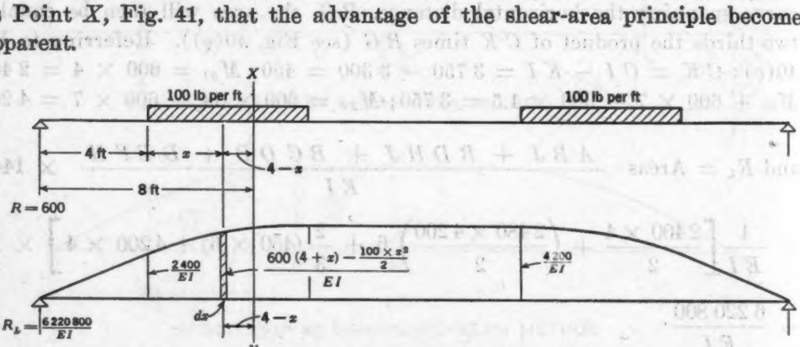

FIG. 41.—DEFLECTION AT ANY POINT BY THE CONJUGATE BEAM METHOD

In finding the static moments about Point X, of the moment areas in the conjugate beam method, recourse must again be made to the calculus for the moment of the area between Points J and X (see Fig. 40(c)). The general expression for the moment of the moment area must be integrated between the limits of J and X (see Figs. 40(c) and 41). An inspection of the following computations plainly shows the relative simplicity of the solution by the shear-area method over that by the conjugate beam method:

By the shear-area method (see Fig. 40(b)):

$$y_x = \phi_L \times x - \frac{I_x}{2};\ \phi_L = \frac{6\,220\,800}{E\,I};\ \text{and, } y_x = \frac{1}{E\,I}\Bigg\{6\,220\,800 \times 8 \times 12$$

$$-\left[\frac{\dfrac{600 \times 4^3}{12} + 600 \times 4 \times 6^2 + \dfrac{200 \times 4^3}{3} + \dfrac{400 \times 4^3}{4}}{2}\right] 1\,728\Bigg\} = \frac{510\,566\,400}{E\,I}$$

By the conjugate beam method:

$$y_x = \frac{1}{EI}\left\{6\,220\,800 \times 8 \times 12 - \left[\frac{2\,400 \times 4}{2} \times \frac{16}{3} + \int_0^4 \left(600\,(4 + x) - \frac{100\,x^2}{2}\right) d\,x\,(4 - x)\right] 1\,728\right\} = \frac{1}{EI}\left\{6\,220\,800 \times 96 - \left[25\,600 + 50\left(192\,x - \frac{16\,x^3}{2} + \frac{x^4}{4}\right)_0^4\right] 1\,728\right\} = \frac{510\,566\,400}{EI}$$

No single method of analysis can be claimed as superior to all others for the solution of all problems. Certain methods are more readily applied to certain types of problems and, therefore, are to be preferred over all others for these specific types. The shear-area method thus supplies one more possible tool which, when used judiciously, can be of real service. The authors are to be commended for bringing this method of analysis to the attention of the Engineering Profession.

R. B. PECK,[18] JUN. AM. SOC. C. E. (by letter).[18a]—The use of the shear-area method is most advantageous, as the authors state, for problems involving distributed load. Where the load is uniformly distributed over entire span lengths—that is, where the moment diagram includes a full parabola—it appears that the method offers no advantages over the moment-area methods because the properties of parabolic half-segments are well known. For uniformly distributed loads occurring in patches, however, so that the moment diagram includes parts of parabolas, the location of the vertices of which is not apparent by inspection, the shear-area method affords a simpler solution.

The equation for deflection is direct and simple in use. If the beam is fixed-ended and the end slopes are known, the solution is rapid. If the beam is simply supported so that the end slopes are not known, it should be emphasized that, although they are easily determined for specific cases by the formulas proposed by the authors, their derivation is inherently less direct than the process of obtaining the reactions of the conjugate beam. Much of the advantage of the shear-area method is lost in this case because of this difficulty in obtaining end slopes, particularly if the computer does not have the aforementioned formulas available.

It will be noticed, however, that a very direct means of computing the end slopes for simply supported beams is found in the method, suggested by the authors, of investigating the loading directly. The deflection formula, Equation (95), will reduce to:

$$y\,E\,I = -\frac{1}{6}\,Q_x + \theta_e\,x + y_e \qquad (169)$$

for simple supports. When written for a point of support, where $y = 0$, it becomes, since $x = L$,

$$0 = -\frac{1}{6}\,Q + \theta_e\,L + y_e$$

---

[18] Troy, N. Y.

[18a] Received by the Secretary August 12, 1935.

which may be solved immediately for the end slope, θ_e. A numerical example is given for illustration.

In order to solve for the deflection at any point in the beam shown in Fig. 42, it is necessary to know one of the end slopes, say θ_L. By Equation (30),

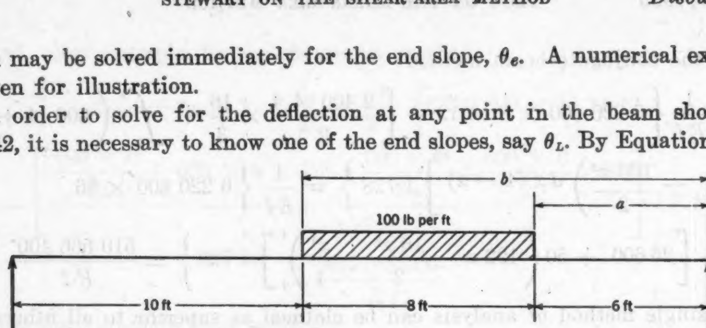

FIG. 42.

$\theta_L = 25\,500$. If, however, instead of Equation (30) the loading is used directly, the expression for the deflection at the right-hand end, using Equation (169), is $0 = -\frac{1}{6}\,Q + \theta_L\,L$, in which Q is taken for the entire span and equals $\frac{R\,x^3}{6} - \int x^3\,dA$. For an area, $\int x^3\,dA = 3\,x_0\,I_{cg} + A\,x^3_0$. Then,

$$0 = \phi \times 24 - \frac{333}{6} \times 24^3 + \frac{3}{6} \times 10 \times \frac{100 \times 8^3}{12} + \frac{100 \times 8 \times 10^3}{6}$$

from which $\theta_L = 25\,500$.

RALPH W. STEWART,[17] M. AM. SOC. C. E. (by letter).[17a]—An interesting mathematical exercise is presented in this paper. The principle which makes the shear-area method possible is the same as that which makes the conjugate beam or elastic weight method possible, namely, in Fig. 1, each curve is the integral of the one above it. This principle is illustrated more simply by drawing the loading, shear, moment, slope, and deflection curves for a cantilever beam using the free end as the origin, thereby eliminating the effect which the reaction has on the shear curve.

In connection with these integrations, as usually performed for specific loading, it is of interest to note that the shear and moment in either the cantilever beam or the simple beam are governed by forces and distances on one side only of the point at a distance, x, from the origin. The slope and deflection, however, are affected by the length of the entire beam and by the loading on both sides of the point at a distance, x. In line with this physical condition the integrations from load to shear and shear to moment are not affected by the valuation of constants of integration, these constants being zero, but the integrations from moment to slope and from slope to deflection require the evaluation and use of constants of integration which are dependent on the entire length of the beam. The authors' treatment of Fig. 1 involves loading which is general rather than specific, thereby leading to two term expressions for the slope and the deflection with constants of integration that equal zero.

[17] Engr. of Bridge Design, Bureau of Eng., Dept. of Public Works, Los Angeles, Calif.

[17a] Received by the Secretary August 19, 1935.

The one obvious advantage which the shear-area method offers in comparison with methods of analysis based on moment areas is that, for beams with uniformly distributed loads, the shear areas are bounded by straight lines, whereas with moment areas a parabolic boundary line is involved. To a computer with meager knowledge of geometry the straight-line figure offers an advantage. The properties of parabolic moment diagrams are so simple, however, and so easily remembered, that any one whose professional practice includes structural engineering can hold them in mind, and by their use can solve beam problems with less work than by the methods set forth in this paper.

As an illustration, the fact that the parabola cuts the rectangle in Fig. 43 into an upper and lower area equal, respectively, to two-thirds and one-third

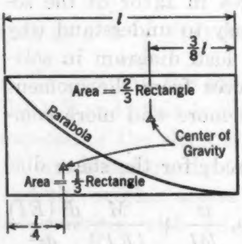

FIG. 43.

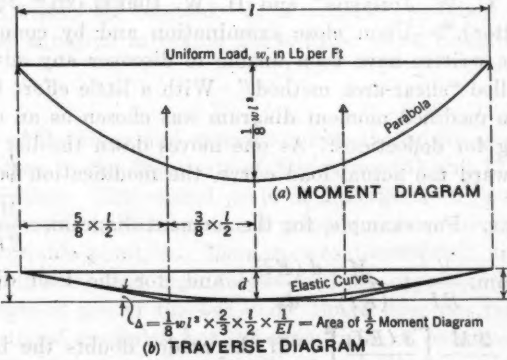

FIG. 44.

of the area of the rectangle, and that the centers of gravity of these areas are located as shown, should not tax the memory of an engineer. Even if forgotten, the integrations to obtain these areas and distances are easier than such integrations as that of Equation (10) and various subsequent integrations in the paper.

Using these parabolic areas and the principle that the change in direction of the tangent between two points on the elastic curve is equal to the area between the two corresponding points on the $\frac{M}{EI}$-diagram, the analysis of beams with uniformly distributed loads can be performed more rapidly and more satisfactorily than by the method set forth by the authors. For example, by the moment-area method, or by the traverse method as illustrated by Fig. 44(*b*),[18] the deflection at the center of a simple beam uniformly loaded is:

$$\frac{5}{16}\, l \left(\frac{1}{8}\, w\, l^2 \times \frac{2}{3} \times \frac{l}{2} \times \frac{1}{E\,I}\right) = \frac{5\, w l^4}{384\, E\, I} \qquad \ldots\ldots\ldots(170)$$

This is certainly simpler treatment than the procedure indicated by the authors' Equations (10) and (11). In fact, their derivation of this maximum deflection appears more tortuous than the usual double integration of the bending-moment equation as taught in most treatises on applied mechanics.

[18] For explanation of Fig. 44(*b*) see "An Improved Method of Finding Beam Deflections", *Civil Engineering*, February, 1934.

An inherent difficulty in the general use of the shear-area method for the analysis of continuous frames is that the shear curve is one step too far removed from the curve of deflections, and the analysis of continuous frames is dependent to a great extent upon equating deflections at certain points to each other, or to zero. The slope is one step closer to the shear curve, and since the theorem of three moments is derived by equating slopes over supports, it is practicable to use the shear-area method to derive it as set forth in the paper.

As a practical tool for the analysis of structures, it appears that the prospect of the shear-area method to gain recognition is not encouraging.

C. W. JOHNSON[19] and H. W. BIRKELAND,[20] JUNIORS, AM. SOC. C. E. (by l tter).[20a]—Upon close examination and by comparison with other methods, the writers have been unable to discover any advantages in favor of the so-called "shear-area method." With a little effort it is easy to understand why the modified moment diagram was chosen as an elastic load diagram in solving for deflections. As one moves down the list of curves from the moment toward the actual load curve, the modification becomes more and more complex. For example, for the moment diagram, $\frac{M}{EI}$ is used; for the shear diagram, $\frac{V}{EI} + \frac{M}{(EI)^2}\frac{d\,(EI)}{dx}$; and, for the load diagram, $\frac{w}{EI} + \frac{M}{(EI)^2}\frac{d^2\,(EI)}{dx^2} - \frac{2\,M}{(EI)^3}\left[\frac{d\,(EI)}{dx}\right]^2$. If the reader doubts the increasing difficulty of using these expressions, let him try an example and be convinced.

Another misleading inference in the paper suggests that the second moment of the modified shear area is easier to find than the first moment of the moment area. This conclusion is inaccurate, of course, because in the two cases the integrations are comparable. For use with the conjugate beam method the writers have long used a simple table of areas and locations of centroids in cases where only deflections at particular points are desired. Such an expedient would be equally necessary and useful in regard to the shear-area method.

The authors have placed great emphasis upon the ease of finding the slopes by this method and the merit of having "eliminated" the moment curve. Compare the usefulness of these two curves and then decide which should be omitted. In the conjugate beam method the most used curve is employed whereas the least used curve is not used. In the shear-area method the valuable moment curve is not used and apparent emphasis is laid on the less important slope curve.

The method does not seem to be readily adaptable to any but the most simple beam problems such as statically determinate, constant section cases with uniformly distributed load. The writers have been unable to find one

[19] Junior Engr., U. S. Bureau of Reclamation, Denver, Colo.

[20] Junior Engr., U. S. Bureau of Reclamation, Denver, Colo.

[20a] Received by the Secretary August 20, 1935.

case in which the procedure could be applied more easily than some other one. To the practicing engineer the method offers nothing that is of sufficient value to investigate as it does not improve upon the methods now in use. However, if the paper were more complete, and included a genuine derivation of the principles, it would be of interest to students, since it calls attention to the second-moment and third-moment principles.

In Fig. 1 the authors have ostensibly set out to show the relation between beam diagrams.[20b] In doing so they start with the load diagram as a calculus curve and attempt to proceed from one curve to another by means of integration.

Since an extremely simple case was chosen, it is unfortunate that the equations were not shown mathematically complete. Some of the constants of integration are shown and others are omitted. It is necessary to show a constant of integration in each equation involving the solution of an integral, such as $y = \int f(x)\,dx$.

In deriving the equations of the shear and moment curves the origin is at the left end; this is likewise true in the first parts of Equations (6) and (7), expressing the slope and deflection. The second parts of Equations (6) and (7) are based on the first-moment and second-moment principles, respectively, and the origins are at any variable point, x. Thus, to avoid confusion, the x occurring with dA under the integral sign might well be expressed as another variable since its origin is not at the left end. Space does not permit a discussion of all the authors' examples, but the same types of omissions and inconsistencies, as mentioned in connection with Fig. 1 and Equations (4) to (7), inclusive, appear throughout.

Although it is not the chief topic of the authors' paper, the writers present a simple and consistent method of showing beam diagrams. The successive curves bear the proper mathematical relationships and the sign conventions are logical. The calculus relationships can be expressed in two simple rules: (*a*) The slope at any point on a curve is equal to the ordinate at the corresponding point in the derived curve; and, (*b*) the difference between the ordinates at any two points on a curve is equal to the area under the derived curve between the two corresponding points.

These two rules do not establish the starting point of the higher degree curve; this point is determined from the constant of integration which is fixed by physical considerations and is often referred to as the initial condition. The equations of the beam diagrams and the sign conventions are, as follows:

(1) Loading (positive when acting upward):

$$w_x = f(x) \quad\text{.......................}\quad (171)$$

[20b] Correction to be made in Fig. 1 (*d*) before paper is finally published in *Transactions*: The curve should have its concave side next to the *X*-axis and should be horizontal at each end. Owing to the authors' penchant for showing the constants at the left end of curves as positive, the fundamental calculus relations between curves are soon lost.

(2) Shear (positive when acting upward on the part of the beam on the right of the cut; an imaginary cut helps to visualize internal shears):

$$V_x = R_L + \int_0^x w_x \, dx \quad \text{.....................(172)}$$

(3) Moment (positive when the lower fibers are in tension):

$$M_x = M_L + \int_0^x V_x \, dx \quad \text{.....................(173)}$$

(4) Slope (positive when deflection curve rises from left to right):

$$\theta_x = \phi_L + \int_0^x \frac{M_x}{EI} \, dx \quad \text{.....................(174)}$$

(5) Deflection (positive when upward from the original position):

$$\delta_x = \delta_L + \int_0^x \theta_x \, dx \quad \text{.....................(175)}$$

In order to keep Equations (171) to (175) general, all terms are shown positive. Therefore, algebraic signs must be included in numerical substitutions, which is the usual practice in mathematics.

This procedure, as applied to the example of Fig. 1, is shown in Fig. 45. Fig. 45(*a*) is a sketch of the beam showing external loads and restraints. Figs. 45(*b*) to 45(*f*) show a series of beam diagrams from load curve to deflection curve, inclusive. Note that, consistent with the foregoing sign convention, the load curve, Fig. 45(*b*), is drawn below the *X*-axis, since a downward acting load is negative. The reason for such a sign convention is to show better the mathematical relationships between the load and shear curves. It is important that the sketch of the beam, showing loading and restraints, is not confused with the load curve. The Cartesian co-ordinate system, with origin at the left end throughout, is used in this method. Values are positive when measured above, and negative when measured below, the *X*-axis.

Since Equations (4) to (7), inclusive, are incomplete, and do not contain a proof of the principles involved, the writers will derive them as mathematical laws that are not limited to beams alone.

The First-Moment Principle.—A special application of the first-moment principle to beams is called Mohr's second law; conjugate beam method; and moment-area principle. Another special application to beams may be called the shear-area method, Part I. A general application, using different terms, is sometimes called the third law of derived curves. Referring to Fig. 46, let the equation of Curve No. 1 be:

$$y_1 = f(x_1) \quad \text{.....................(176)}$$

Integrating Equation (176), the equation of Curve No. 2 is obtained; thus:

$$y_2 = y_{2A} + \int_a^{x_2} y_1 \, dx_1 \quad \text{.....................(177)}$$

Note that instead of taking the constant of integration at the origin and starting the integration from there, the constant is taken at Point *A* (Fig. 46), and the integration starts from that point. This is done in order to remove any doubt about the universal truth of the law to be derived.

Integrating again, the equation of Curve No. 3 is obtained:

$$y_3 = y_{3A} + \int_a^{x_3} y_{2A}\, dx_2 + \int_a^{x_3} \int_a^{x_2} y_1\, dx_1\, dx_2 \qquad (178)$$

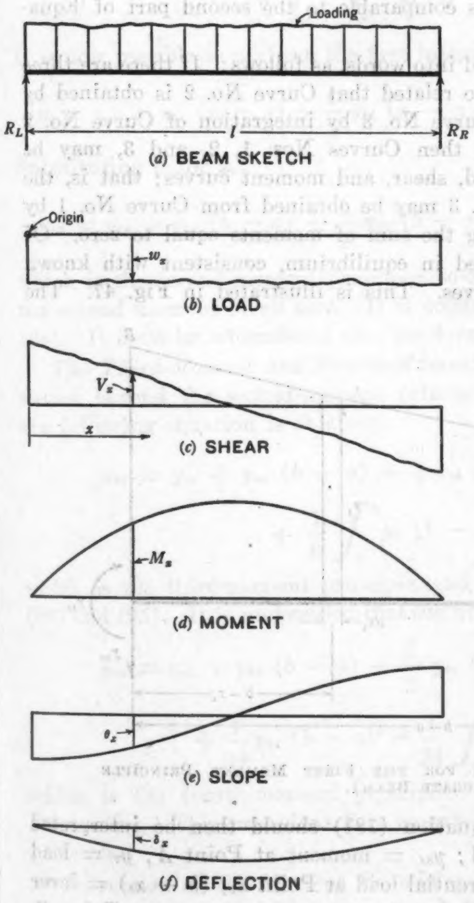

FIG. 45.—BEAM DIAGRAMS.

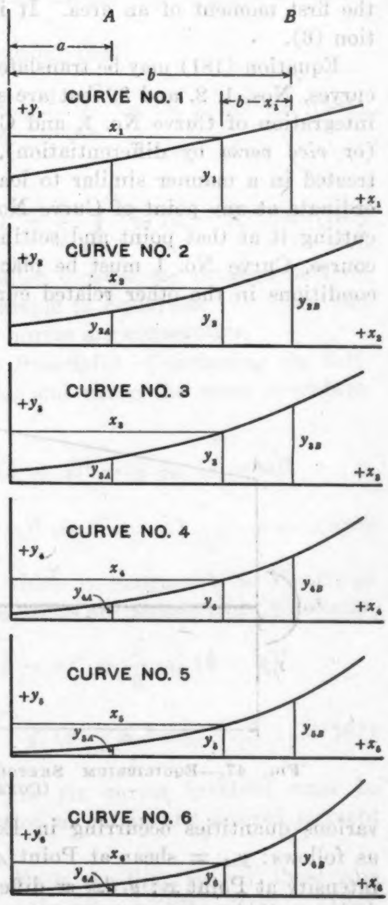

FIG. 46. — CONSECUTIVE CALCULUS CURVES.

Rewriting Equation (178) with the order of integration reversed:

$$y_3 = y_{3A} + \int_a^{x_3} y_{2A}\, dx_2 + \int_a^{x_3} \int_{x_1}^{x_3} y_1\, dx_2\, dx_1 \qquad (179)$$

It is now possible to perform the first integration::

$$y_3 = y_{3A} + y_{2A}\,(x_3 - a) + \int_a^{x_3} y_1\,(x_3 - x_1)\, dx_1 \qquad (180)$$

Substituting b for x_3,

$$y_{3B} = y_{3A} + y_{2A}\,(b - a) + \int_a^b y_1\,(b - x_1)\,dx_1 \ldots\ldots\ldots \quad (181)$$

which is the first-moment principle, so-called because the integral involves the first moment of an area. It is comparable to the second part of Equation (6).

Equation (181) may be translated into words, as follows: If there are three curves, Nos. 1, 2, and 3, that are so related that Curve No. 2 is obtained by integration of Curve No. 1, and Curve No. 3 by integration of Curve No. 2 (or *vice versa* by differentiation), then Curves Nos. 1, 2, and 3, may be treated in a manner similar to load, shear, and moment curves; that is, the ordinate at any point of Curve No. 3 may be obtained from Curve No. 1 by cutting it at that point and setting the sum of moments equal to zero. Of course, Curve No. 1 must be placed in equilibrium, consistent with known conditions in the other related curves. This is illustrated in Fig. 47. The

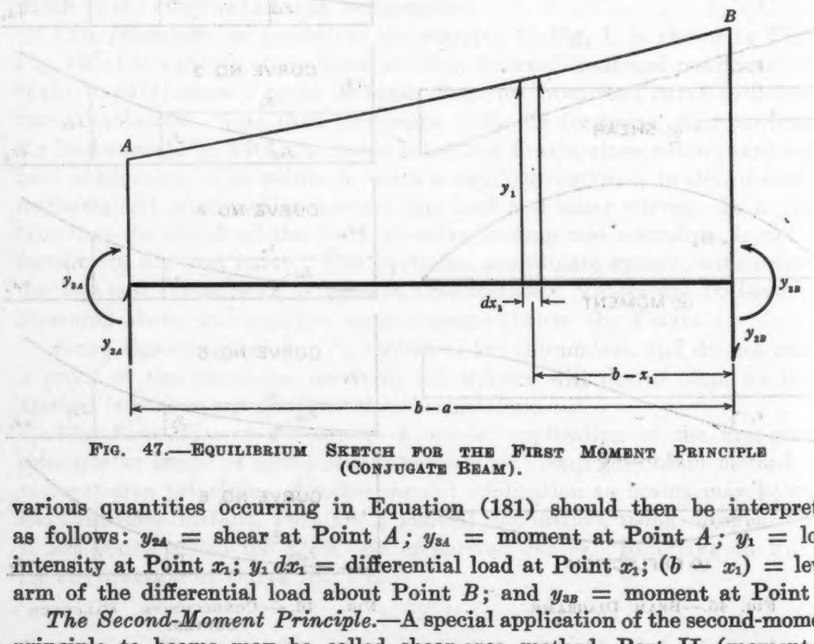

FIG. 47.—EQUILIBRIUM SKETCH FOR THE FIRST MOMENT PRINCIPLE (CONJUGATE BEAM).

various quantities occurring in Equation (181) should then be interpreted as follows: y_{2A} = shear at Point A; y_{3A} = moment at Point A; y_1 = load intensity at Point x_1; $y_1\,dx_1$ = differential load at Point x_1; $(b - x_1)$ = lever arm of the differential load about Point B; and y_{3B} = moment at Point B.

The Second-Moment Principle.—A special application of the second-moment principle to beams may be called shear-area method, Part II (moment of inertia of shear diagram). Referring to Fig. 46, the equation of Curve No. 4 is obtained by integration of Equation (180):

$$y_4 = y_{4A} + \int_a^{x_4} y_{3A}\,dx_3 + \int_a^{x_4} y_{2A}\,(x_3 - a)\,dx_3$$

$$+ \int_a^{x_4}\int_a^{x_3} y_1\,(x_3 - x_1)\,dx_1\,dx_3 \ldots\ldots\ldots\ldots\ldots\ldots (182)$$

Rewriting Equation (182) with the order of integration reversed:

$$y_4 = y_{4A} + \int_a^{x_4} y_{3A}\, dx_3 + \int_a^{x_4} y_{2A}\, (x_3 - a)\, dx_3 + \int_a^{x_4} \int_{x_1}^{x_4} y_1\, (x_3 - x_1)\, dx_3\, dx_1 \ldots\ldots\ldots\ldots\ldots (183)$$

It is now possible to perform the first integration; thus:

$$y_4 = y_{4A} + y_{3A}\, (x_4 - a) + \frac{1}{2}\, y_{2A}\, (x_4 - a)^2 + \frac{1}{2} \int_a^{x_4} y_1\, (x_4 - x_1)^2\, dx_1 \,.(184)$$

Substituting b for x_4:

$$y_{4B} = y_{4A} + y_{3A}\, (b - a) + \frac{1}{2}\, y_{2A}\, (b - a)^2 + \frac{1}{2} \int_a^b y_1\, (b - x_1)^2\, dx_1 \,.(185)$$

which is the second-moment principle, so-called because the integral involves the second moment of an area. It is comparable to Equations (7), (92), and (94). It must be remembered that the four curves are consecutive.

The Third-Moment and Fourth-Moment Principles.—Continuing the derivation beyond the second-moment principle, and using the same procedure, the following equation is obtained,

$$y_{5B} = y_{5A} + y_{4A}\, (b - a) + \tfrac{1}{2}\, y_{3A}\, (b - a)^2 + \tfrac{1}{6}\, y_{2A}\, (b - a)^3 + \frac{1}{6} \int_a^b y_1\, (b - x_1)^3\, dx_1 \ldots\ldots\ldots\ldots\ldots (186)$$

which is the third-moment principle, and which is comparable to Equations (93) and (95). It is understood that the five curves are consecutive. Similarly,

$$y_{6B} = y_{6A} + y_{5A}\, (b - a) + \frac{1}{2}\, y_{4A}\, (b - a)^2 + \frac{1}{6}\, y_{3A}\, (b - a)^3 + \frac{1}{24}\, y_{2A}\, (b - a)^4 + \frac{1}{24} \int_a^b y_1\, (b - x_1)^4\, dx_1 \ldots\ldots\ldots (187)$$

which is the fourth-moment principle. The six curves involved must be consecutive. This procedure may be extended to obtain any desired moment principle.

Discussion of the Moment Principles.—From the first, second, third, and fourth-moment principles, represented by Equations (181), (185), (186), and (187), respectively, the following points may be noted:

(1) The first-moment principle is the only one of the group that lends itself to use in connection with an equilibrium sketch, because the numerical coefficients of all terms are unity (1.0) in this one case only; and,

(2) A problem, which in ordinary procedures would involve a multiple integration, has been reduced to one with a single integration. It is well to note that the intermediate curve or curves are not entirely eliminated since the constants of integration of all these curves are used, and, therefore, must be evaluated.

In solving a problem by beam diagrams, a choice must be made between the following procedures: (1) To apply a series of successive, straight integrations to obtain the equations of all curves; (2) to apply the first moment principle, repeatedly if necessary and desired, along with such successive integrations as are necessary to determine the constants of integration of the intermediate curves; and, (3) to apply the second or higher moment principle, along with the first-moment principle and successive integrations to determine the constants of integration of the intermediate curves.

It is futile, of course, to say that one procedure is better than the others, for one must bear in mind the possible complications accompanying the moment principles.

GARRETT B. DRUMMOND,[21] ESQ. (by letter).[21a]—There will be many who recognize in this paper another approach to the solution of beams; but it is certainly not remiss to search deeper and recognize another emphasis of the mathematical fundamentals of elasticity.

Consider the familiar expression of the calculus:

$$\int f(x)\ dx = y = F(x) \qquad (188)$$

which, with limits, becomes,

$$\int_a^b f(x)\ dx = F(b) - F(a) \qquad (189)$$

but $F(b)$ is the ordinate on the integral curve at $x = b$, and $F(a)$ is the ordinate at $x = a$; which leads to the statement which is the basis of graphical integration:

The area under the derived curve between any two ordinates is equal numerically to the difference between the corresponding ordinates on the integral curve.

Assumptions (3), (4), and (5) of the paper are a consequence of the foregoing mathematical statement.

Papers such as this contribute to a broader viewpoint of the geometry of statics. It is not sufficient that designers be able to apply the so-called laws of mechanics without the facility of visualizing just what happens to a beam or other structure. The shear-area method provides another approach to that visualization.

Thus, the structural engineer is able to express the so-called mathematical principles in ordinary language. Shear being the sum of all the forces and the moment the sum of these forces times their distances from any given point, if the point is moved a short distance the moment will be increased by the shear times the distance. In addition, the rate of change of the shear is the unit intensity of the load.

In other words, if there are no loads on a beam, the shear across the beam is constant and the moment curve is a straight line. If all the loads on any

[21] Asst Prof. of Mathematics, Oklahoma Agri. and Mech. Coll., Stillwater, Okla.

[21a] Received by the Secretary September 4, 1935.

span are in the same direction the shear in that span either has the same sign at all points or changes sign at one point in the span. Furthermore, the moment curve has a continuous slope in one direction or changes direction of slope at one point.

This geometrical conception of the action of any structure is fundamental, not only to statically determinate, but to statically indeterminate, structures. It has been stated that if a structure does not fail, it holds together. If that is true, continuity requires that there be certain geometric relations between its parts.

These physical interpretations of mathematical statements should be stressed more and more to students. It is true that, often, a teacher of mechanics uses his integral calculus with a disregard for the true mathematical correctness of his juggling; but teachers of mathematics far too often advance mathematical laws without any effort to establish a link in the mind of the student with the more concrete evidences of their universal application. The authors have presented another demonstration of the relationship between derived curves and their integrals, and also have added to the geometrical analysis of the elastic functions of beams.

HAROLD E. WESSMAN,[22] ASSOC. M. AM. SOC. C. E. (by letter).[22a]—Several writers of "engineering problems" texts have stated the general mathematical law of which the moment-area method and the shear-area method are special cases. In one text[23] appears the statement that:

"In any curve, the length of the ordinate from the tangent to the curve at any point (called the first point) to any other point on the curve (called the second point) equals the algebraic sum of the moments of the areas between the ordinates of the corresponding points in the second lower curve, moments being taken about the ordinate through the second point."

Because this general law has such significance for engineers, one might expect to find it stated in some calculus text also. The writer has never seen an explicit statement of it, however, in the texts with which he is familiar. He is curious to know, simply for purposes of information, whether the authors have ever encountered it in any mathematical text. Teachers of calculus for engineers could well afford to give the general law more emphasis.

The special application of this law in the moment-area theorems of Mohr and Green is familiar to many engineers. The application *via* the shear-area concept of the authors is not so well known. That is not strange when one realizes that, in college, the embryo engineer is usually introduced to the double integration method of finding beam deflections, a method which begins by expressing the relationship between curvature and moment in the familiar equation, $\frac{d^2 y}{dx^2} = -\frac{M}{EI}$. He performs the calculus operations involved in solving this equation to find slopes and deflections. He is then, in many

[22] Assoc. Prof. of Structural Eng. and Mechanics, Coll. of Eng., Univ. of Iowa, Iowa City, Iowa.

[22a] Received by the Secretary September 5, 1935.

[23] "Engineering Problems Manual", by F. C. Dana and E. H. Willmarth, p. 46.

places, exposed to the moment-area method (often cluttered up with an imposing title) which parallels the calculus method, but which fortunately places the emphasis upon geometrical concepts.

In teaching the subject of deflections, the writer always portrays, geometrically, the five curves of load, shear, moment (or curvatures), slope, and deflection similar to those shown in Fig. 1, but he supplements these with a picture of a deformed segment of a beam. It is logical to reason geometrically from curvature of beams to deflections of beams. Since curvature at a point is expressed in terms of the moment at the same point, the moment-area method has some physical significance for the student. It does not seem quite so satisfactory to reason from the rate of change of curvature to the slope of the beam and then to deflection, even though in some cases it may be simpler to evaluate a triangular shear area rather than a curved moment area.

In the classroom, every teacher is confronted with the task of selecting the minimum essentials in this age of voluminous theory and with the importance of making those essentials clear to the student; hence, it is advisable, particularly in undergraduate work, to give the student the best possible tool and to make him familiar with that tool, rather than give him a nodding acquaintance with a variety of tools which have the same purpose.

This is not to be construed as a depreciation of the authors' paper. They have performed a service in presenting this special concept. Such contributions give the members of the profession an opportunity to weigh and then select that which is best suited for particular needs.

AMERICAN SOCIETY OF CIVIL ENGINEERS

Founded November 5, 1852

DISCUSSIONS

DISTRIBUTION OF STRESSES UNDER A FOUNDATION

Discussion

BY MESSRS. CLEMENT C. WILLIAMS, D. P. KRYNINE, AND L. C. WILCOXEN

CLEMENT C. WILLIAMS,[23] M. AM. SOC. C. E. (by letter).[23a]—In his excellent review of theory and experiments relative to pressures under a foundation, the author has performed a helpful service in that his presentation is pointed toward a practical evaluation of their significance. The rather amorphous state of foundation literature represents a stage preliminary to its crystallization into usable principles involving known soil factors. The paper seeks to give point to the theories and experiments that cluster about the geometry of stress distribution in an isotropic elastic solid.

In most experiments relating to pressure distribution under a foundation slab sand has been utilized as the soil. Rankine's theories contemplate a material like dry sand. Within the shear limits of internal friction, the behavior of dry sand in transmitting pressure is similar to that of a granular sandstone, since the cementitious binder of the latter performs no essential function until friction is overcome, except in so far as the solid stone has a weak tensile strength. That there is a close correlation between the theories that are based on either an hypothetical elastic solid, or on a sand bed (which, within limits, behaves similarly to an elastic solid), should not occasion surprise; nor, on the other hand, should it lead to a generalized conclusion applicable to all foundation soils.

Not enough experimental observations have been made with loads resting on elastic soils. The limited observations made by the writer, by William S. Housel, Assoc. M. Am. Soc. C. E., and by others, indicate a behavior different in essential respects to that of granular material under a bearing plate.

As an extreme departure from a load resting on an elastic solid, the case of a box containing a load floated in a lake of water may be cited. The box is supported at a certain flotation depth, but the pressure on the bottom of the lake is not increased (except in so far as the water surface may be raised

NOTE.—The paper by A. E. Cummings, Assoc. M. Am. Soc. C. E., was published in August, 1935, *Proceedings*. This discussion is printed in *Proceedings* in order that the views expressed may be brought before all members for further discussion.

[23] Pres., Lehigh Univ., Bethlehem, Pa.

[23a] Received by the Secretary September 16, 1935.

slightly) and the pressure is evenly distributed over the bottom of the box. In a fluid, the pressures so increase with the depth that the upward reactions on the bottom supports the load.

In a viscous material, such as heavy oil or asphalt, a similar phenomenon occurs, except that flow occurs slowly and only after a long period of time is the theoretical flotation sinking attained. In heavy asphalt, the sinking stops short of the fluid flotation depth, showing that the shear stresses developed have a certain permanent sustaining capacity for holding the load in equilibrium.

The behavior of plastic earths under load has certain points of similarity to viscous fluids. Whereas the pressures assume the typical bell-shaped distribution pattern in a sand bed under load, by virtue of the internal friction, in a plastic soil that is essentially devoid of internal friction, this pressure pattern is fundamentally modified. The spread of the load is probably much wider by virtue of shear and tension than observations seem to indicate, because of the experimental difficulty of measuring small increments of pressure. It is probable also that the depth to which the pressure is perceptibly transmitted in plastic soils is much less than is commonly assumed, owing to the wider spread of the load and the accompanying effect of immeasurably small pressures distributed over a large area, which is much greater than has been generally recognized. An artificial foundation bed for experimentation that would correspond more closely than sand to the prototype would be a thick layer composed of small rubber bands. Instead of using such an artificial bed for laboratory investigations, however, typical earths themselves should be used, because the present plethora of discordant foundation discussion has resulted largely from not basing theories and experiments on soils as they actually occur in Nature.

A relatively small clay content will convert sand to a plastic material in so far as friction and cohesion are concerned. Limited observations made by the writer indicate that, with fine sand of fairly uniform grain, 20% clay will make the mass essentially plastic. Probably with graded sand having a lower percentage of void space, even a smaller proportion of clay would be required. Practical foundations should be considered as saturated, for such will almost certainly be their condition at times, and experiments on dry soils are likely to be misleading.

The bell-shaped pattern of pressure distribution has relatively little significance, therefore, in the practical design of a particular footing, partly because only in clean sand or gravel, or on solid rock, is such a distribution likely to occur. In the second place, even if it should occur when the load is first applied, adjustment in time would tend to make the pressures fairly uniform. Moreover, shifting eccentricities of practical loadings tend to render inapplicable conclusions that may be predicated on an assumption of a fixed point of application of a load. Since the higher pressures at the center of a footing result only from greater rigidity of the soil in that region, the unequal distribution of the pressures will not result in settlement of a footing that is proportioned for a uniform distribution of soil pressure. Any giving way at the center would immediately distribute pressures toward the periphery.

Therefore, even if any flexure of the footing slabs that may occur would tend to accentuate the non-uniformity of soil-pressure distribution, a footing designed for uniform soil pressure would generally not result in failure.

In expressing appreciation of Mr. Cumming's excellent paper, which so succinctly sets forth the conception of a foundation as an hypothetical elastic structure, the writer wishes to venture the hope that more experimental and theoretical attention may be devoted to a consideration of actual soils with a view to determining their structural behavior under load. At any rate, more experimentation on plastic soils as a typical foundation material is needed, in order to establish values at the other extreme of soil types.

D. P. KRYNINE,[24] M. AM. SOC. C. E. (by letter).[24a]—The most comprehensive discussion of the Boussinesq formula and related problems that has ever appeared in the English language is contained in this paper. For advanced students of soil mechanics the completeness of references and the interesting historical data may be of great value; and readers less advanced are given a concise and clear presentation of the material which furnishes an excellent view of the subject as a whole. In reading this paper, however, the writer faced some difficulties which he wishes to clarify.

Conception of Isotropy.—Bodies termed "isotropic" in reality may possess quite different properties, depending on their degree of isotropy. If the material in a body possesses exactly the same properties throughout, including the stress-transmitting capacity, any point of any line drawn within that body will be a part of an isotropic "continuum," and such a state of isotropy may be termed "monotonous." On the other hand, if the material consists of units or particles interspersed with voids or some other material, with different stress-transmitting capacities, the body may possess "statistical" isotropy. Owing to the presence of a great number of particles pressed against each other, stresses within such a body may be generated so as to simulate a "continuum," and this similarity is the greater, the greater the degree of isotropy approaches the "monotony" referred to; for instance, if two straight lines, 1 in. long, drawn within a sand and a clay mass, pierce 100 and 100 000 soil particles, respectively, it is evident that the clay mass is much more properly termed "monotonously" isotropic than the sand mass. Furthermore, attracted moisture, which is almost solid in the case of a moist clay mass, approaches more the stress-transmitting capacity of the soil particles than water in the voids of a sand mass. Hence, formulas of the theory of elasticity, the Boussinesq formula among them, developed for the case of an isotropic elastic "continuum" should be applied to clays rather than to sands. It does not follow, however, that clays are elastic, and sands inelastic. Each sand particle is an elastic body, as demonstrated by the rebound after releasing a load from a sand mass; but the reason why the Boussinesq formula cannot be applied unconditionally to sands, lies in their lack of monotonous isotropy. Since statistical isotropy requires the presence of a great number of particles, it does not exist at all where this

---

[24] Research Assoc. in Soil Mechanics, School of Eng., Yale Univ., New Haven, Conn.

[24a] Received by the Secretary September 20, 1935.

condition is not fulfilled. Hence, an earth mass, especially a natural sand mass, is not isotropic close to its boundary.

The explanations advanced are required in order to understand the following apparent inconsistency in Mr. Cummings' paper. First, he quotes Boussinesq himself who stated that the distribution of stress across planes parallel to the surface is the same in all isotropic bodies and a few pages following a numerical example dealing with stress distribution in sand shows that an actual vertical pressure is almost twice that computed according to the Boussinesq formula, and so do the experiments described. The reader is thus induced to believe that sands are not isotropic and perhaps not elastic; but the situation clears up if one realizes that under the term, "isotropic," Boussinesq could mean monotonously isotropic bodies only, such as those studied in the theory of elasticity.

Interrelationship Between the Degree of Isotropy and the Value of the Concentration Factor.—Commenting on the opinion of Mr. Cummings, as to the values of the concentration factor ($n = 3$ for clays and $n = 6$ for sands), the writer agrees with it in so far as shallow depths are concerned, but wishes to offer an interpretation. At each point of the earth mass, loaded with its own weight, there is a vertical pressure, p_z, and a horizontal pressure, $p_x = p_y$. The ratio, $\frac{p_x}{p_z} = \frac{p_y}{p_z} = K$, is the coefficient of pressure at rest, according to the terminology of Professor Terzaghi. The value of K in monotonously isotropic elastic bodies (confined water, some metals, etc.), is equal to 1. This value decreases as isotropy ceases to be monotonous; for instance, it equals about one-fourth in the case of coarse sands. Simultaneously, the concentration factor, n, increases; and this can be shown mathematically. In Fig. 6 the vertical and the horizontal angular distances are designated by θ and θ', respectively; d is the depth of a point, A, at which the vertical and horizontal pressures, p_z and p_x, respectively, are to be determined; and z is the variable depth of a point, Q. Equation (3) represents the vertical normal stress, p_z, which may be conceived as the vertical projection of the full stress p; thus:

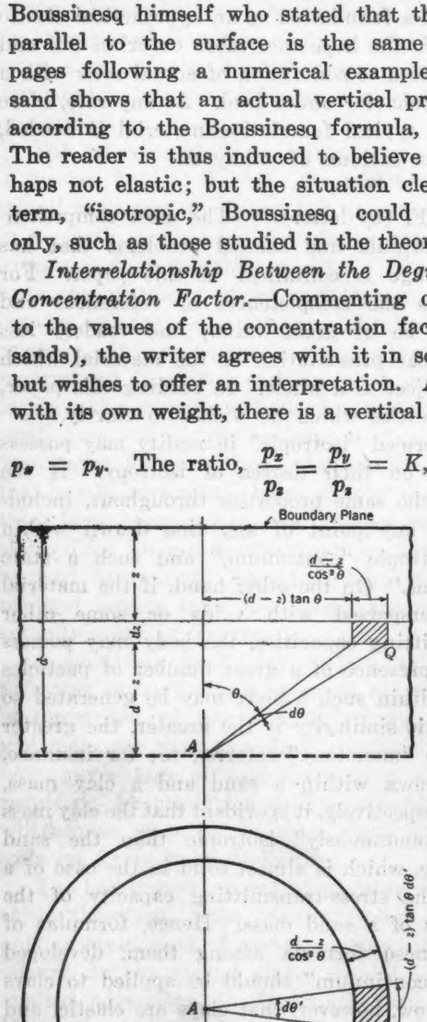

FIG. 6

$$p = \frac{nP}{2\pi R^2}\left(\frac{z}{R}\right)^{n-2} = \frac{nP}{2\pi R^2}\cos^{n-2}\theta \quad (15)$$

It will be assumed that a projection of the stress, p, on the horizontal plane does not depend on the value of the Poisson ratio. At the point, Q, there is a small earth element (shaded area in Fig. 6). If w is the unit weight of the earth material in question, the weight of this small element is:

$$dP = w\left[\frac{d-z}{\cos^2\theta}\right]\left[(d-z)\tan\theta\, d\theta'\right]\left[dz\right] = \frac{w(d-z)^2\sin\theta}{\cos^3\theta}\,dz\,d\theta\,d\theta' \quad \ldots(16)$$

In Equation (16) the three dimensions of the earth element at the point, Q, (its length, width, and height) are written separately in brackets. According to Equation (15) the value of the elementary stress acting along the direction, QA, is:

$$dp = \frac{n\,dP}{2\,\pi\,(d-z)^2}\cos^n\theta \quad \ldots\ldots\ldots\ldots\ldots\ldots(17)$$

and the horizontal projection of this elementary stress:

$$dp\,\sin^2\theta = \frac{n\,dp}{2\,\pi\,(d-z)^2}\cos^n\theta\,\sin^2\theta \quad \ldots\ldots\ldots(18)$$

Taking the sum of the horizontal projections (Equation (19)) of the elementary stresses reaching Point A from all parts of the earth mass lying above it, the horizontal pressure at Point A would be obtained. Hence:

$$p_x + p_y = 2\,p_x = \int_{\theta=0}^{\theta=\frac{\pi}{2}}\int_{z=0}^{z=d}\int_{\theta'=0}^{\theta'=2\pi}\sin^2\theta\,dp \quad \ldots\ldots(19)$$

Introducing into Equation (19) the values of dP and dp from Equations (16) and (17), the first step is to integrate with respect to both z and θ', and then with respect to θ; thus:

$$p_x = \frac{1}{2}\,n\,w\,d\int_0^{\frac{\pi}{2}}\cos^{n-3}\theta\,\sin^3\theta\,d\theta$$

$$= \frac{1}{2}\,n\,w\,d\;\frac{2}{n}\left[-\frac{\cos^{n-2}\theta}{n-2}\right]_0^{\frac{\pi}{2}} = \frac{1}{n-2}\,w\,d \quad \ldots\ldots\ldots(20)$$

Since the value of the vertical pressure at Point A is $p_z = w\,d$, the value of the coefficient of pressure at rest, K, would be: $K = \frac{p_x}{p_z} = \frac{1}{n-2}$, from which:

$$n = 2 + \frac{1}{K} \quad \ldots\ldots\ldots\ldots\ldots\ldots\ldots\ldots(21)$$

Equation (21) expresses the relation between the concentration factor, n, and the coefficient of pressure at rest, K. It is an approach to the solution of this problem since further research may prove that some other causes also influence this relation. For a monotonously isotropic elastic body, $\frac{p_x}{p_z} = 1$ and, hence, $n = 3$. If the horizontal pressure exerted by a clay is

three-fourths of the vertical, the value of n in that case is about 3.3. For a sand possessing an angle of friction of $\phi = 35°$ under given circumstances,

$$K = \frac{p_x}{p_z} = \tan^2\left(45° - \frac{\phi}{2}\right) = \tan^2 27° \, 30' = \frac{1}{4}$$

Hence, according to Equation (21), the value of its concentration factor is $n = 6$. It is also obvious that there is a certain relation between the value of the concentration factor, n, and the angle of friction, ϕ, of a given sand.

The writer wishes to emphasize, however, that the few known values of K have been determined from experiments practically all of which were in rather shallow test containers. Hence, the corresponding values of the concentration factor, n, cannot be applied unconditionally for computations of stresses at greater depths. The writer's belief is that the concentration factor, n, is a function of depth also; apparently, it decreases with the depth, tending to approach the asymptote at $n = 3$. Evidently, the latter value is a minimum, since one cannot visualize any material more free from voids than a "continuum." Probably, at a certain depth within the earth all matter obeys the Boussinesq law with a concentration factor, $n = 3$, and the difference between the stress distribution in sand and clay is merely a surface phenomenon.

The writer bases his opinion on the experiments of Messrs. Terzaghi[25] and Hatch,[26] who proved that the coefficient of friction of sand decreases as the normal pressure increases; and this means that the coefficient of pressure at rest, K, is greater and the factor of concentration, n, smaller, at a relatively greater depth than close to the ground surface. The statement to which Mr. Cummings objects, namely, that the distribution of stress is independent of the type of material, should be corrected by adding the phrase, "at a certain depth." It is true that this unknown depth may be very considerable.

Stresses at the Plane of Contact.—Mr. Cummings' remark that the distribution of pressure on the under side of the experimental test plates in the experiments described is responsible for the stress distribution in the earth mass, cannot be over-emphasized. An interpretation of the fact should be given, however. According to the third Newton law, action and reaction are equal and opposite, and it appears at first glance that if the load on a foundation or experimental plate is uniform, the reaction of the earth mass under it should also be uniform. Such a manner of thinking has proved disastrous in the history of civil engineering and has retarded the development of soil mechanics for many years. What actually matters is not the distribution of load around the foundation, but the distribution of stresses within the footing close to its plane of contact with the earth. The structure and the earth mass together form a statically indeterminate system, and the stress distribution depends on the elastic properties of both bodies in contact. In all cases stresses on both sides of the plane of contact are equal, thus satisfying

[25] "Handbuch der physikalischen und technischen Mechanik," edited by F. Auerbach and W. Hort, Vol. IV, Pt. 2, p. 523, Leipzig, 1931.

[26] "Tests for Hydraulic-Fill Dams," by Harry H. Hatch, M. Am. Soc. C. E., *Transactions*, Am. Soc. C. E., Vol. 99 (1934), pp. 228–229.

Newton's third law (Fig. 7(*a*)). As a rule, the stress distribution in question is not uniform, although it may become so in a particular case.

In reference to the interesting statement by Mr. Cummings that for very large areas the pressure is approximately uniform, the writer wishes to state

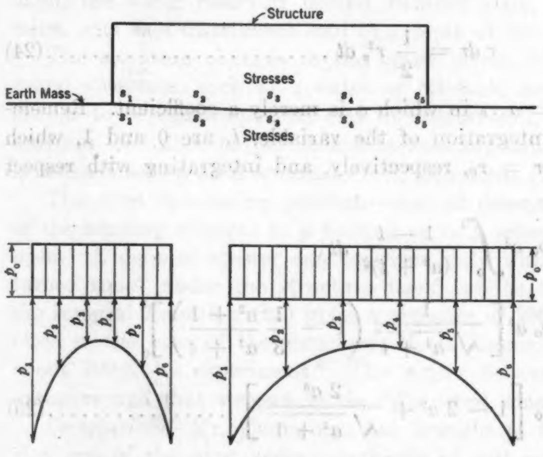

FIG. 7

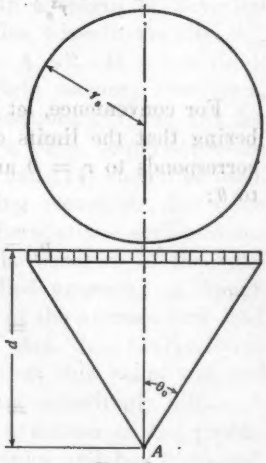

FIG. 8

that in some cases there is only an appearance of uniformity. In Fig. 7(*b*) a narrow structure, and in Fig. 7(*c*), a wide structure are represented; both are subjected to the same uniform unit load and both are rigid and constructed on rigid clay, so that the stress would be a minimum at the center. The ordinates, p_1, p_2, p_3, etc., of the stress distribution curve are exactly equal at corresponding points of both structures; but the rate at which the stress increases per foot of width of the foundation is less in the case of the wide foundation. This may create the impression of a rather uniform stress distribution close to the middle of a wide structure.

Mathematics of the Stress Distribution Formulas.—If trigonometric functions were used in developing Equation (7), it would be in a more convenient form for application. In Fig. 8, θ_o, designates a half angle at the vertex of the cone formed by radii vectors drawn from a given point, *A*, within the earth mass to the perimeter of a round foundation. Then, Equation (7) becomes,

$$p_z = p_o\,(1 - \cos^3 \theta_o) \ldots\ldots\ldots\ldots\ldots\ldots\ldots (22)$$

Equation (22) is a particular case of a general formula. Actually, integrating Equation (6) for a general case (that is, for a concentration factor, *n*):

$$p_z = p_o\,(1 - \cos^n \theta_o) \ldots\ldots\ldots\ldots\ldots\ldots\ldots (23)$$

from which, by making $n = 6$, the stress distribution for Case II may also be obtained. Equation (23) was first developed by Dr. O. K. Fröhlich, of Holland.[22]

[22] "Druckverteilung im Baugrunde," p. 50, Julius Springer, Vienna, 1934.

To integrate Equation (12), Mr. Cummings uses an infinite series; the problem was also solved by Dr. Fröhlich by a transformation to trigonometric functions.[19] The formula, however, may be integrated in a closed form by substituting t for $\frac{r^2}{r_e^2}$, thus:

$$r\,dr = \frac{1}{2}\,r_e^2\,dt \qquad (24)$$

For convenience, let $d = a\,r_e$ in which a is merely a coefficient. Remembering that the limits of integration of the variable, t, are 0 and 1, which corresponds to $r = 0$ and $r = r_e$, respectively, and integrating with respect to θ:

$$p_z = 3\,p_0\,a^3 \int_0^1 \frac{1-t}{(a^2+t)^{\frac{5}{2}}}\,dt$$

$$= 6\,p_0\,a^3 \left[\frac{1}{\sqrt{a^2+t}}\left(1 - \frac{1}{3}\,\frac{a^2+1}{a^2+t}\right)\right]_0^1$$

$$= 2\,p_0\left[1 - 2\,a^2 + \frac{2\,a^3}{\sqrt{a^2+1}}\right] \qquad (25)$$

By making $a = 1$ in Equation (25), the true value of the vertical pressure, p_z, at a depth, $d = r_e$, may be obtained. It is equal to 0.83 p_o, and not infinity, as indicated by Fig. 4, Case III. A mathematical tool, like any other, can give adequate results only within the limits of its applicability. This is why in this case an infinite series proved inadequate to reflect the actual physical condition between $a = 1$ and $a = 0$. By making $a = 0$, in Equation (25), p_z becomes equal to 2 p_o or 200% of the average surface pressure as obtained from Dr. Fröhlich's integrals. Case IV may be dealt with in a similar manner.

Limits of Application of the Formulas Discussed.—So far as may be concluded from this paper, the following methods are available for computing stresses within an earth mass: (*a*) By Equations (1) or (3) for the case of a concentrated load; (*b*) by Equation (7) for uniform load distribution; and (*c*), by Equations (12) and (14) for parabolic load distribution. A case is also mentioned by Mr. Cummings in which a distribution would be a minimum at the center and infinite at the edge; but no formula is given for this case.

In comparing the curves shown in Fig. 4, the author reaches the conclusion that "the character of the pressure distribution at the surface (uniform or parabolic) is especially important near the surface but loses its importance as the depth increases." This statement, although quite true, should be generalized and strengthened as follows: "At a certain depth, about twice the diameter of the loaded area, ($d \geq 4\,r_e$), any structure acts practically as a concentrated load." In other words, if stresses are to be determined at a depth greater than twice the diameter of the loaded area, the designer need

[19] "Druckverteilung im Baugrunde", p. 52.

not worry about how the loads are distributed along the structure, nor need he worry as to whether or not the structure is rigid. The Washington Monument, in Washington, D. C., has a base of about 125 by 125 ft; hence, it acts as a concentrated load at a depth of 250 ft beneath the base. On the other hand, the water reservoir behind Boulder Dam, with a length of, say, 100 miles, acts as a distributed load to a depth of 200 miles, beneath the site.

The situation changes in the upper layers ($d < 4\ r_e$). If a non-rigid, round structure, such as a water or oil tank, non-rigid masonry structures, etc., is to be constructed on clay or similar soil, Equations (7) and (8) for uniform load distribution should be applied; and if a rigid, round structure is constructed on sand or similar soil, Equations (12) and (14) should be used.

The most interesting problem—that of determining accurately, the value of the bending moment in a footing or in a spread foundation—still remains open. A definite answer can be given only when the behavior of the "disturbed zone" under the structure itself can be studied properly. Although the integral Equation (25) gives a pressure of 200% of the average unit load close to the base of the structure, M. L. Enger, M. Am. Soc. C. E., found about 300% by experiment.[27] The writer believes that this value was not excessive and that stresses in the "disturbed zone" are exceedingly high.

Conclusion.—Mr. Cummings has brought to the attention of the profession one of the most serious problems of soil mechanics and has displayed, in this connection, an unusually broad knowledge of the technical literature. No one can be expected to solve such problems alone; hence, if in discussing this interesting and important paper, corrections and additions are made, this cannot diminish its value.

L. C. Wilcoxen,[28] Assoc. M. Am. Soc. C. E. (by letter).[28a]—The distribution of stresses in an elastic soil under a foundation, based on certain specific assumptions, has been developed mathematically by Mr. Cummings. His conclusions are logical, and he has done well to stress the limitations of his formulas to the conditions assumed.

Examination of the general conditions affecting the distributions of stresses under a foundation more clearly sets forth the significance of the limitations prescribed by the author. The distribution of stresses is modified by: (*a*) The load distribution on the footing; and (*b*) the degree of flexibility of the footing. In practice, there are three distinct types of simple foundations, each having its characteristic stress distribution: (1) The uniformly loaded, perfectly flexible foundation; (2) the concentrated load on a semi-flexible foundation; and (3) the rigid (non-flexible) foundation, in which the character of the load is not a factor. Naturally, there are modifications and hybrids of these three types. Their recognition, however, explains much of the conflicting evidence regarding the behavior of foundations.

The uniformly loaded, perfectly flexible foundation produces a uniform surface load on the soil, as Mr. Cummings has assumed in Cases I and II.

[27] Second Progress Rept. of the Special Committee on Stresses in Railroad Track, *Transactions*, Am. Soc. C. E., Vol. LXXXIII (1919–20), p. 1409, and Vol. 93 (1929), p. 372.

[28] Asst. Engr., City Engr.'s Office, Detroit, Mich.

[28a] Received by the Secretary September 20, 1935.

The concentrated load on a semi-flexible foundation (and with the proper degree of flexibility) produces a surface load that is parabolic in sections. This covers Cases III and IV. It may also yield a uniform surface load as in Cases I and II, and as will be explained.

The rigid foundation, regardless of the type of loading, produces a maximum surface loading at its perimeter, decreasing toward the center. This type of distribution has been demonstrated by the writer,[29] using the photo-elastic method. The soil loading produces an inverted arch, or dome of maximum stress, the bottom of which (in the case observed) was at a depth, 0.7 *D*, below the foundation. This dome of stress is probably somewhat akin to the cone developed under a small "foundation" when the latter is driven through a soil.

In all these different cases, the foundation flexibility is the key to the resulting type of surface stress distribution. Deformation is probably as important in foundation problems as retaining wall movements (however small) are, in determining soil reactions. The latter has recently been demonstrated in a striking manner by Charles Terzaghi, M. Am. Soc. C. E.[30] The former remains to be demonstrated.

Given a concentrated load on a rigid footing, it has been stated that the maximum surface stress is at the perimeter, decreasing toward the center. If flexibility of the footing could be introduced progressively, the pattern of the surface reaction on the footing would change progressively. It would first become uniform; later, it would assume the parabolic distribution, and, ultimately, it would become a concentrated reaction under the load itself. It is one of these intermediate cases which was reported by Frederick Converse, Assoc. M. Am. Soc. C. E., and referred to by the author.[31] Failure by Mr. Converse to report the nature and extent of the footing deformation made the experiment incomplete.

The classical experiment[31] by M. L. Enger, M. Am. Soc. C. E., has been assumed by the author to have been a parabolic surface loading, as in Cases III and IV. This is probably an error, although in this case, it is not important because the data which he borrows are at a depth of at least one footing diameter below the footing. At this level, Dean Enger has shown such a distribution to be correct.

In the original report of this experiment the lines of equal stress were extrapolated from the uppermost plane of observed values (6 in. below the footing) upward to the foundation. Although not supported by tests, and although no conclusions were drawn from it, the diagram showing the greatest surface load at the center has gained wide credence. The footing was relatively rigid, at least in one case (a heavy plate, $13\frac{1}{2}$ in. in diameter, with a load as great as 18 000 lb applied by a jack with a large base). Under this footing, a dome of maximum stress probably occurred with the distribution

[29] Progress Rept. of the Special Committee on Earths and Foundations, *Proceedings*, Am. Soc. C. E., August, 1933, p. 1054.

[30] *Engineering News-Record*, February 1 and 22, March 8 and 29, and April 19, 1934, Vol. 112, pp. 136, 259, 315, 403, and 503.

[31] "Distribution of Pressure Under a Footing," *Civil Engineering*, April, 1933, Vol. 3, No. 4, p. 207.

[31] *Engineering Record*, January 22, 1916, Vol. 73, p. 106; and *Transactions*, Am. Soc. C. E., Vol. 93 (1929), p. 372.

of the soil reaction, being a maximum at the perimeter and decreasing toward the center. Fig. 9 shows the original stress diagram (*a*) modified, and (*b*) in accordance with the writer's theory of rigid foundation surface stress distribution.

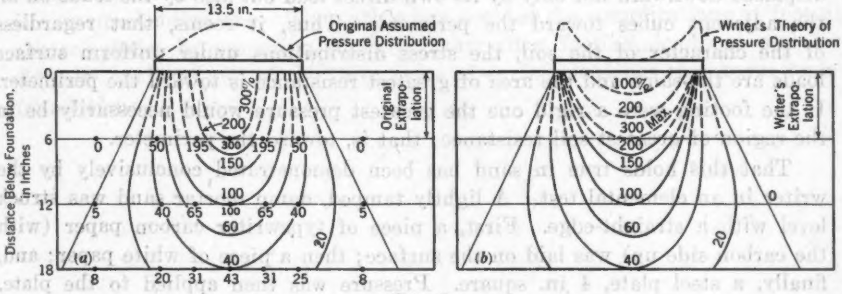

FIG. 9

That the pressure under a rigid foundation is greatest at the center is a theory that is widely held. The writer is aware that in many cases the opinion is authoritative, especially when the soil is a granular one. Nevertheless, he offers the following facts and deductions in support of his own view.

It has been demonstrated[20] that, with a uniform surface loading, in both plastic and granular soils, settlement was greatest at the center. Fig. 10 (*a*)

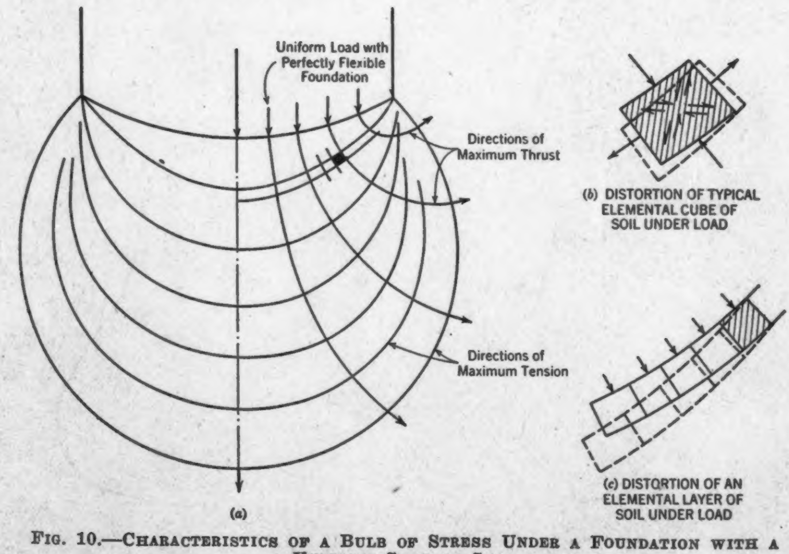

FIG. 10.—CHARACTERISTICS OF A BULB OF STRESS UNDER A FOUNDATION WITH A UNIFORM SURFACE LOAD

is a diagram of such a bulb of displacement and Fig. 10 (*b*) is a magnified incremental cube. With an increased footing load this cube would be distorted as indicated by the dotted diagram. The tests indicate that this deforma-

tion, and, hence, its stress distribution, would be the same regardless of whether the soil is cohesive or granular.

Fig. 10 (*c*) is a diagram of an incremental layer of soil as distorted by an increased load. It is apparent that each successive cube toward the center is displaced downward not only by its own direct load but also by the loads on all the adjacent cubes toward the perimeter. Thus, it seems, that regardless of the character of the soil, the stress distributions under uniform surface loads are the same and the area of greatest resistance is toward the perimeter. If the footing were a rigid one the greatest pressure would necessarily be in the region of greatest soil resistance; that is, toward the perimeter.

That this holds true in sand has been demonstrated conclusively by the writer in an elemental test. A lightly tamped, damp mortar sand was struck level with a straight-edge. First, a piece of typewriter carbon paper (with the carbon side up) was laid on the surface; then a piece of white paper; and, finally, a steel plate, 4 in. square. Pressure was then applied to the plate,

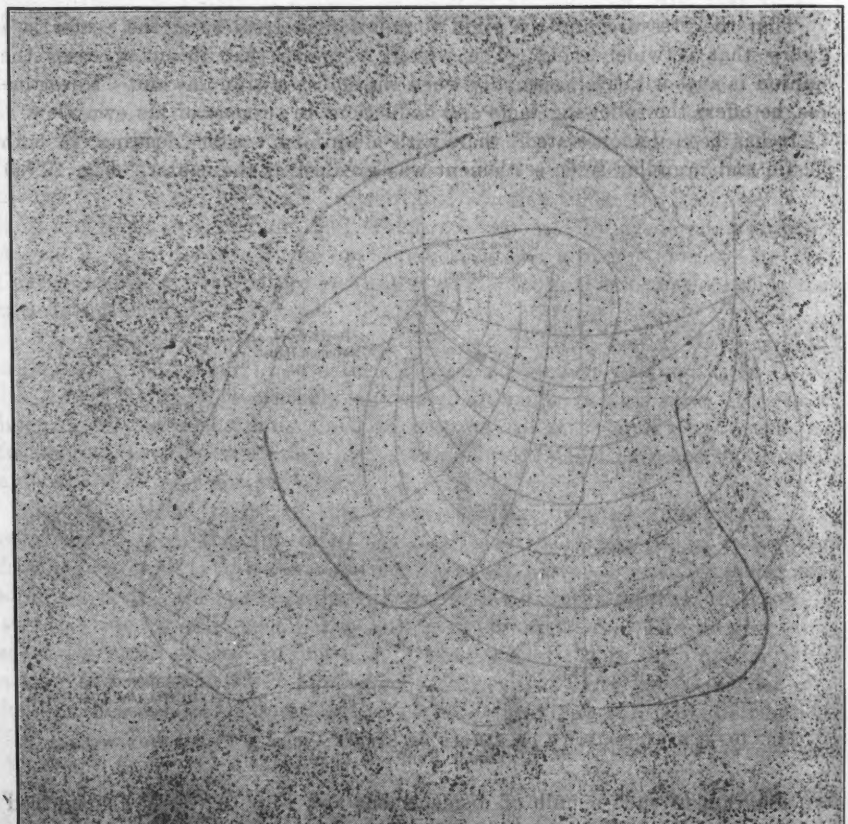

FIG. 11

by twice plunging a round-ended fence post down upon it. The results (see Fig. 11) showed that the region of greatest carbon transfer (and, hence, the greatest pressure) occurred under the part of the foundation near the perimeter.

The problem of analyzing the distribution of pressure under a foundation is a comprehensive one. The author has avoided the complications of footing characteristics by assuming surface, rather than footing, loadings, and has skilfully analyzed two of the three types of surface loadings that occur under foundations.

AMERICAN SOCIETY OF CIVIL ENGINEERS
Founded November 5, 1852

DISCUSSIONS

FAILURE THEORIES OF MATERIALS SUBJECTED TO COMBINED STRESSES

Discussion

BY MESSRS. J. J. SLADE, JR., T. MCLEAN JASPER, AND I. K. SILVERMAN

J. J. SLADE,[9] JR., ESQ. (by letter).[9a]—The interpretation of the results presented by Professor Marin offers some serious difficulties, the principal of which is due to the large radial scatter of the representative points. It is apparent, however, that none of the theories outlined by the author is adequate to represent the phenomenon throughout the range of values of $\frac{s_2}{s_1}$. In noting this the author states (see "Conclusion") that "the precisely correct theory of failure is probably a combination of a number of these theories, depending upon the ratio, $\frac{s_1}{s_2}$."

Assuming a material essentially homogeneous, such as steel, it is not likely that the failure values, s_1 and s_2, of the principal stresses would jump, at some ratio, $\frac{s^2}{s_1}$, from those given by one theory to those given by another; that is, it is more conformable with experience that the transition should be gradual. Such transitions, then, would most likely occur close to the points of intersection of the representative curves. Tracing the various possibilities it is seen that, although one may obtain a locus much closer to the average of the test data than any of those given by the simple theories, still there are serious discrepancies. For instance, near the ratio, $\frac{s^2}{s_1} = 1$, the average of the tests falls between loci of the general shear and the maximum strain-energy theories. These observations do not rule out any of the simple theories presented, however, but only their mathematical form; most of these expressions have been obtained on the assumption that Hooke's stress-strain relation holds, and failure, by any reasonable definition, occurs beyond the linear relation.

NOTE.—The paper by Joseph Marin, Jun. Am. Soc. C. E., was published in August, 1935, *Proceedings*. This discussion is printed in *Proceedings* in order that the views expressed may be brought before all members for further discussion.

[9] Assoc. Prof. of Eng. Mechanics, Rutgers Univ., New Brunswick, N. J.

[9a] Received by the Secretary July 31, 1935.

In view of this the writer proposes a different approach to the problem. Considering sufficient homogeneity of the material and accuracy of tests to determine the failure point, it will be assumed: (*a*) That there is a law of failure; (*b*) that the curve representing this law is continuous and continuously changing; and (*c*) that, for a given value of the ratio, $\frac{s_2}{s_1}$, the resultant of the principal stresses is single valued. As was stated, Assumption (*b*) is a requirement that conforms with experience. Requirement (*c*) states, in other words, that, if two identical samples are subjected to identical conditions, the values of the principal stresses at failure will be identical for the two. It is important to notice that the test results will not generally be identical, but these results are subject to errors of interpretation and mechanical errors which cannot be avoided. The scatter of the points representing the tests presented by Professor Marin will be considered later.

In order to develop the present analysis it will be convenient to adopt the polar co-ordinates, ρ and θ, which are connected with the co-ordinates, x and y, by the relations $x = \rho \cos \theta$; and $y = \rho \sin \theta$; or,

$$\rho = \sqrt{x^2 + y^2} \qquad (43)$$

and,

$$\theta = \arctan\left(\frac{y}{x}\right) \qquad (44)$$

It is thus seen that ρ is the resultant of the principal stresses divided by s_t. For brevity, ρ will be called the resultant and x and y, the principal stresses. In terms of these co-ordinates the law of failure embodying the foregoing three requirements will be given by a functional relation,

$$\rho = F\,(\theta) \qquad (45)$$

Besides the aforementioned requirements, it is seen that $F(\theta)$ is periodic in θ (this is so by the very nature of the representation of the law; for instance, the value of ρ cannot change by adding 360° to θ). Therefore, $F(\theta)$ is ideally suited to be expanded in a Fourier series:

$$F(\theta) = b_0 + \sum_{k=1}^{\infty} a_k \sin k\,\theta + \sum_{k=1}^{\infty} b_k \cos k\,\theta \qquad (46)$$

With very extensive data the coefficients of this expansion may be determined readily by the method of least squares. A number of the terms of the series may be discarded *a priori* by Requirement (*d*) that the curve must pass through points, ± 1, on the axes, and Requirement (*e*) that the curve must be symmetrical about the two lines, $\theta = \pm 45$ degrees. The number of the remaining terms of the expansion, Equation (46), that may be retained, will depend on the completeness of the available data. In another connection, the writer has discussed the significant flexibility of curves,[10] particularly of curves represented by a series in which the coefficients are adjusted by the method of least squares or related procedures. It is sufficient to state that,

[10] *Proceedings*, Am. Soc. C. E., September, 1935, p. 1053.

depending on the data, there is a point beyond which added terms of the series will give a poorer representation of the function than will be given by the series with these terms omitted. The first two terms of the series, Equation (46), that satisfy Requirements (*d*) and (*e*) are:

$$F(\theta) = 1 + a \sin 2\theta \ldots\ldots\ldots\ldots\ldots\ldots (47)$$

Equation (47) will be tried as a first approximation to the law of failure. There is only the constant, *a*, to be determined, so that the method of least squares leads to the simple formula:

$$a = \frac{1}{n} \sum_{k=1}^{n} \frac{\rho_k - 1}{\sin 2\theta_k} \ldots\ldots\ldots\ldots\ldots\ldots (48)$$

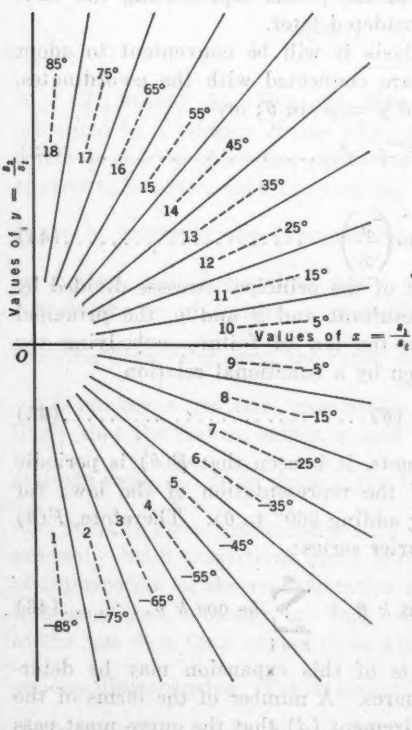

FIG. 20.—CLASS SECTOR DIVISION OF THE STRESS PLANE

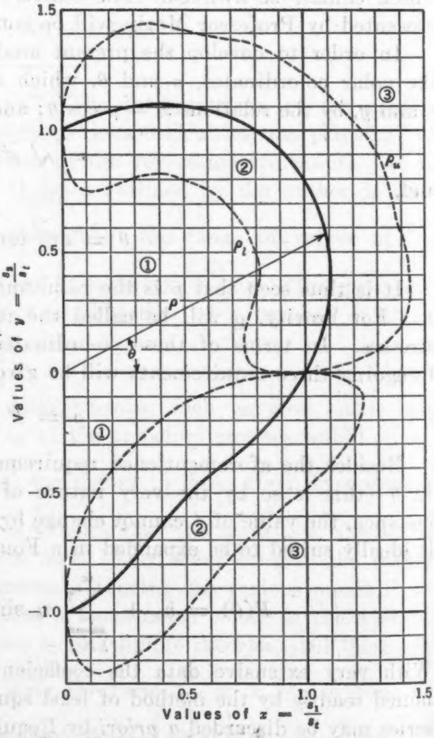

FIG. 21.—FAILURE CURVE WITH REGIONS OF ACCIDENTAL VARIATION

for the best value of *a*. In Equation (48) ρ_k is the resultant of the recorded tests; θ_k, the corresponding angle in the polar representation; and *n*, the number of items. Equation (45) has been used to substitute ρ for F. To every experimental result there corresponds a definite set of co-ordinates, ρ_k and θ_k, which may be readily obtained from the data made available to the writer by Professor Marin; but instead of computing each term of the series,

Equation (48), separately, the data will be grouped as follows: The right half of the stress plane (where all the experimental data fall) will be subdivided into eighteen 10° sectors numbered as shown in Fig. 20, and to the points falling within each sector will be assigned the angle of the sector mid-line, as shown in the same diagram. This subdivision is not only convenient but necessary for the statistical analysis of the problem. The magnitude of the angular opening of the class sectors adopted, has been dictated by personal judgment; it is desirable to make this magnitude small, but if it is made too small, the classes into which the data are thereby grouped will not contain a sufficient number of items with which to compute their statistical elements.

Adopting this class subdivision and inserting the values in Equation (48), obtained from the data on steel tubes presented by Professor Marin (which is the most extensive), the magnitude, 0.278, is obtained for the best value of a. Thus, the best two-term Fourier approximation to the failure law for steel tubes is:

$$\rho = 1 + 0.278 \sin 2\,\theta \ldots\ldots\ldots\ldots\ldots\ldots\ldots(49)$$

TABLE 2.—COMPARISON OF FAILURE CURVE WITH TEST RESULTS ON STEEL TUBES

Sector (1)	No. of items (2)	θ, in degrees (3)	Sector means (4)	Dispersion about means (5)	ρ (6)	Deviations of means (7)	Standard errors of means (8)	Variation limits (9)	ρ_l (10)	ρ_u (11)
1	0	—85	....	....	0.951	....	....	0.285	0.666	1.246
2	1	—75	(0.806)	....	0.862	—0.056	....	0.343	0.519	1.205
3	3	—65	0.778	0.026	0.789	—0.011	±0.014	0.335	0.454	1.124
4	1	—55	(0.940)	....	0.739	+0.201	....	0.315	0.424	1.054
5	60	—45	0.759	0.107	0.722	+0.027	±0.014	0.308	0.414	1.030
6	14	—35	0.877	0.057	0.739	+0.138	±0.015	0.315	0.424	1.054
7	17	—25	0.800	0.125	0.789	+0.011	±0.030	0.335	0.454	1.124
8	20	—15	0.856	0.084	0.862	—0.006	±0.019	0.343	0.519	1.205
9	25	— 5	0.911	0.098	0.951	—0.040	±0.019	0.285	0.666	1.246
10	4	5	0.981	0.076	1.049	—0.068	±0.038	0.285	0.764	1.334
11	4	15	1.091	0.166	1.139	—0.048	±0.083	0.343	0.796	1.482
12	6	25	1.253	0.067	1.212	+0.041	±0.028	0.335	0.877	1.547
13	11	35	1.247	0.109	1.261	—0.014	±0.033	0.315	0.946	1.576
14	13	45	1.357	0.186	1.279	+0.078	±0.052	0.308	0.971	1.587
15	7	55	1.186	0.043	1.261	—0.075	±0.016	0.315	0.946	1.576
16	2	65	1.092	0.039	1.212	—0.120	±0.027	0.335	0.877	1.547
17	0	75	....	....	1.139	....	....	0.343	0.796	1.482
18	0	85	....	....	1.049	....	....	0.285	0.764	1.334

Before discussing Equation (49) to determine its meaning as a mathematical expression for the theory of failure under bi-axial stresses, it is well to test its adequacy to represent the given data. For this purpose Table 2 has been constructed. The first column of this table lists the class numbers given in Fig. 20. The second column gives the number of experiments with representative points falling within the corresponding sectors. The third lists the corresponding sector mid-angles, also shown in Fig. 20. The mean resultant of the observed points for each class is given in Column (4). The standard radial deviation was computed for each class about the class mean and the results listed in Column (5), Table 2. Column (6) gives the values of ρ computed for the values of θ listed in Column (3). In Column (7) are listed the differences, Column (4)—Column (6); these, then, are the deviations

of the sector means from the failure curve, Equation (49). For every sector, from the number of items in the class and the corresponding standard deviation, the standard error of the mean was computed and the results are listed in Column (8).

In the first place, it should be noted that the deviations from the failure curve of the sector means do not show any marked trend; their distribution is not incompatible with one of a random nature. Now, of the thirteen classes for which the statistical elements can be computed, the deviations from the curve of the means of five of them are less than the standard errors in the mean, and five others come well within three times the standard errors. Of the remaining three, two may be disposed of by the following arguments: In Sector 6, ten of the fourteen items represent experiments by Cook and Robertson, which, it will be noticed, show consistently high values for the resultant—as compared with tests by Scoble, for instance, which show consistently low results. This sector, therefore, is not a fair sample, and the high value of the deviation cannot be given full weight. Sector 16, with a high negative deviation, has only two items, from which a standard deviation of 0.039 was computed. Two items, however, cannot give a fair estimate of the dispersion, which is consistently high for the entire range of tests, averaging 0.091 for the thirteen classes and being 0.107 for Sector 5 which has sixty items. With such high dispersion it is not beyond the bounds of reasonable probability that the average of two experiments, particularly when performed by the same person (Guest), should deviate $-$ 0.120 from the curve. The remaining class, Sector 15 with seven items, might be considered in like manner, but it is quite probable that one in thirteen classes should deviate from the norm by more than three times the standard error. Of the two classes with a single item each (Sectors 2 and 4) one deviates less than the average standard deviation, the other less than three times this deviation—a reasonable variation for single items.

Altogether, this analysis seems to show a high probability that Equation (49) is a close first approximation to the law of failure under bi-axial stresses for steel tubes.

The writer believes that it is important to make explicit recognition of the fact that the scatter of the experimental points is doubtless due more to errors of observation and faults of technique than to variations in the strength of the material, provided, of course, that the strength is kept within certain specification bounds. For the purpose of design it is desirable to set limits to the actual variation in the strength of the material, but there are no data available to the writer from which to make such an estimate. However, a rough estimate of the observational variation limits may be made from the data presented by Professor Marin. In the octant included between Line $\theta = 0°$ and Line $\theta = -45°$, where most of the experimental points fall, the circle of radius = 1 and the center at the point (1, $-$ 1) follows quite well the trend of the lower limit of variation. The equation of this circle referred to the origin is:

$$r = \sin \theta' + \cos \theta' - \sqrt{\sin 2 \theta'} \quad \ldots\ldots\ldots\ldots\ldots (50)$$

in which r is the radius vector and θ' equals θ in the fourth quadrant taken with a positive sign. The lower limits of experimental variation from Equation (49) will thus be given, in the fourth quadrant, by,

$$l = \rho - r \text{.........................} (51)$$

Assuming an essential symmetry in the accidental variations two curves may be constructed in the four quadrants:

$$\rho_1 = \rho - l \text{.........................} (52)$$

and,

$$\rho_u = \rho + l \text{.........................} (53)$$

where, for all quadrants, l is computed from the fourth quadrant by Equations (50) and (51). The values for the limits of variation thus determined are given in Column (9) of Table 2. Columns (10) and (11) give ordinates of ρ_1 and ρ_u. In Fig. 21 are given the graphs of Equations (49), (52), and (53) in the right half of the stress plane. These loci divide the plane into three regions. Assuming material essentially homogeneous, and reasonably accurate laboratory technique, then one can state that in Region 1 no sample will be found to fail, all samples will be observed to fail somewhere in Region 2, and no samples will be found to persist in Region 3. These limits, no doubt, can be greatly narrowed when more is known regarding the differences between observed results and actual failures. It may be noted that three results of experiments by Becker (Sector 14) fall beyond the tentatively assigned upper limit.

From the available data little can be said about the distribution of failures throughout Region 2; but taking as typical the limits, ±0.315, and a standard deviation of 0.105 (this value, which is close to the average of the standard deviations, is taken so as to make the ratio, $\frac{0.315}{0.105} = 3$, an even number) one may construct a distribution curve from Table 22 of the closing discussion of the writer's paper.[11] From the first section of Table 22, for the symmetric distribution function, for the value, $\lambda = 3$, the quantities listed in Table 3 are obtained.

TABLE 3.—DISTRIBUTION OF OBSERVATIONAL VARIATIONS

Percentage of samples...	1	5	10	15	20	30	40	50	60	70	80	85	90	95	99
Deviation...	−0.233	−0.184	−0.151	−0.126	−0.104	−0.066	−0.031	0.0	0.031	0.066	0.104	0.126	0.151	0.184	0.233

The meaning of Table 3 is that, in testing a large number of samples, 5% of them, for instance, will be observed as weak or weaker than the value given by Equation (49), less 0.184; or, that 70% of samples will be observed as weak or weaker than the value given by Equation (49), plus 0.066.

[11] "An Asymmetric Probability Function", *Proceedings*, Am. Soc. C. E., September, 1935, p. 1054 *et seq.*

Fig. 22 shows this distribution function. For comparison the actual distribution is given of the tests in Sector 5 about the class mean. The two are not strictly comparable because neither the means nor the standard deviations coincide; but the comparison is made, nevertheless, to show that, in general, the distribution of observed failures in Region 2 follows that required by theory.

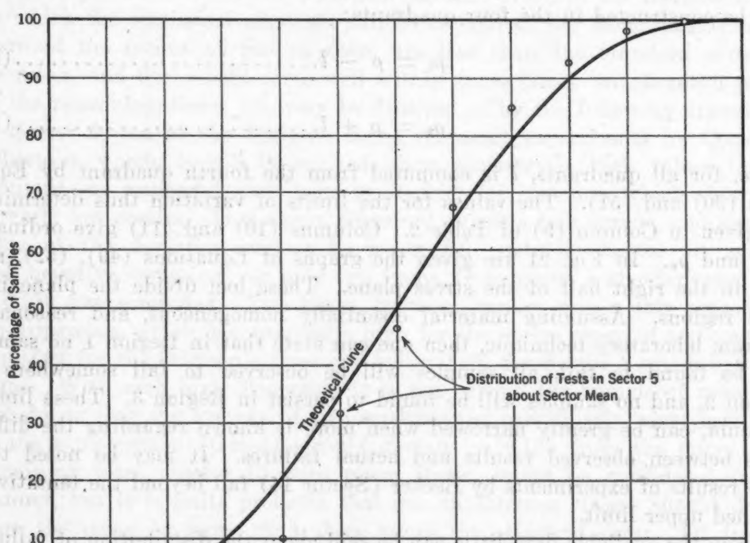

FIG. 22.— DISTRIBUTION OF FAILURES ABOUT FAILURE CURVE

The present statistical analysis of the problem has led to Equation (49) as a first approximation to the law of failure for steel tubes under bi-axial stresses. The available statistics do not warrant a closer approximation, but they seem to give to this equation a high probability of approximating closely the true law. It remains to discuss this law from the point of view of a possible theory of failure that might give rise to it.

The value, $a = 0.278$, found for the constant of Equation (47) suggests strongly that this constant might be Poisson's ratio; or, perhaps (as will appear subsequently in the discussion of the failure of brass tubes), some function of this ratio. One might indeed expect, *a priori*, to find this important constant included in the law of combined stress failure. Assuming $a = \sigma$ for the moment, and using the relation, $\sin 2\theta = 2 \sin \theta \cos \theta$, and the co-ordinate transformations, Equations (43) and (44), then the law of failure, Equation (49), becomes,

$$\sqrt{x^2 + y^2} = 1 + \frac{2 \sigma x y}{x^2 + y^2} \quad \text{.......................(54)}$$

or, more compactly (using the value for ρ given by Equation (43)),

$$x^2 + y^2 - \left(\frac{2\sigma}{\rho}\right) x y = \rho \quad \ldots\ldots (55)$$

In this form the law is seen to bear a striking resemblance to the expressions for several of the theories presented by the author. Equation (55), in fact, may be considered as the equation of a continuously varying ellipse. In Sectors 9 and 10 this curve coincides closely with the maximum strain-energy theory, but elsewhere it intersects or parallels the curves representing the other theories and thus does not seem to bear out the author's conjecture that the correct theory may be a combination of several of these theories depending on the ratio, $\frac{y}{x}$. In the writer's opinion the correct theory of failure, an approximation to the mathematical expression for which is given by Equation (49) or Equation (55), can be formulated only after taking into account: (*a*) The non-linear character of the stress-strain relation in the neighborhood of failure; (*b*) the modification of Poisson's ratio in that region; and (*c*) the relation of the direction of the plane of fracture to θ in the polar representation.

The experiments on brass tubes given in the author's paper would seem to indicate that the constant, a, of Equation (49) is not simply equal to Poisson's ratio, for the substitution of $\sigma = 0.35$ in Equation (55) gives a poorer representation of the results than a much smaller quantity would give. There are not enough tests given on brass tubes, however, to make a significant statement regarding the form of this constant. The few results given on copper tubes, on the other hand, more nearly confirm the conjecture that $a = \sigma$. The experiments on steel rods, on an average, give higher values than are obtained by Equation (49) but this is, perhaps, what should be expected.

In a tube the condition of failure can be attained more uniformly than in a solid rod. In the latter failure may occur at a point before failure can be detected experimentally. Where failure does not occur uniformly there is a chance for the phenomenon of "wire-drawing" to add its reinforcing effect to the test rod. In this case Equation (49) would give the first failure, or "point" failure, and whether this can be detected depends on the achievement of very exact laboratory technique. Cast iron presents characteristics of failure that seem to be definitely different from those of the more elastic and homogeneous materials. Experiments on this material show a scatter of the representative points which is smaller than that for tests on steel, so that a few careful experiments that plot in the first quadrant of the stress plane would no doubt give a good indication of the failure characteristics of this material. A negative value of the constant, a, of Equation (47) is necessary to represent the cast-iron data properly, but the law thus determined might not follow through into other quadrants. Another term in the Fourier series may be necessary to approximate closely enough the law of failure for this material a term which becomes insignificant in the case of the failure of steel tubes. This case illustrates the importance of formulating carefully the correct theory of failure.

In conclusion, the writer wishes to express his appreciation of Professor Marin's work of unifying and presenting this valuable information collected from such wide sources; his paper is a great step toward the correlation of theory with experiment in this interesting branch of mechanics, which marks the way to greater efficiency in design.

T. McLean Jasper,[12] M. Am. Soc. C. E. (by letter).[12a]—In discussing the paper by Professor Marin it is well to point out two fundamental differences which might cause confusion in the discussion of theories of failures. It is believed, that the general testing methods adopted to discover the theories of material failure have not been given proper differentiation as between the failure of a structure because of its shape and the failure of a material based on its fundamental strength qualities.

When buckling is introduced into the test sample as a possible method of failure of a structure, it is obvious that failure can occur at values of stress that are much below the elastic limit or yield point of the material. Such a failure depends on the shape and on the elastic properties of the test pieces, rather than on the yield or general break-down of the material.

Examples of structure failure, in which buckling occurs at varying values of stress depending on the relative slenderness of the test samples, are contained in the column problem, the tube collapse problem, and the thin tube torsion problem. Many of the theories of material failure are based on test samples in which buckling, as a method of failure, enters, and the confusion which has associated itself with various theories, as shown in the author's Fig. 19, is largely attributable to lack of appreciation of this fact. The writer's experience with testing has brought to light failure of slender steel columns at less than one-third the yield strength of the material. The slender tube has collapsed at less than one-third the yield strength of the steel, and the slender torsion tube has collapsed at less than two-thirds of the torsional yield strength of the steel. In each case as the slenderness of the test sample has been reduced, the failure point of the various aforementioned structures has increased progressively.

Many of the experimenters have applied as experimental test samples one or more of the aforementioned methods which are associated with this buckling and as different investigators have varied the relative slenderness of test shapes, they do not check even within large percentages with each other.

A good example of what the writer wishes to convey is contained in the experimental work of Guest,[13] who is responsible for the maximum shear theory of failure. The record of his work shows that great care was taken in his experimentation, and since it was recorded in such detail, it allows a careful study of the test procedure. In his experimental work, Guest used thin cylinders and performed as many as twenty tests on a single test sample. He used a combination of torsion, internal pressure, and tension or compression, or various combinations of these testing methods. In certain cases,

[12] Research Dept., A. O. Smith Corporation, Milwaukee, Wis.

[12a] Received by the Secretary August 28, 1935.

[13] "On the Strength of Ductile Materials under Combined Stress", by J. J. Guest, *Philosophical Magazine*, July, 1900, p. 69.

he repeated the combinations of stress application more than once on a single test sample. For instance, the first test might be that of simple shear, and after various other tests were made on the same sample, he again resorted to simple shear. Invariably, when he repeated identical tests on the same sample, he obtained the same results.

The point the writer wishes to make is this; Since his standard of measurement depended on the stress-strain diagram and the deviation from proportionality, it is obvious, that if this point is exceeded in terms of yielding of the metal, then with each test a new yield point is established. If, on the other hand, elastic buckling only is responsible for the phenomena, the limit of proportionality of the structure can be exceeded without interfering with the yield of the metal and such elastic buckling will repeat itself indefinitely. If Guest had changed the slenderness of his test sample appreciably, he would have obtained quite different results.

There is exceeding good evidence that elastic structures fail very nearly according to the mathematical theory of elasticity, especially in the zone in which the elastic properties of the materials impose the controlling factor. The failure of materials, such as separation into two parts can occur only in tension or in shear according to the strict interpretation of these terms. The writer has obtained fatigue fractures from different samples of the same bar of steel which occurred separately as tension and as shear.

It is very probable, that neither the maximum shear theory nor the maximum stress theory can explain the break-down of the steel or other materials in bi-axial or tri-axial loading. The writer leans toward the idea that some form of maximum energy will yield the most reliable answer to the problem of the theory of failure of a material.

This discussion is not presented with the idea that the answer to the problem of material failure is known definitely. The method of determining the answer must be disassociated from buckling. It is possible that different materials may yield to different solutions; for instance, glass probably will produce a different result than steel. Steel will possibly have a different solution than aluminum. On the other hand, the failure of structures has yielded to consistent ideas, so that the service problem of the application of materials has not suffered because the various theories of material failure do not coincide.

I. K. Silverman,[14] Jun. Am. Soc. C. E. (by letter).[14a]—The conditions causing plasticity have been of great interest not only to physicists but also to engineers, since the limiting states of stress are intimately bound up with working stresses and factors of safety.[15] Civil engineers use the Rankine or maximum stress theory almost exclusively, whereas mechanical engineers favor the maximum shear theory, especially for ductile materials.

The author lists sixteen theories. The best known of these are Theories (1), (4), (7) to (11), (14), and (16). Theory (5) reduces to that of Theory (7); Theory (12) reduces to Theories (10) and (11); and, Theories (6), (13), (14),

[14] With U. S. Bureau of Reclamation, Denver, Colo.

[14a] Received by the Secretary September 16, 1935.

[15] "Factor of Safety and Working Stress," by C. R. Soderberg, *Transactions*, Am. Soc. Mech. Engrs., APM 52-2.

and (15) seem to have very little experimental support. By comparing the hypotheses of Theories (11) and (13) it is seen that the fundamental ideas thus expressed are diametrically opposed. The statement of Theory (11) is based upon the experimental fact that materials can withstand large hydrostatic pressures without failing. What is the basis for the statement expressed in Theory (13)?

These various theories can be compared by examining the case of pure shear, in which $s_1 = -s_2$, and from which a relation between the yield stress in shear and that in uni-axial stress may be obtained. Writing this relation as,

$$s_r = k\, s_t \qquad (56)$$

the value of k for the various theories mentioned by the author, are given in Table 4.

TABLE 4.—COMPARISON OF k-VALUES

Theory No. (1)	Special condition (2)	Value of constant, k (3)	Theory No. (1)	Special condition (2)	Value of constant, k (3)	Theory No. (1)	Special condition (2)	Value of constant, k (3)
1	....	1	8	....	0.6†		By Equation	
2	....	0.83	9	$a = 1$	0.577		28(a):	
3	....	0.83	9	$a = 1.3$	0.54	12	$\sigma = 0.3$	0.62
4	$\sigma = 0.25$	0.8	10	$\sigma = 0.25$	0.63	12	$\sigma = 0.35$	0.61
4	$\sigma = 0.30$	0.77	10	$\sigma = 0.3$	0.62	12	By Equation	
4	$\sigma = 0.35$	0.74	10	$\sigma = 0.35$	0.61		28(b)‡	0.577
5	....	0.5	11	....	0.577	13	....	0.5
6	....	0.5	12	By Equation		14	....	0.71
7	....	0.5		28(a):* $\sigma = 0.25$	0.63	15	....	0.5
						16	....	0.6†

* Same as Theory No. 10. † Assumed. ‡ Same as Theory No. 11.

Experiments by Becker[16] have shown that k is approximately 0.6, and that, apparently, for the state of stress expressed by $s_1 = s_2$ failure occurs when $s_1 = s_2 = 1.2\, s_t$. This value may have been influenced by the fact that the tests were not purely by-axial. More recent experiments[17] seem to support the theory of Huber-Hencky-von Mises.

[16] *Bulletin No. 32,* Univ. of Illinois, Vol. 13.

[17] W. Lode, *Zeitschrift für Physik,* Vol. 36, 1926; also, Ros and Eichinger, *Proceedings,* Second International Cong. for Applied Mechanics, Zurich, 1926.